NEAR-SURFACE INVESTIGATIONS OF THE DAMMAM DOME ON THE KFUPM CAMPUS USING THE GRAVITY METHOD

BY

MUHAMMAD HANIF

A Thesis Presented to the
DEANSHIP OF GRADUATE STUDIES

KING FAHD UNIVERSITY OF PETROLEUM & MINERALS

DHAHRAN, SAUDI ARABIA

In Partial Fulfillment of the
Requirements for the Degree of

MASTER OF SCIENCE

In

GEOPHYSICS

MAY 2018

KING FAHD UNIVERSITY OF PETROLEUM & MINERALS

DHAHRAN- 31261, SAUDI ARABIA

DEANSHIP OF GRADUATE STUDIES

This thesis, written by **Muhammad Hanif** under the direction of his thesis advisor and approved by his thesis committee, has been presented and accepted by the Dean of Graduate Studies, in partial fulfillment of the requirements for the degree of **MASTER OF SCIENCE IN GEOPHYSICS.**

Prof. Stewart A. Greenhalgh
Advisor

Dr. Abdulaziz Al-Shaibani
Department Chairman

Dr. SanLinn I. Kaka
Member

Prof. Salam A. Zummo
Dean of Graduate Studies

Dr. Umair bin Waheed
Member

21/5/13
Date

To Allah ﷻ, my parents, wife, and families who support my studies

وَهُوَ الَّذِي خَلَقَ اللَّيْلَ وَالنَّهَارَ وَالشَّمْسَ وَالْقَمَرَ ۖ كُلٌّ فِي فَلَكٍ يَسْبَحُونَ

And it is He who created the night and the day and the sun and the moon; all [heavenly bodies] in an orbit are swimming (21:33)

ACKNOWLEDGMENTS

Praise be to Allah ﷻ, may praise and peace be upon the Messenger of Allah, upon his family, his Companions and those who follow his guidance. I would like to express my gratitude to Allah ﷻ for His tawfiq and hidayah so that I can complete this thesis with a good result. Secondly, thanks to my parents Dra. Siti Fathiyah Banser and Dani Kusnandar, SE for their prayer all the time. My wife Sofa Tsani Aflacha, S.Si whose support, times, and much cheers for my son and daughter, Musa & Maryam.

Prof. Stewart Greenhalgh for his immense help and patience in teaching and advising this research. Dr. Sannlinn Ismail Kaka and Dr. Umair Bin Waheed for the guidance and help of some suggestions on this research.

Special thanks to Dr. Abdullatif Al-Shuhail for his help and support to my study in KFUPM. Dr. Abdulaziz Al-Shaibani and all Geosciences faculty and staff for all support, guidance, and attention to my study. Thank you to all CPG crews: Eng. Ayman Al-Lehyani, Eng. Abdulatif Ashadi, Adnan Al-Mubarak, Ahmed Al-Shaibani, Khalid Abdurrahman, Hameed Bhay, Mojtaba, and special thanks for Dr. Lamidi Babalola for the field trip.

Dr. Tauhid Nur Rahman, Agi Sugilar, ST., Ben Hilman, ST., Jodi Caesardana, ST., Faris Pramadhaniwali, S.Si., Mojtaba, for all your help in the differential GPS data acquisition and processing. All Indonesian and PPMI Dhahran squads, Mas Andy, Uda Septri, Mas Pram, Tausif Bhay, Uda Yose, Bang Yusri, Kang Adha, Bang Yusron, and special thanks for my roommate Kang Jemi for his prayers, support, and good culinary taste.

Finally, I hope this research can be beneficial for all the readers. If you have any suggestions or corrections for this manuscript, please kindly send it to hanifgeos@gmail.com.

TABLE OF CONTENTS

LIST OF TABLES

LIST OF FIGURES

LIST OF ABBREVIATIONS

CBA	:	Complete Bouguer Anomaly
DEM	:	Digital Elevation Model
DGPS	:	Differential Global Positioning System
FAC	:	Free Air Correction
FFT	:	Fast Fourier Transform
SRTM	:	Shuttle Radar Topography Mission
SVD	:	Second Vertical Derivative
USGS	:	United States Geological Survey

ABSTRACT

Full Name : Muhammad Hanif

Thesis Title : Near-surface Investigation of The Dammam Dome on KFUPM using The Gravity Method

Major Field : Geophysics

Date of Degree : May 2018

This thesis presents a near-surface investigation to explore the fault structures and cavity potential in the Dammam Dome. The gravity acceleration has been measured on the Dammam Dome in KFUPM campus. The total acquisition area is approximately 5 km^2 with the grid station is roughly 50 meters. The instruments are using Scintrex CG-5 Gravimeter and Leica GPS 1200+. Basic data correction such as tide, drift, latitude, free-air, Bouguer, and terrain has been carefully done to generate complete Bouguer anomaly (CBA) map. The regional field was then removed from the total gravity field using a spatial filtering technique to obtain the residual anomaly map due to near-surface geological variations. The second vertical derivative (SVD) map of the residual field was calculated and analyzed to better define geological faults and other features such as cavities. Sixty-seven dominant fault structures were interpreted. The dominant structural trends are NW-SE and NE-SW, with average fault strike directions of N 39^o W and N 48^o E. From the second vertical derivative and fault dip modeling analysis in the 4 fault lines, the dominant type of faults in the area are thrust faults and the fault dip are 21^o, 15^o, 28^o, and 67^o. These structures as well as the sand filled subsurface cavities are most probably controlled by the doming mechanism and dissolution.

Keywords: Dammam Dome, Cavity, Gravity, Bouguer Anomaly Map, Fault, Near-Surface, Saudi Arabia

ملخص الرسالة

الاسم الكامل: محمد حنيف

عنوان الرسالة: قرب التحقيق السطحي لقبة الدمام في جامعة الملك فهد باستخدام طريقة الجاذبية

التخصص: جيوفيزياء

تاريخ الدرجة العلمية: مايو 2018

تقدم هذه الأطروحة تحقيقات في المنطقة القريبة من السطح لاستكشاف هياكل الصدوع وإمكانيات التجاويف في قبة الدمام. تم قياس تسارع الجاذبية في قبة الدمام في حرم جامعة الملك فهد للبترول والمعادن.وتبلغ المساحة الإجمالية لجمع البيانات حوالي 5 كيلومتر مربع ، بشبكة محطات تبلغ حوالي 50 مترًا. تمت عملية جمع البيانات باستخدام Scintrex CG-5 Gravimeterو.+Leica GPS 1200 تم إجراء تصحيح البيانات الأساسية مثل المد والجزر وخطوط العرض وبوغير والتضاريس بعناية لإنشاء خريطة شذوذ بوغير الكاملة.(CBA) ثم تم إزالة الحقل الإقليمي من حقل الجاذبية الكلي باستخدام تقنية الترشيح المكاني للحصول على خريطة الشذوذ المتبقية بسبب الاختلافات الجيولوجية القريبة من السطح.تم حساب وتحليل المشتقة الرأسية الثانية (SVD) للحقل المتبقي من أجل تحديد الصدوع الجيولوجية و الملامح الجيولوجية الأخرى مثل التجاويف بشكل أفضل.تم تفسير البيانات بسبعة وستين صدع جيولوجي. الاتجاهات الهيكلية السائدة هي NW-SE و-NE SW، مع متوسط اتجاهات الصدع N 39 Wو.N 48 E من التحليل للمشتقة الرأسية الثانية و نمذجة انحدار الصدع لخطوط الصدع الأربعة ، فإن النوع المهيمن من الصدوع في المنطقة هي صدوع الدفع ، وانحدارات الصدوع هي 21 و 15 و 28 و 67.هذه الهياكل بالإضافة إلى التجاويف تحت السطح المملوءة بالرمال هي على الأغلب خاضعة لسيطرة آلية التفكيك والالتحام.

الكلمات المفتاحية: قبة الدمام ، تجويف ، جاذبية ، صَدْع ، قريب من السطح ، المملكة العربية السعودية

CHAPTER 1

INTRODUCTION

1.1 Preamble

Dammam Dome is situated in Dammam city, Eastern Province of Saudi Arabia. Unlike any other Saudi Arabia terrain, this region is unique due to the Hormuz Salt formation growth under this formation. This ellipsoid shape of group formation is rising 7 m/Ma (Weijermars, 1999). The terrain is indicated by the build-up of carbonate rocks on the flat extent of the Dammam Peninsula. There was situated the first discovery of a hydrocarbon-bearing structure within the Arabian mainland. The Standard Oil Company of California (SOCAL) first discovered oil in Dammam Dome from drilling the Dammam-7 Well in March 1938 (Al-Fahmi et al., 2014). Outside the Kingdom of Saudi Arabia, the structure is associated with a massive hydrocarbon reservoir in Kuwait (Milton, 1967), the surface exposure in Qatar (Al-Saad & Ibrahim, 2002), and similar to the elongated Awali Dome on the Island of Bahrain.

The main rock structures of the Dammam Dome are fractured carbonates with joints, karst features, and small-scale reverse faults (Al-Fahmi et al., 2014). Dissolution on the carbonate rocks structure can cause a karst phenomenon and resulting in subsurface cavities (Weijermars, 1999). The geological units have also been subject to faulting due to compressional stress from Zagros Orogeny, tangential stress associated with the dome's growth or development of local structures (Al-Fahmi et al., 2014)

Knowing the subsurface properties at shallow as well as greater depths is important for geoscientists as well as civil and petroleum engineers. The deeper structure controls to a large extent the hydrocarbon accumulations whilst variations in the surface topography and near-surface geology can corrupt the seismic images from the reservoir. This case can lead to seismic horizon picking errors (Setiyono et al., 2015), in addition to creating geo-hazard disasters (Khaldaoui et al., 2015).

Near-surface exploration using geophysical methods can be applied to delineate the subsurface structure of an area, especially for mapping potential cavities and faults. For example, ground penetrating radar (Chamberlain et al., 2000; Momayez et al., 1996), electrical resistivity tomography (Gambetta et al., 2011; Metwaly & Alfouzan, 2013; Putiška et al., 2012), seismic refraction and reflection (Fiore et al., 2013; Pernod et al., 1989), transient electromagnetic methods (TEM) (Guoqiang et al., 2004), and microgravity surveying (Bishop et al., 1997; Butler, 1984; Pánisová & PaŠteka, 2009; Styles et al., 2005) are all useful techniques for locating anomalies in the subsurface.

1.2 Literature Review

The literature records many studies describing qualitative investigation of cavities by utilizing geophysical tools. The gravity method is a non-destructive and passive remote sensing technique that utilizes changes in the Earth's natural gravitational field (caused by anomalous subsurface masses or density variations) to elucidate subsurface structure. It is especially sensitive to lateral subsurface density variations (Nettleton, 1971). Some researchers have already applied the method for investigating cavities. A qualitative

approach of gravity exploration for detecting shallow cavities in large caverns in Iraq was presented by Colley (1963). Butler (1984) developed microgravity analysis using the derivatives of the gravitational potential and concluded that the procedure is an effective means for delineating air and sediment filled cavities. Martín et al. (2011) integrated the techniques of regional residual separation using polynomial fitting, global geopotential model, and spectral analysis and successfully detect the cavities.

Some geotechnical studies of the study area began in the 1980s, including the evaluation of potential geohazards caused by solution cavities in shallow limestone beds (Abdullatif, 2010; Abu Taleb & Egeli, 1981; Crosch et al., 1985; Davies & Lord, 1980; Jado & Johnson, 1983). Weijermars (1999) reported fractures and joints in the Middle and Lower Rus units. The near-surface studies on this area are limited to ground penetrating radar and has found its capability to delineate cavities on 1-2 m depth (Al-Shuhail et al., 2004b).

Table 1 shows the summary of karstification on the Dammam Dome (Al-Fahmi et al., 2014).

Table 1 Summary of Karstification Data (Al-Fahmi et al., 2014)

No.	Karst Features	Location		Area (square meters)	Formation
		North	East		
1	Filled cave	26°18'52"	50°04'47"	1,000	Dam
2	Synform	26°18'48"	50°05'56"	8,987	Rus
3	Synform	26°19'23"	50°06'37"	Uncertain	Rus
4	Synform	26°18'59"	50°06'45"	20,255	Rus
5	Sinkhole	26°19'12"	50°07'05"	4,115	Rus
6	Sinkhole	26°19'03"	50°07'58"	300	Rus
7	Sinkholes	26°18'43"	50°08'19"	400	Dammam
8	Sinkhole	26°18'17"	50°07'23"	16,323	Rus
9	Synform	26°18'16"	50°06'24"	14,020	Rus
10	Sinkhole	26°18'21"	50°06'07"	650	Rus

My study adds to the characterization of near-surface density and structure model of the Dammam Dome on the KFUPM campus. It focuses on finding possible large structures (e.g fractures and karst features) and interpreting the lateral density distribution with its patterns. The methodology integrates the gravity survey with high accuracy of topography mapping acquired by differential GPS and laboratory data on rock features (eg; density) from the literatures.

1.3 Study Area

The study area is a part of Dammam Dome that situated on the King Fahd University of Petroleum & Minerals (KFUPM) campus, Dhahran city, Kingdom of Saudi Arabia (See Figure 1 & Figure 2). The bounding coordinates are 26°19’5.31’’ N to 26°17’34.68’’ N and 50°09’0.18’’ E to 50°8’18.75’’ E. The study area bordered with the blue line on Figure 2 is approximately 5 km^2 area. The gravity measurements were acquired mainly

on the roads and access paths inside the KFUPM campus both within the academic and housing complexes.

Figure 1 Location of Dammam Dome (on the red box) situated on the Eastern Province of Saudi Arabia from Google Earth® 2018

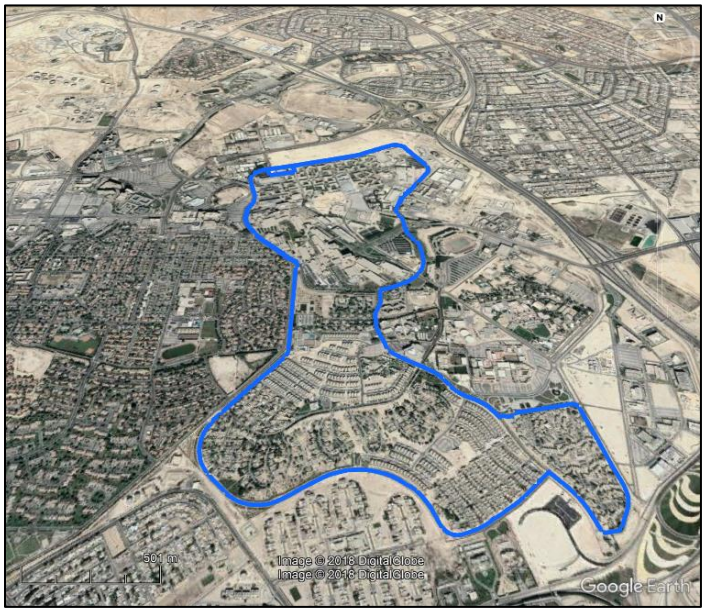

Figure 2 3D map view of study area (blue line bordered) taken from Google Earth ® 2018

In this study, a total of 500 field measurements of vertical gravity, roughly in a regular grid of 50 x 50 m has covered the area. The gravity data were acquired using Scintrex CG5 gravimeter and the topography control was carried out with a Leica 1200+ differential GPS. See Figure 3 below for the station position and the interpolated elevation model on the study area.

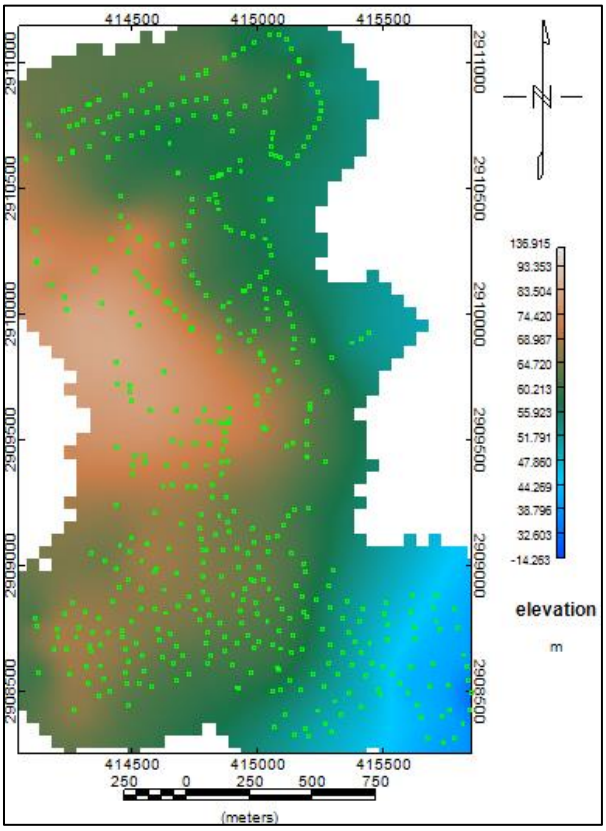

Figure 3 Station position and the elevation model on the study area

1.4 Motivation

The presence of faults and subsurface cavities poses an enormous hazard possibility because they have a collapse potential. This constitutes a risk to people as well as land and building damage. The delineation of faults and cavities are important aspects in the

geotechnical applications. Drilling is a common method of site investigation to detect the physical parameter of subsurface, but it has some limitation in the cost and the depth reached. To overcome the problem, non-invasive and cost effective geophysical methods can be used for near-surface fault. Due to importance of subsurface properties, a joint inversion approach of geological and gravity data is proposed to map the subsurface rock distribution and to detect the cavities potential in the study area.

1.5 Thesis Objectives

To date there have not been any attempts using the gravity method to image the near-surface structure and cavity potential on the Dammam Dome. However, the gravity technique has been applied widely elsewhere for subsurface cavity detection, but mainly using a qualitative approach. In this thesis, the objectives are to quantitatively map the near-surface structure and cavity potential using the gravity method. It is intended to estimate the subsurface density distribution of the area. Therefore, the aim of this work is to analyze and interpret the near-surface structure and likelihood of cavities occurrence of Dammam Dome on KFUPM campus by studying the fault structure. Furthermore, the gravity data will be inverted with the rock density and structure constrains from laboratory measurements and literatures to get the fault dip estimation.

1.6 Thesis Outline

This MSc thesis consists of six chapters. Apart from this first introductory chapter; it comprises the following chapters:

Chapter 2

Covers the literature review of the gravity method and the geological background from previous investigations on both the geophysical and geological side.

Chapter 3

Explains the methodology, how the data are acquired, quality controlled, and processed together.

Chapter 4

Details the synthetic model generation for fault dip in the study area.

Chapter 5

Explains the result over the target area as well as the interpretation.

Chapter 6

A summary and recommendations for future work.

CHAPTER 2

GEOLOGY OF THE DAMMAM DOME

2.1 Geological Setting of the Dammam Dome

The geological units are Tertiary (T) and Quaternary (Q) as shown in Figure 5. The former is sub-divided into the Rus (Tr), Dammam (Tdm), Hadrukh (Th), and Dam (Td) formations. The Quaternary deposits which are labeled using two lower case letters which express the predominant lithology or facies: sabkha (Qsb), coastal deposits (Qcd), and eolian sand (Qes). There are also areas of reclaimed land (Re), which are composed of landfill materials. On the study area, it was indicated that there are Rus Formation and Umm Er Radhuma (UER) Formation.

Rus Formation

Rus Formation as part of Lower Eocene has been divided into three members: lower, middle, and upper part. The lower part of formation shows alteration of marls and thin dolomitic limestone beds with abundant slumps and geodes. The middle Rus consists of a vuggy weathered, well-jointed calcarenite with abundant mud balls. The upper Rus consists of fine-grained chalky limestone with few marls and clay layers at the top. The thickness found on the Dammam Dome outcrop is 50 m.

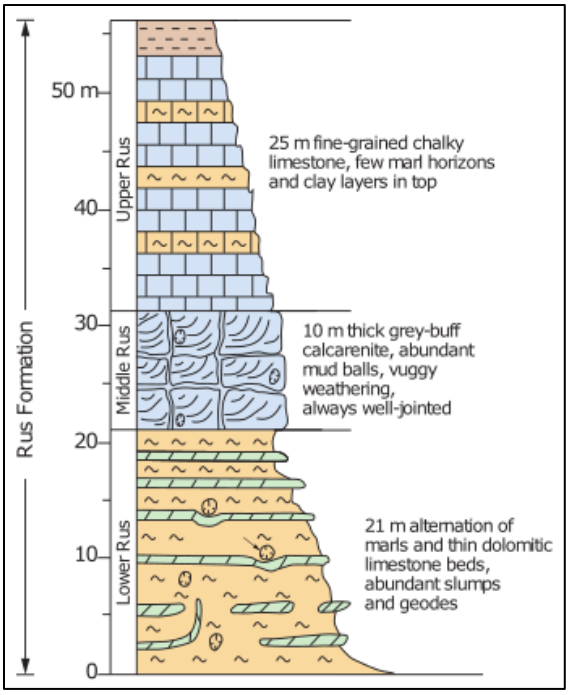

Figure 4 Stratigraphic column of Rus Formation (Al-Fahmi et al., 2014)

Umm Er Radhuma Formation

The formation is the lowermost Cenozoic formation. Umm Er Radhuma (UER) Formation was described as a 3m-thick section of vuggy dolomite located about 488 m east of Jabal Umm ar Ru'us in a topographically low area along the core of small anticline (Tleel, 1974). The other outcrop is located within the KFUPM campus and was reported to be part of the upper UER from its distinctive lithology (Weijermars, 1999). The thickness can reach up to 500 m meter on the subsurface (Alsharhan et al., 2001).

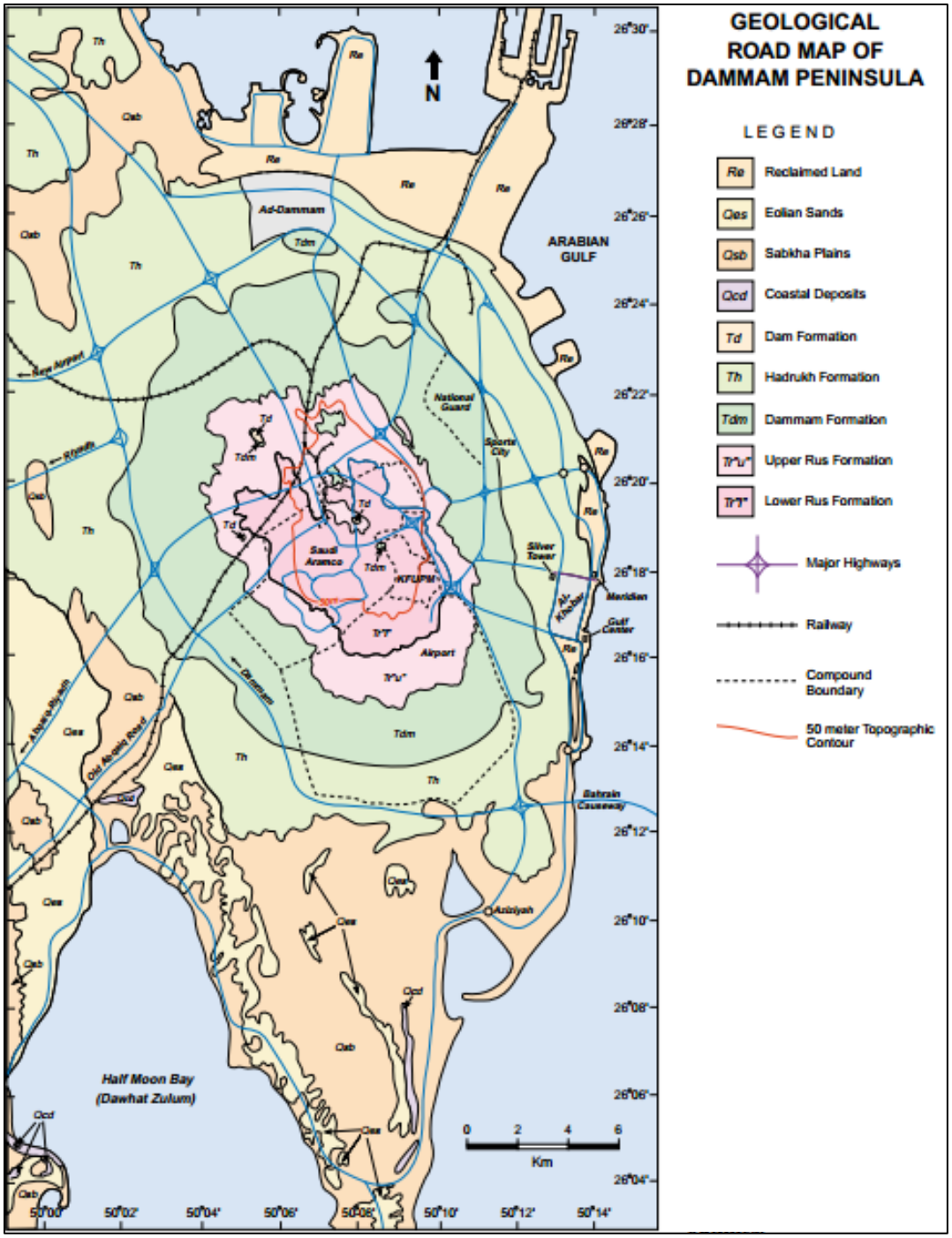

Figure 5 Geological map of Dammam Peninsula. Indicated geological boundaries are between the Lower and Upper of Rus Formation, between Rus and Dammam formation and Quatenary and Sabkha outlines (Weijermars, 1999).

2.2 The Karst System of Dammam Dome

The karst phenomena exist over large areas of the eastern part of Saudi Arabia (Hariri, 2013). They are formed as solution features such as sinkholes, collapse dolines and caverns. Caves are repositories for sediments moved in to form the surface and for sediments derived from within the cave (Al-Fahmi et al., 2014). The landforms are particularly associated with carbonate and evaporite formation of the Arab, Hith, Sulaiy, Umm er Radhuma (UER), Rus, Dammam, Dam, and Salt Dome formations.

The presence of karst within the UER Formation (marked as Location 2 in Figure 6) can be inferred from synforms within the lower Rus Unit at some areas in Dammam Dome. The small sinkholes are a bowl shaped morphotype but the larger ones have indefinite shape and are simply referred to as synforms. The large synforms are identified from some exposed units that dip with some angle to the flat surface (Crosch et al., 1985). It is also identified from bedding inclination measurements for some rock strata dipping in an opposite direction to the general gentle dip of the dome locations where bedding is expected to dip away from the central region of the dome.

In conclusion, the karst features can be identified by exploring the possible potential for dipping layer or fault feature.

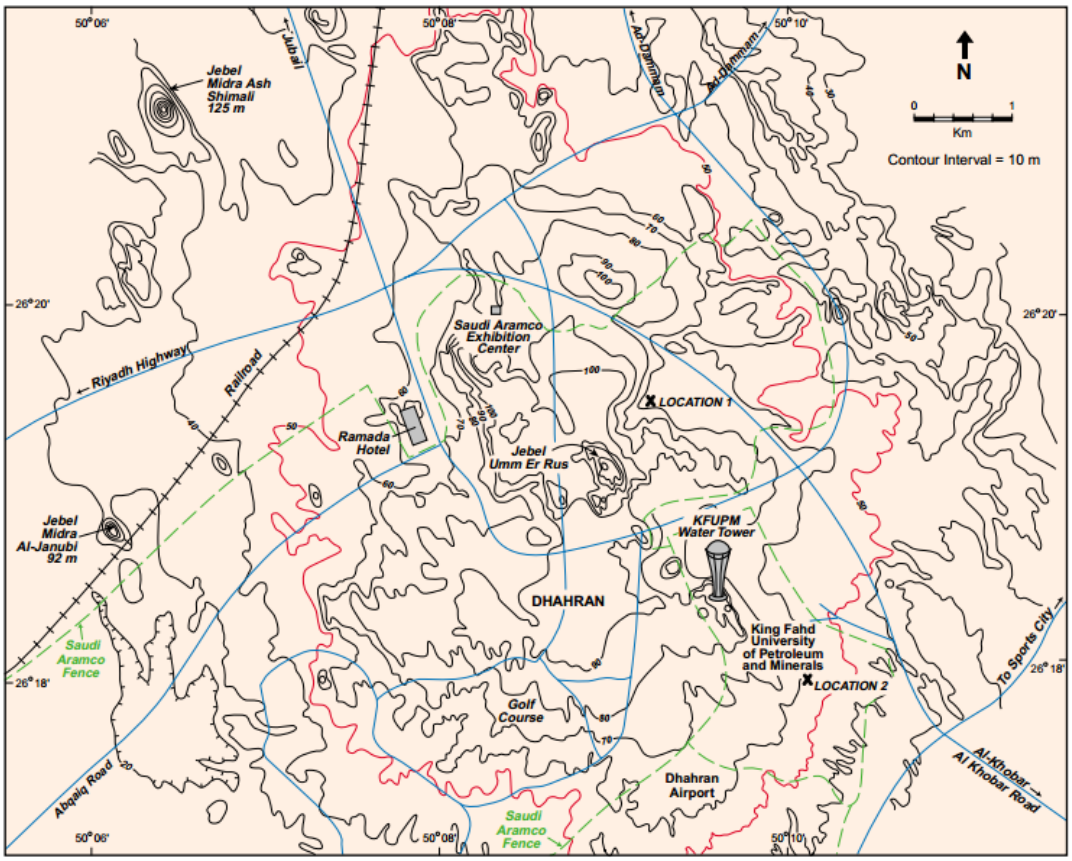

Figure 6 Map of high resolution topography showing 10 m contour interval of the Dammam Dome main area (Weijermars, 1999)

The existence of karst around the Dammam Dome has been demonstrated by some researchers using excavation methods such as in KFUPM (Jado and Johnson, 1983) and North Dhahran (Crosch et al., 1985). It shows that the location is subject to potential hazard from sinkholes, dolines, or caverns. Abdullatif (2010) has mapped several types of cavities from the outcrop of the Rus Formation.

CHAPTER 3

METHODS AND PROCEDURES

3.1 Overview

The detection of subsurface cavities is possible using certain geophysical methods, especially the gravity method provided by the cavity is sufficiently large and not too deep. The method may detect the presence of the cavity (air-filled, water-filled or sediment-filled) provided there is enough density contrast between the cavity fill and the surrounding rock layers. In this chapter, I review the gravity method, the surveying procedure, and the elevation and position determination, which are crucial for making corrections to the observed gravity data and the interpreted result.

The gravity method measures the lateral variation in the vertical component of the gravitational field at the surface of the earth. This variation is caused by the subsurface density distribution. Moreover, this method is appropriate to investigate the subsurface geological structures such as detecting faults, geological boundaries and mapping basins. Cavities are one of the features that can be mapped by this method. This structure can be a void or filled by a mass of sediments. Therefore, they usually have a lower density than the surrounding rock layer and therefore produce a negative gravity anomaly.

Newton's Law of Gravitation is the basic law that addresses gravity measurements:

$$F_g = G\frac{M_1 M_2}{R^2} \qquad (1)$$

where Fg is the gravitational force due to the two masses M_1 and M_2 a distance R apart, and G is the universal gravitational constant (6.672×10^{-11} Nm^2/kg^2).

From the equation above the gravity acceleration (g) due to a body of mass M,

$$g = \frac{GM}{R^2} \qquad (2)$$

Gravitational acceleration g is measured in Gal where 1 Gal = 1 cm/s^2 = 0.01 m/s^2. However, most targets of interest usually produce much smaller anomalies, especially in engineering and environmental studies. Therefore, these studies require surveys with micro-Gal resolution (1 micro-Gal=0.001 mGal). The term microgravity survey is used instead of gravity survey which is generally used for regional gravity surveys.

3.2 Gravity Surveying

3.2.1 Data Acquisition

In addition to the anomalous subsurface mass variation, which is the objective of the gravity survey, the gravity observations are the combined effects of all regional geological features plus instrumental effects, position on the Earth's surface, elevation and terrain effects plus planetary attraction. Theoretical formulae, geological data, and empirical observations are used to remove the extraneous effects of temporal and spatial variations in the gravity field which are unrelated to the subsurface geology. After removing all the unintended effects, the target features can be isolated (Hinze *et al*., 2013). Figure 7 is a flow-chart which illustrates the methodology of gravity interpretation.

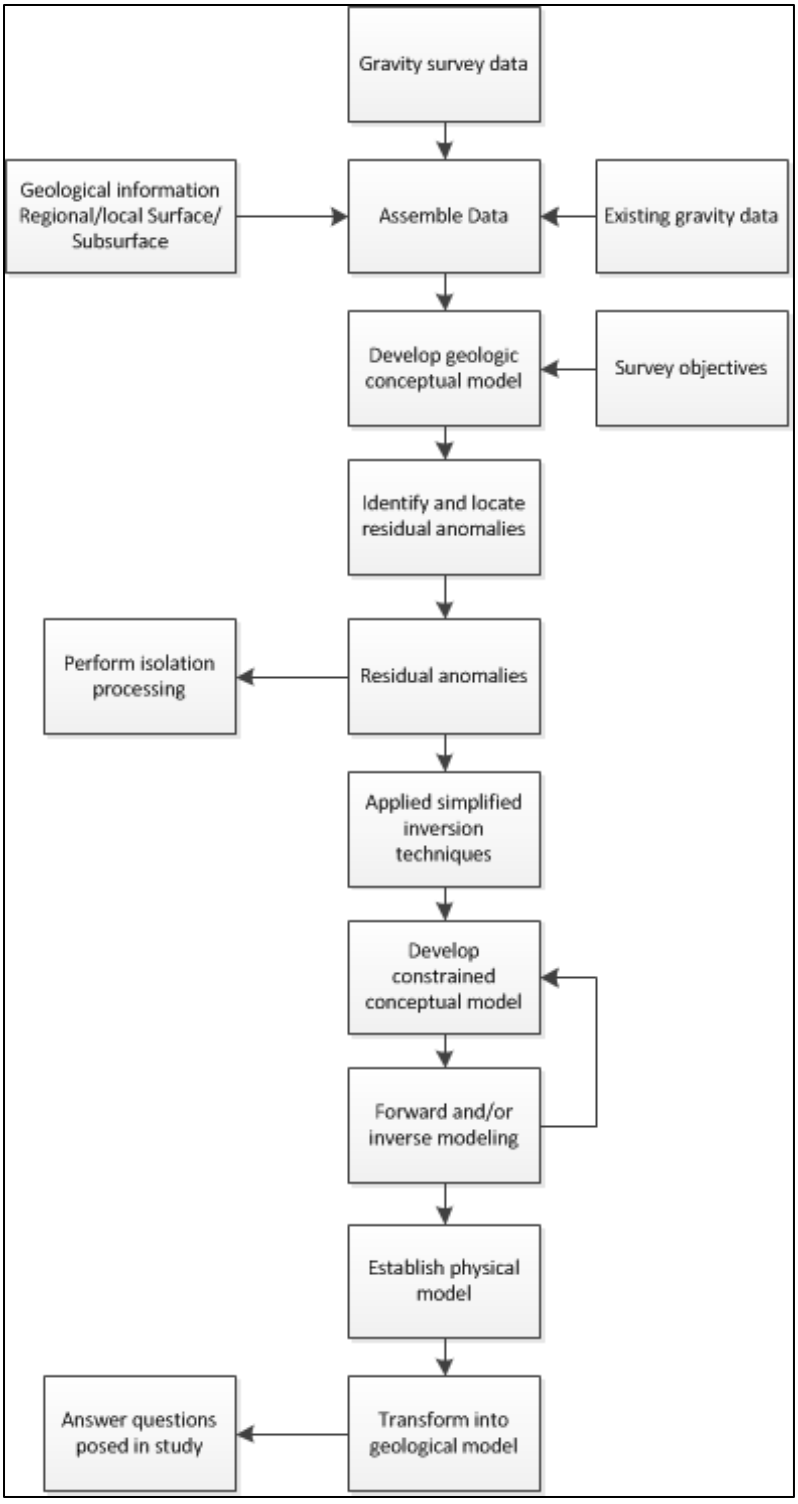

Figure 7 Flow-chart showing the components involved in the interpretation of gravity data and their relationship (Hinze et al., 2013)

To observe the gravity field, it needs some basic tools for doing the measurements as shown in Figure 8. The main one is the gravimeter which measures relative gravity. The other tools are for position determination and leveling (Figure 9).

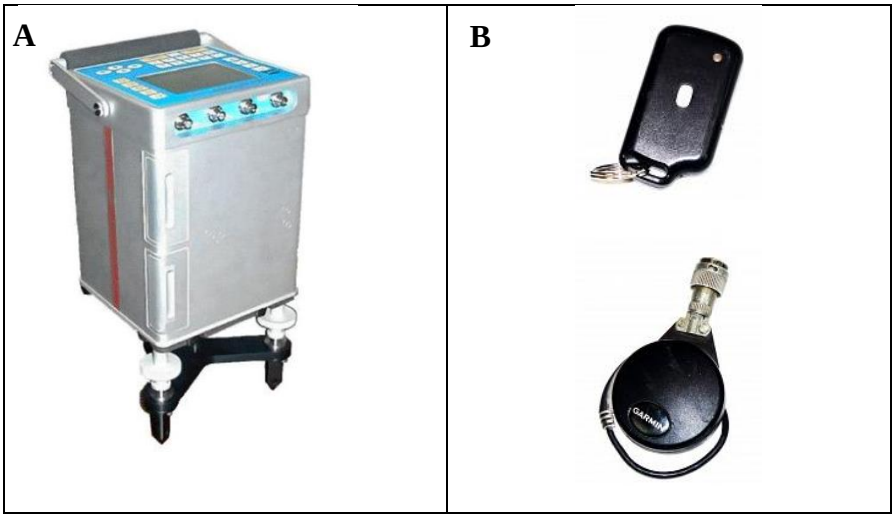

Figure 8 Instruments used in the data acquisition: a) Scintrex CG5 gravimeter on the tripod, b) remote & attached GPS

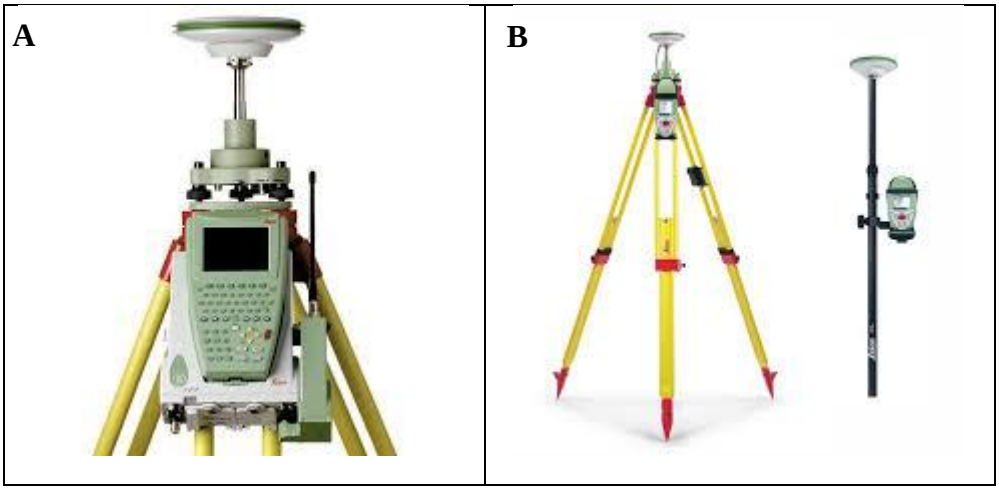

Figure 9 a) Differential GPS Leica1200+ GPS base and b) rover instrument

3.2.2 Data Reduction

The raw gravity data need to be corrected for instrument drift and earth tide effect. The latter is the gravitational attraction due to the Sun and the Moon, which varies systematically throughout each day. After correction, we obtain the observed gravity value ($\boldsymbol{g_{obs}}$).

1. Drift Correction

The instrument drift correction is largely due to stress relaxation in the elastic system due to the stretching of the quartz fiber in the gravity-meter. After an initial stabilization period, it can be considered a linear function of time, see Figure 10.

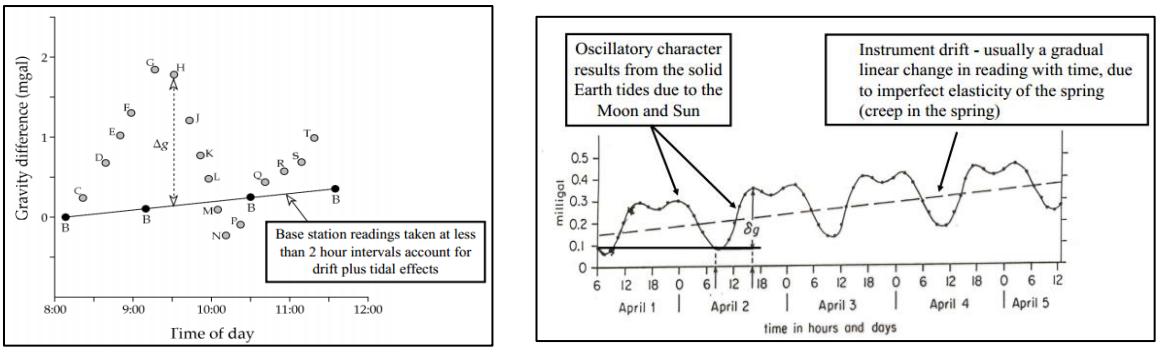

Figure 10 Left: gravity reading from the survey stations (grey dot) should be corrected by total of drift and tide correction reading from the base station (black dot) to get the observed gravity value. Right: Tide and drift correction in a graph showing the variation of corrections in terms of time (Greenhalgh & Marescot, 2013).

2. Tide Correction

The gravitational effect of the sun and the moon not only produce a changing shape of ocean surface or fluid tides but also distort the shape of the earth (Telford et al., 1990). As its effect is much less for rocks than for water, the amount of external forces is much

less than the ocean distortion. The ocean tides have amplitudes in the range of meters, but the solid earth tides are in the range of centimeters. The theoretical gravity tide correction is calculated using the venerable formulas of (Telford et al., 1990).

To get the value of observed gravity ($\boldsymbol{g_{obs}}$), the gravity reading at the survey station should be corrected by the amount of tide and drift correction that is done in the base station periodically.

3. Complete Bouguer Anomaly

The complete Bouguer Anomaly (CBA) is the gravity anomaly after application of a series of corrections to consider the known variations in the field, such as due to latitude, elevation etc. It can be formulated as follows (Hinze et al., 2013)

$$CBA = g_{obs} - g_{\theta} + FAC - BC + T \qquad (3)$$

$\boldsymbol{g_{obs}}$ is the observed gravity reading after earth tide and drift corrections obtained by repeated measurements at a fixed base station. The Bouguer anomaly basically measures how gravity changes from one station to another.

From the equation (3), $\boldsymbol{g_{obs}}$ must be corrected by several factors, was explained below:

a. Latitude correction ($\boldsymbol{g_{\theta}}$)

Gravity varies as a function of latitude on the surface of the reference ellipsoid. A Chebychev approximation is used to measure the effect with a maximum error of 0.004 mGal (Telford et al., 1990),

$$g = 978.03185\ (1 + 0.005278895\ \sin^2\theta + 0.000023462 \sin^4\phi\ )\ \text{Gal} \qquad (4)$$

This formula assumes that the points are on the surface of the reference ellipsoid. There are free air and Bouguer effects need to be calculated if there is difference in elevation of the reference elevation.

In many exploration surveys covering limited areas, the station locations are not referenced to global latitude. As a result, the latitudinal effects on the stations of the survey are referenced to a single station (usually the base station) and determined by assuming a linear gradient of the normal gravity as a function of north–south distance (distance is not far from extremities of area). This gradient in mGal/m can be determined by differentiating above equation with respect to north-south distance $\boldsymbol{x_{N-S}}$ so that

$$\frac{\partial g_\theta}{\partial g_{x_{N-S}}} = 0.8144 \times 10^{-3} \sin(2\theta) \qquad (5)$$

assuming a mean radius for the Earth of 6,367.45 km and the spherical coordinate.

b. Free air correction

The attraction of the Earth can be considered to be the same if its mass were concentrated at its center. So, the further out from the center of the earth the less the gravity. All stations must be corrected for this effect relative to a datum level (eg: sea level). The elevation difference of the gravity-meter from the datum must be determined. The correction will be calculated as:

$$g_0 - g_{obs} \cong \Delta g \cong -2\frac{g_0}{R} \qquad (6)$$

$$\text{FAC} = 0.3085\, h \qquad (7)$$

where g_0 represent the attraction of gravity on the geoid and the g_{obs} is the observed gravity at the station, while h (in meter unit) represents the difference in elevation of g_0 and g_{obs}.

c. Bouguer correction

This correction is dependent on the slab of rock which lies between the datum level and the h station elevation (in meter unit). It will have the opposite sign to the free air correction. The correction depends on the ρ average density (in g/cm^3 unit) of the material between the station and datum according to the formula:

$$BC = 0.04185\,\rho\,h \qquad (8)$$

Densities of rocks ρ as shown in Figure 11 below are determined by certain factors such as rock type, mineralogy, degree of compaction, etc. The Bouguer density used for the correction in this study is 2.3 g/cm^3 because the residual anomaly lies in the Rus and UER Formation which has average density of 2.3 g/cm^3 (Abdullatif, 2010). The laboratory test is measured from the outcrop samples on each formations has been done by Abdullatif (2010) to get the precise density of the formation, shown on Table 2.

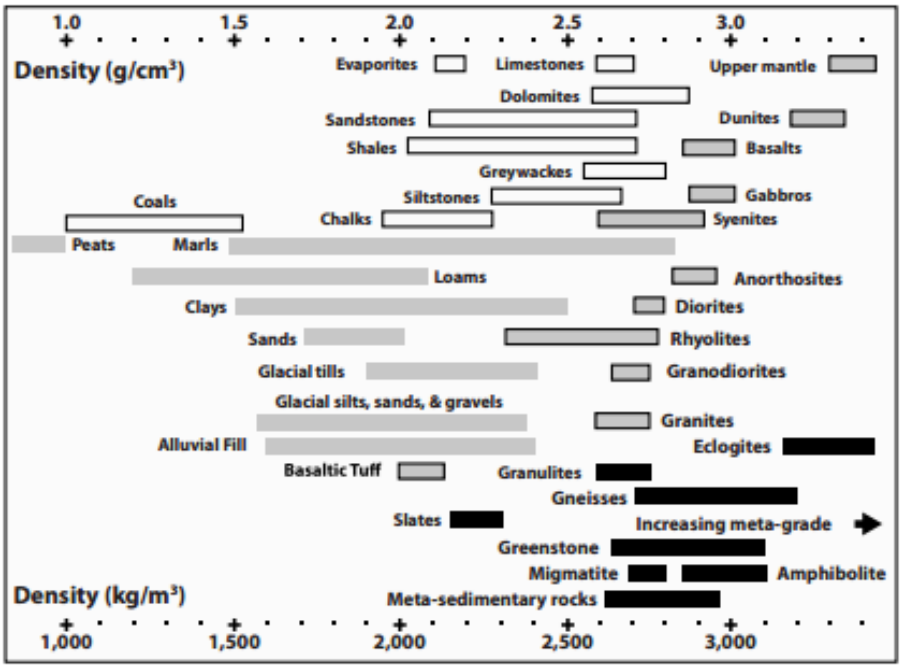

Figure 11 Natural densities (saturated bulk density) of igneous, metamorphic, and sedimentary rock types (after Hinze et al., 2013).

Table 2 Summary of laboratory testing result for the Lower and Middle Rus Formation carbonates studied in outcrops (after Abdullatif, 2010).

Formation	Lower Rus			Middle Rus		
Geomechanical Parameter	Average	Minimum	Maximum	Average	Minimum	Maximum
Point load Strength I Index (Mpa)	5.20	0.56	24.3	6.90	0.5	13.21
Uniaxial Compressive Strength (Mpa)	100.10	12.12	506	152.92	15	288.86
Porosity (%)	10.39	5	16	8.83	5	14
Dry Density (g /cm^3)	2.28	1.7	2.52	2.56	2.14	2.86
Permeability (md)	84.57	5.08	316.27	58.35	2.98	278.72
Young's Modulus *E* (Mpa)	42748	4047	183236	80322	13879	207503
Poisson's Ratio	0.22	0.10	0.38	0.21	0.10	0.35
Schmidt Hammer	33	12	54	50	36	60

d. Terrain correction

This correction is added to compensate for the difference between the actual surface topography and assuming flat infinite slab as in the Bouguer correction. The terrain correction is always positive and requires a detailed elevation map of the entire area. It can often be ignored when topography is gentle. It will remove the effect of hills by adding its upward attraction at the station and compensates for valleys by adding the attraction it would exert at the station if filled with rock.

The correction is extremely tedious and usually done using Hammer charts as shown in Figure 12, which require the average elevation in each compartment and the known distance to each station.

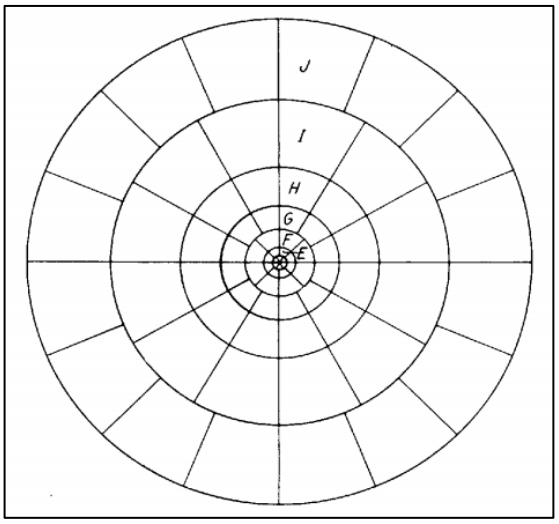

Figure 12 Hammer chart to measure terrain correction on gravity survey (Telford et al., 1990)

The usual procedure is to divide the area into compartments and compare the elevation within each compartment with the station elevation (Telford et al., 1990). This can be

done by outlining the compartments on transparent sheet as shown on Figure 10 overlying a topographic map. Based on its radius this correction is divided into inner zone r_1 and outer zone r_2, and n indicates the total zone.

$$T = 0.04191\frac{\rho}{n}\left(r_2 - r_1 + \sqrt{{r_1}^2 + z^2} - \sqrt{{r_2}^2 + z^2}\right) \qquad (9)$$

After all the data reduction done, the Bouguer anomaly can predict the density distribution in the subsurface as shown in the Figure 13.

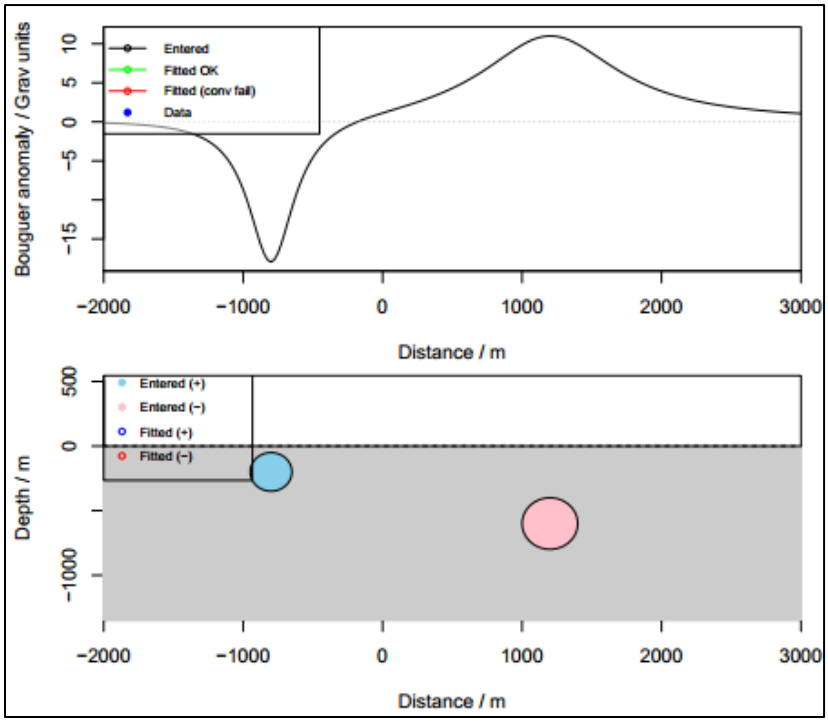

Figure 13 The basic idea of gravity surveying. The lower panel shows a cross-section through the ground. The red circle (right) represent denser region and blue circle (left) indicates less dense region. The above panel shows the Bouguer anomaly that measured at the surface (Pumphrey, 2014).

3.2.3 Station Elevation and Position Determination

Observed gravity is affected by differences in the rock density on the subsurface but it is also affected by the elevation and ground surface. Hence, to see slight differences in density contrast, the elevation measurement must be done in an accurate way. For small scale surveys, for example 1 km distance, the heights need to be measured to an accuracy of $\pm$1 cm. To get this accuracy the altitudes must be surveyed in the traditional manner using theodolite and levelling stave or we can apply the recent technology of differential GPS.

By using differential GPS methods, we can get up to $\pm$5-10 mm accuracy by using static method. Due to the limited time of study, I use the kinematic techniques to get the efficient elevation data. Figure 10 illustrate how one concept of altitude measurement using real time kinematic (RTK) differential GPS to get accuracy of $\pm$1 cm.

In this study, the methods were applied using Leica 1200+ GPS instrument to obtain the accurate position and elevation of the station (See Appendix B).

3.3 Regional Residual Anomaly Separation

The Bouguer gravity data are presented in either map or profile form for analysis and interpretation, depending on the objectives and coverage of the survey and the attributes of the observed anomalies. These data are the summation of all anomaly sources regardless of their depth or distance from the observation point and any errors in the processing of the data (Hinze et al., 2013).

The gravity anomaly (A) resulting from the reduction of observed gravity data thus consists of three separate components; the residual anomaly (Ar) which is the target of the survey, the regional anomaly (AR) which contains the larger spatial wavelength components of the gravity related to deeper geological features, and the noise (N) which is spatially smaller than the residual. That is,

$$A = Ar + AR + N \qquad (10)$$

Noise may originate from the instrumentation system and the observer, the reduction and processing of data, and geophysical interpretation. These effects can be minimized by adding together a series of observations in which measurements include a coherent signal with random errors or signals superimposed. This procedure, commonly referred to as stacking, attenuates the random errors or noise by a factor of $\sqrt{n}$ with respect to the coherent signal, where n is the number of elements in the series. This procedure is used widely in geophysics to minimize random errors or noise (Hinze et al., 2013).

Generally, the noise, N, is negligible and disregarded, in which case the anomaly of interest, the residual gravity anomaly, is simply

$$Ar = A - AR \qquad (11)$$

In actual practice, the subtraction is directly performed graphically or arithmetically using polynomial filtering, spectral analysis, or indirectly performed by emphasizing the residual anomaly at the expense of the regional anomaly (Hinze et al., 2013).

Elimination of the regional gravity anomaly from the observed anomaly is a critical step in the identification and analysis of gravity anomalies. There are some methods to do this

separation such. Improper definition of AR can cause errors in the attributes of the residual anomaly, its amplitude, gradients, trend, etc.

3.3.1 Spectral Analysis

Spectral analysis is a process to identify the different spatial wavelengths (or wavenumbers) present in the Bouguer anomaly map, which in turn relate to depth information. The residual field can be separated from the regional field by a process of wavenumber filtering to retain only the large wavenumbers or small wavelength features. Besides that, the result from this analysis will be used for the window length in the moving average process. Spectral analysis uses the Fourier analysis mathematical method that is carried out on the selected profile line on the chosen gravity anomaly (Elkins, 1951)

The one-dimensional Fourier transform is used to transform any function from the spatial (or time) domain into the wavenumber (or frequency) domain. This transform is useful in geophysics because of the ease of convolving functions and filtering data in the wavenumber domain. The two-dimensional Fourier transform is equally useful for transforming and filtering map data, for example the gravity field as a function of distance east and north. The 2D forward and inverse Fourier transform is:

$$F(k_x, k_y) = \int_{-\sim}^{\sim} \int_{-\sim}^{\sim} f(x,y)\, e^{-i2\pi(k_x x + k_y y)} dx dy \qquad (12)$$

$$f(x,y) = \left(\frac{1}{2\pi}\right)^2 \int_{-\sim}^{\sim} \int_{-\sim}^{\sim} F(k_x, k_y)\, e^{-i2\pi(k_x x + k_y y)} dk_x dk_y \qquad (13)$$

where k_x and k_y refer to the 2D wavenumber in the x and y directions. $f(x, y)$ is the function of gravity field as function of map coordinate x, y and i is the complex conjugate. A 2D power spectrum shows the wavenumbers (or their reciprocals, wavelengths) wavelengths at which signals are most prominent on the map.

3.4 Second Vertical Derivative

The second vertical derivative (SVD) enhances near-surface effects at the expense of deeper anomalies. Second vertical derivatives are a measure of curvature of the Bouguer anomaly, and large curvatures are associated with shallow anomalies.

The second vertical derivatives can be obtained from the horizontal derivatives because the gravity field satisfies Laplace's equation

$$\nabla^2 g = \frac{\partial^2 g}{dx^2} + \frac{\partial^2 g}{dy^2} + \frac{\partial^2 g}{dz^2} = 0 \qquad (14)$$

$$\frac{\partial^2 g}{dz^2} = -\left(\frac{\partial^2 g}{dx^2} + \frac{\partial^2 g}{dy^2}\right) \qquad (15)$$

According to this equation, the second derivative of the vertical component of the gravity field outside the sources can be calculated by applying the operator O to $g(x, y)$ (Buttkus, 2000),

$$O = -\left(\frac{\partial^2}{dx^2} + \frac{\partial^2}{dy^2}\right) \qquad (16)$$

$$\frac{\partial^2}{dz^2} g(x, y) = -\left(\frac{\partial^2}{dx^2} + \frac{\partial^2}{dy^2}\right) g(x, y) \qquad (17)$$

Application of the operator O to gravity field data $g(x, y)$ with the 2D wavenumber spectrum $G(k_x, k_y)$ yields

$$g(x,y) = O\{g(x,y)\} = -\left(\frac{\partial^2}{dx^2} + \frac{\partial^2}{dy^2}\right) \int_{-\sim}^{\sim} \int_{-\sim}^{\sim} G(k_x, k_y)\, e^{i2\pi(k_x x + k_y y)} dk_x dk_y$$

$$= \int_{-\sim}^{\sim} \int_{-\sim}^{\sim} 4\pi^2 \left(k_x{}^2 + k_y{}^2\right) G(k_x, k_y) e^{i2\pi(k_x x + k_y y)} dk_x dk_y \qquad (18)$$

Or in the wavenumber domain:

$$V(k_x, k_y) = 4\pi^2 \left(k_x{}^2 + k_y{}^2\right) G(k_x, k_y) \qquad (19)$$

The second derivative to the vertical component of the gravity field thus corresponds to a 2D filter with wavenumber response function

$$H(k_x, k_y) = 4\pi^2 \left(k_x{}^2 + k_y{}^2\right) \qquad (20)$$

The wavenumber response function $H(k_x, k_y)$ is multiplied by $G(k_x, k_y)$ to get vertical derivative in wavenumber domain $V(k_x, k_y)$. The resulting function then back transformed into the spatial domain $v(x, y)$. The averaging procedures is needed to avoid the amplification of measurement errors due to this method.

The purpose of second vertical derivative method to the gravity data is to identify the shallow structures, fault type and to estimate the fault dipping. The criteria used for determining whether a fault is normal or reverse are as follows (Reynolds, 1997):

$$\left|\frac{d^2 g}{dz^2}_{max}\right| > \left|\frac{d^2 g}{dz^2}_{min}\right| \text{ for normal faults} \qquad (21)$$

$$\left|\frac{d^2 g}{dz^2}_{max}\right| < \left|\frac{d^2 g}{dz^2}_{min}\right| \text{ for thrust faults} \qquad (22)$$

CHAPTER 4

SYNTHETIC STRUCTURAL DIP GENERATION

This chapter explains the synthetic fault model to estimate the fault dip in the study area. The combined analysis between the synthetic model and the second vertical derivative value can predict the fault dip of the structure.

4.1 Synthetic Model Generation

From the analysis of second vertical derivative value (SVD), the fault dip can be modelled based on the empirical formulation. Therefore, the fault model is built with various dip angle from 10 to 90 degrees. Assuming the minimum thickness of Umm Er Radhuma Formation on this study is 100 meters (Alsharhan et al., 2001) and 0.25 g/cm^3 contrast density with the top in 20 meters depth and bottom in 100 meters depth. It is based on the estimation of the thickness of Rus Formations and depth of Umm Er Radhuma (UER) Formation (Al-Fahmi et al., 2014; Weijermars, 1999).

To model the background subsurface layer, the average density is obtained by the mean of measured density of the layers on the study area. The density for Lower Rus Formation is 2.28 g/cm^3 or the average density value from the laboratory test and for Middle Rus Formation is 2.14 g/cm^3 is the minimum density value from the laboratory test. All these tests has been done to 49 outcrop samples on the study area (Abdullatif, 2010). The density value for Umm Er Radhuma (UER) is 2.56 g/cm^3 from the average density for

dolomitic limestone (Telford et al., 1990). The difference between the Umm Er Radhuma Formation and the average background density is 0.25 g/cm^3 is used to model the synthetic fault model for the dip estimation.

Table 3 Background density on the study area for synthetic model generation

Formation	Density (g/cm^3)
Middle Rus	2.14
Lower Rus	2.28
Umm Er Radhuma	2.56
Average	2.31

See Table 3 for the explanation of subsurface density assumption for the modeling on the Figure 12.

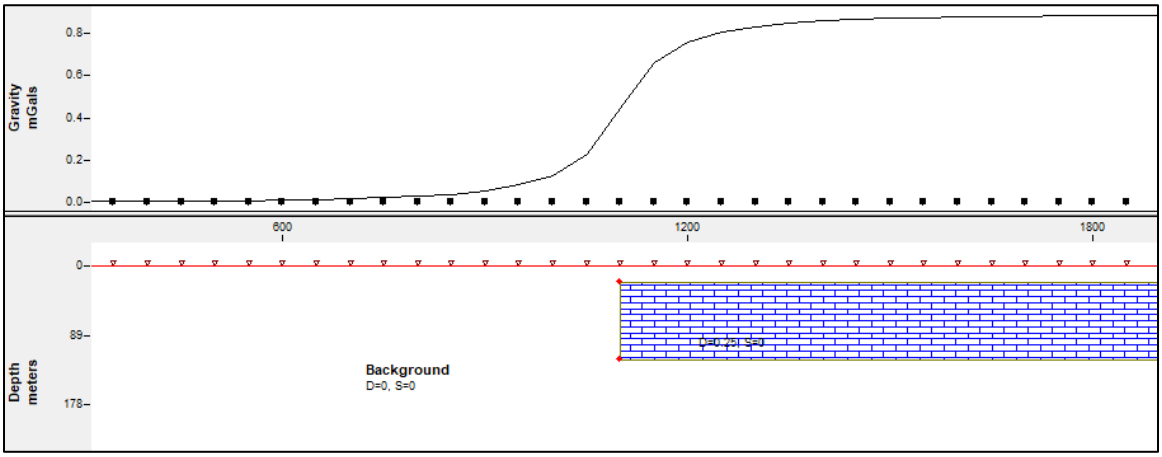

Figure 14 Synthetic fault model in semi-infinite slab with fault dip 90º, 100 meters thickness and 0.25 g/cm^3 contrast density

On the Figure 14, the synthetic model was built based on the geological features on the study area. It is built to get the idea of fault dip variations to the Bouguer anomaly value. The density contrast is plotted as 0.25 g/cm^3 as the UER Formation consists of dolomitic

limestone which has average density of 2.56 g/cm^3 and the resulting background layer has average density 2.31 g/cm^3.

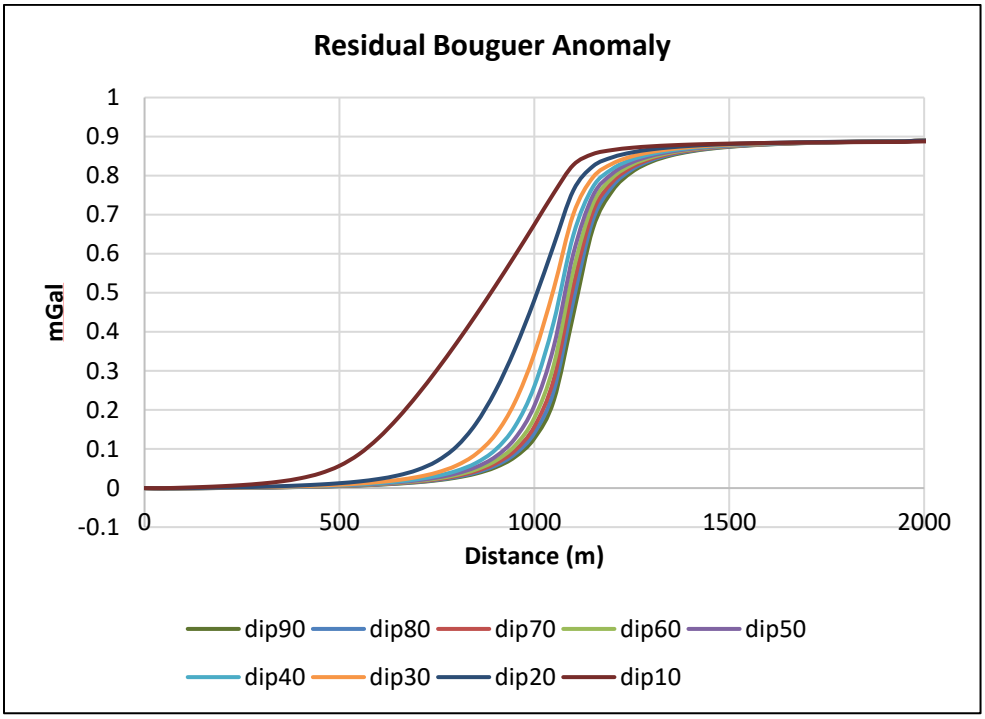

Figure 15 Residual complete Bouguer anomaly of the synthetic model

To get the idea of change in dip angle, the synthetic model is modified in to different fault dips from 10, 20, 30, to 90 degrees. These generated synthetic models is then forward modelled to get the complete Bouguer anomaly response on the Figure 15. After getting the residual anomaly profile, the second vertical derivatives profile must be generated as the method is effective to map the fault edge and near-surface structure.

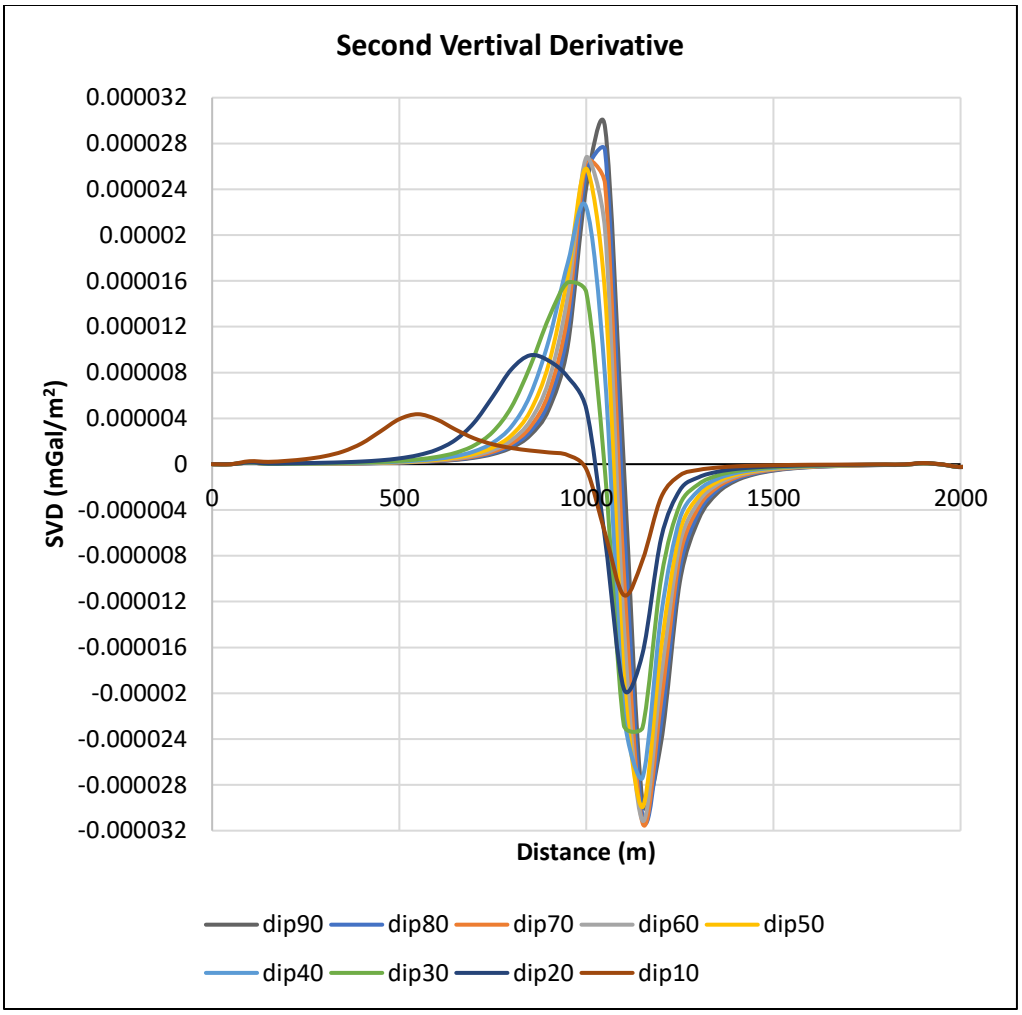

Figure 16 Second vertical derivative of the synthetic model

After getting the second vertical derivative profile shown in Figure 16, the normalized second vertical derivatives profile needs to be generated. This value will help us defined the fault dip in the study area and indirectly will define its fault type.

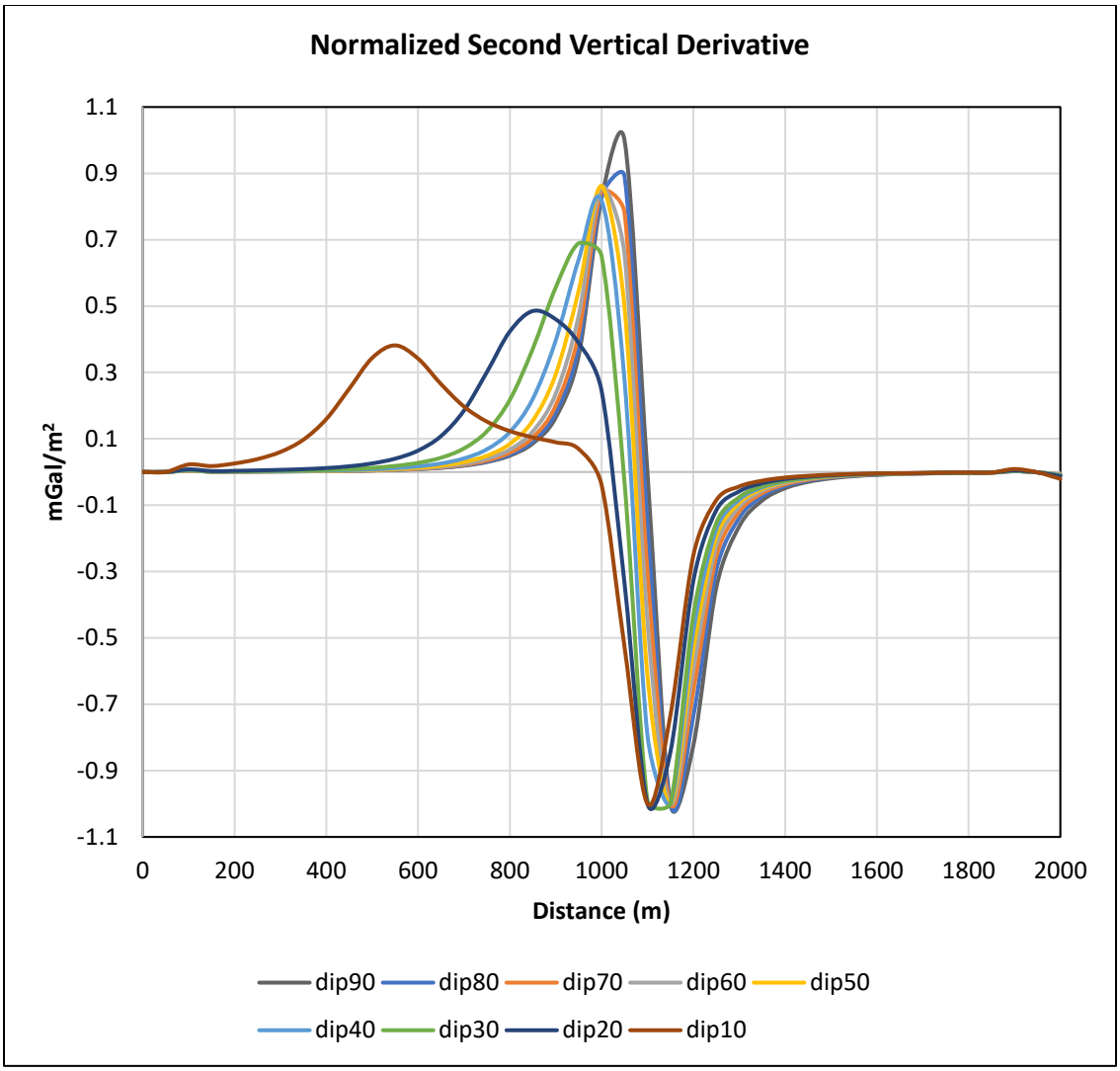

Figure 17 Normalized second vertical derivative for various fault dip angle

The normalized second vertical derivative profile in Figure 17 is generated by dividing the absolute maximum value of the second vertical derivative anomaly. This normalized profile is built to get the same scale of all dip model.

The value between the maximum and minimum value of each dip angle in this profile is called delta second vertical derivative (ΔSVD). The value is then plotted to get the relationship between the fault dip and ΔSVD.

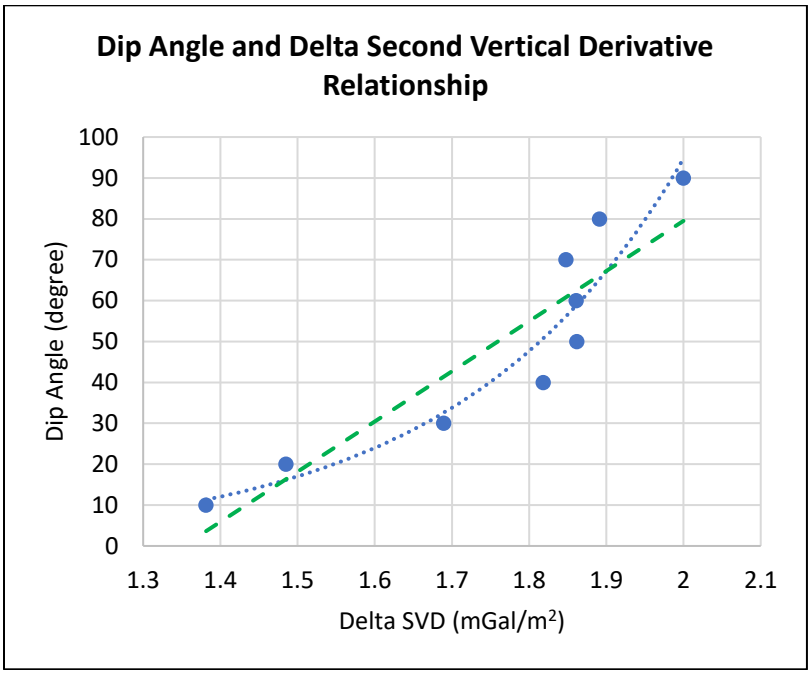

Figure 18 Synthetic fault dip angle relation with the delta second vertical derivative value

On Figure 18, the relation between the fault dip and the delta second vertical derivative map are plotted and is shown a good fit with the exponential model, refer to

Table 4. So, the model to predict the fault dip (y) from the delta second vertical derivative (x) is $y=0.0986e^{3.434x}$.

Table 4 Curve fitting model of the delta second vertical derivative synthetic model

Model	**Formula**	**R^2**
I. Exponential	$0.0986e^{3.43x}$	0.94
II. Linear	123x - 166	0.83

CHAPTER 5

RESULTS AND ANALYSIS

5.1 Bouguer Anomaly

The gravity data acquisition was carried out at 500 stations (see Figure 19) and then some data reduction explained in Chapter 2 was performed to correct the observed values and obtain the Bouguer anomaly (See Appendix A).

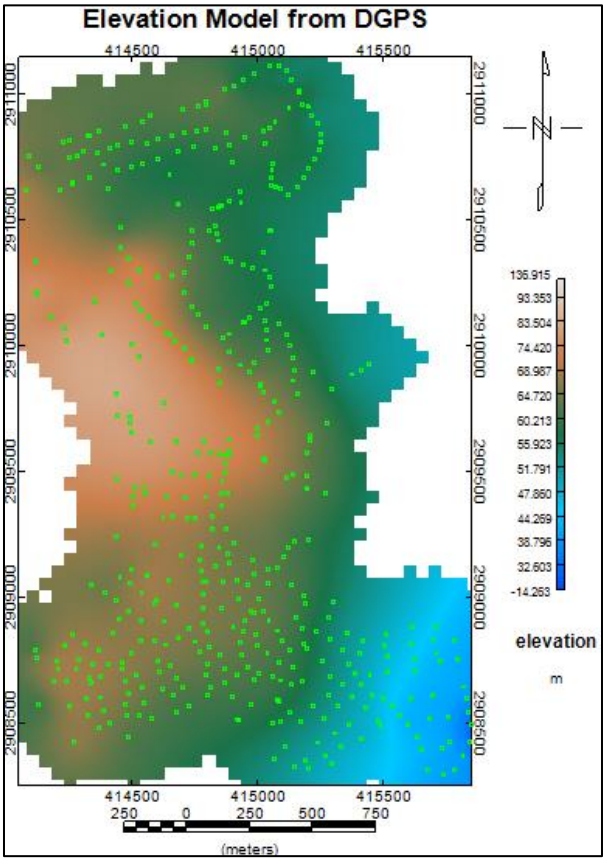

Figure 19 Map of gravity stations on the KFUPM Dammam Dome topography map. The green dots are stations position.

The Bouguer density used in generating the Bouguer anomaly profile is 2.31 g/cm^3, which is the average density determined by laboratory tests (Abdullatif, 2010). The interpolation of the model in this study is carried out using kriging and the resulting standard deviation was 1.57%.

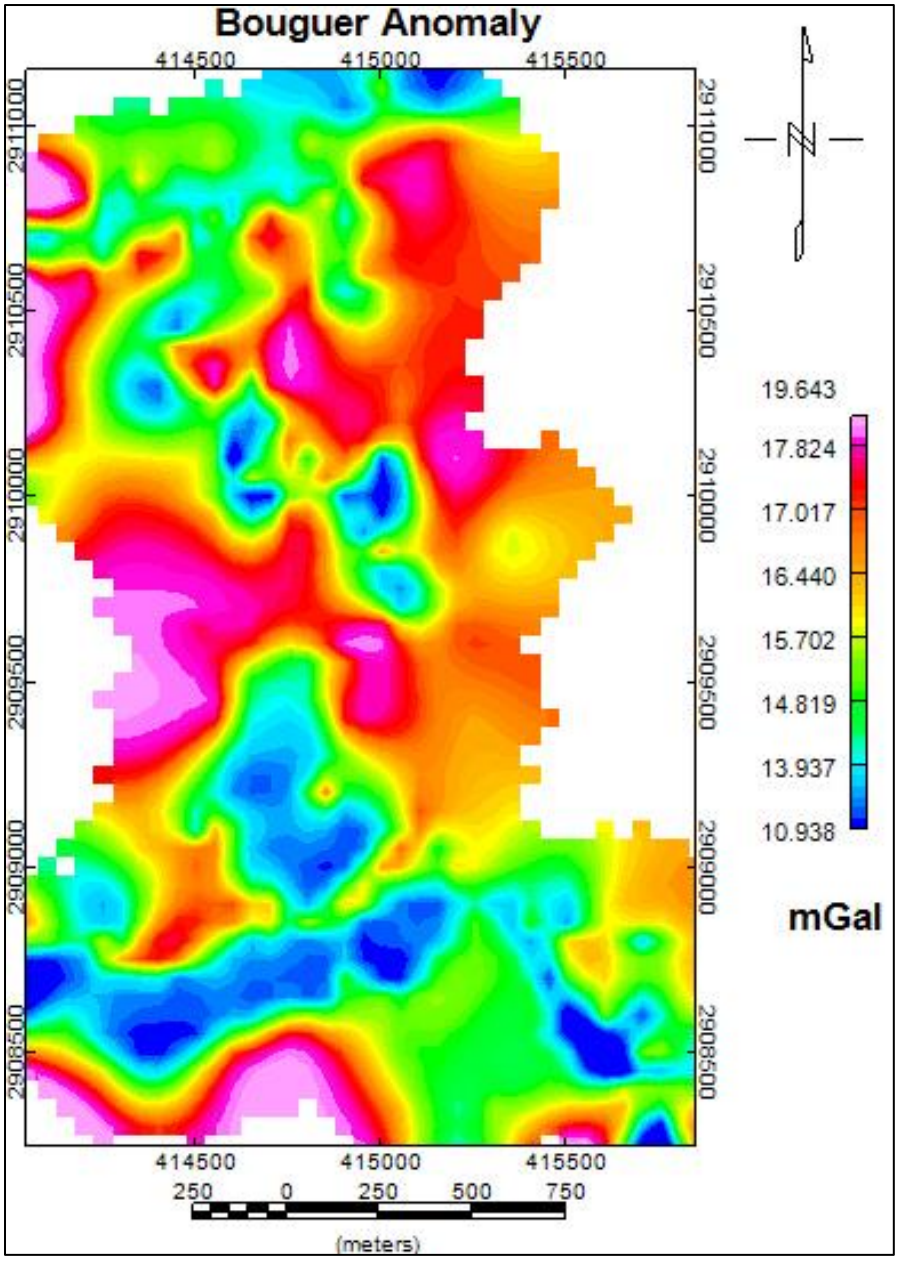

Figure 20 Bouguer anomaly map showing the variation of gravity anomalies in the area

5.2 Terrain Correction

The Bouguer anomaly map needs to be corrected for terrain effects to eliminate the effects of topography and nearby buildings on the campus. From the differential GPS measurement, the maximum accuracy of 2 centimeters in position and elevations were acquired (Appendix B). The terrain correction was measured using the Digital Elevation Model from SRTM satellite provided by USGS which has 1-arcsecond or 30 m resolution with 5 m vertical precision (Elkhrachy, 2016).

The digital elevation model (DEM) map on Figure 21 is used to be an elevation control for topography of the surrounding station. The scope area of DEM map is enlarged from the border of study area to accommodate the terrain correction of the outermost stations.

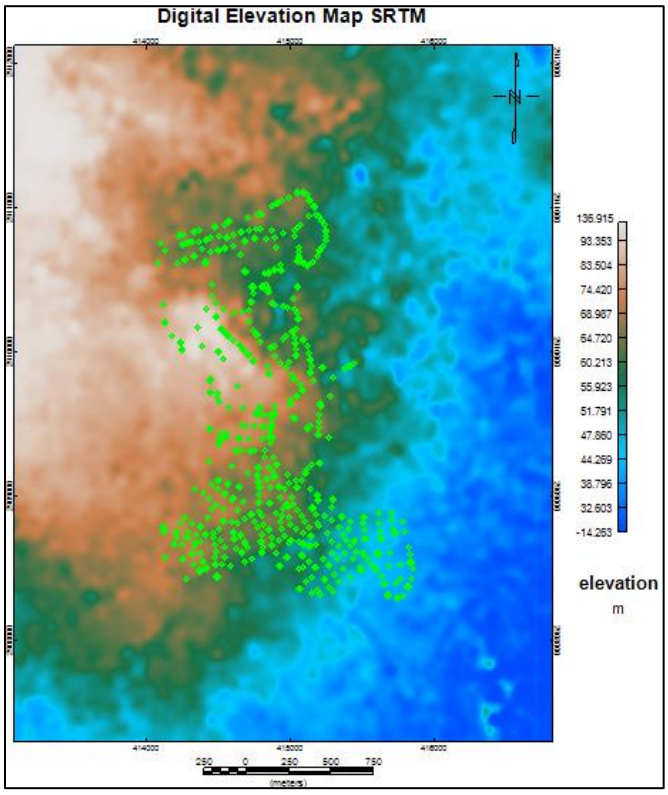

Figure 21 Digital Elevation Map from SRTM satellite

Each station was terrain corrected using Hammer method resulting a terrain correction map as shown on Figure 22. We can see from the figure that the largest value 0.062 mGal of the correction is on the western side of KFUPM which dominated by the building and the hills.

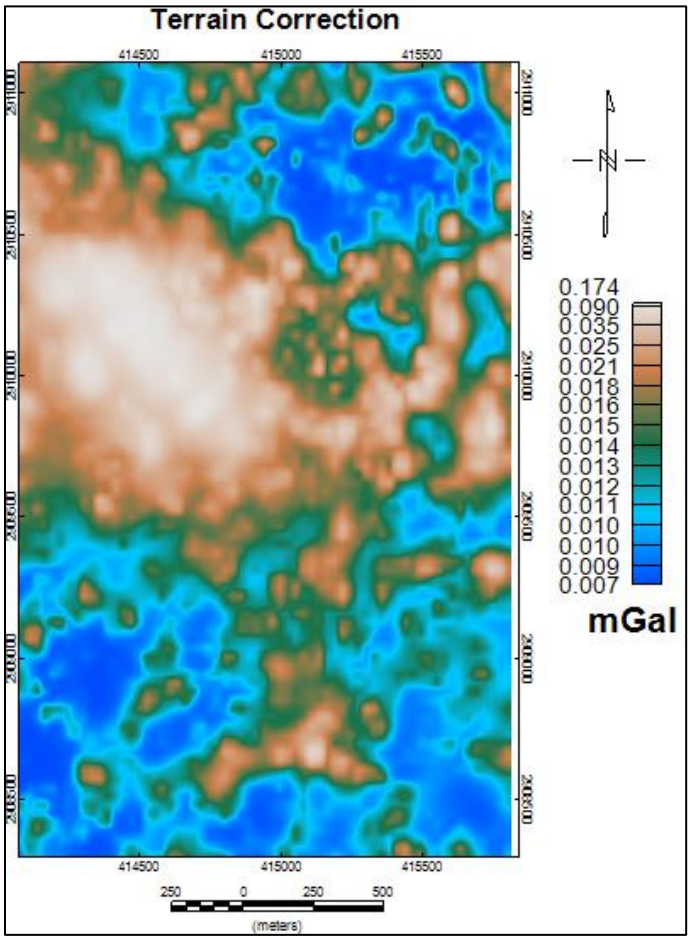

Figure 22 Terrain correction of the study area derived from the Hammer chart method using DEM map. The value range is from 0.009 to 0.062 mGal

After getting the correction of terrain, the Bouguer anomaly profile is added by the amount of terrain correction in each station. The result is called complete Bouguer Anomaly (CBA) as shown in Figure 23 below.

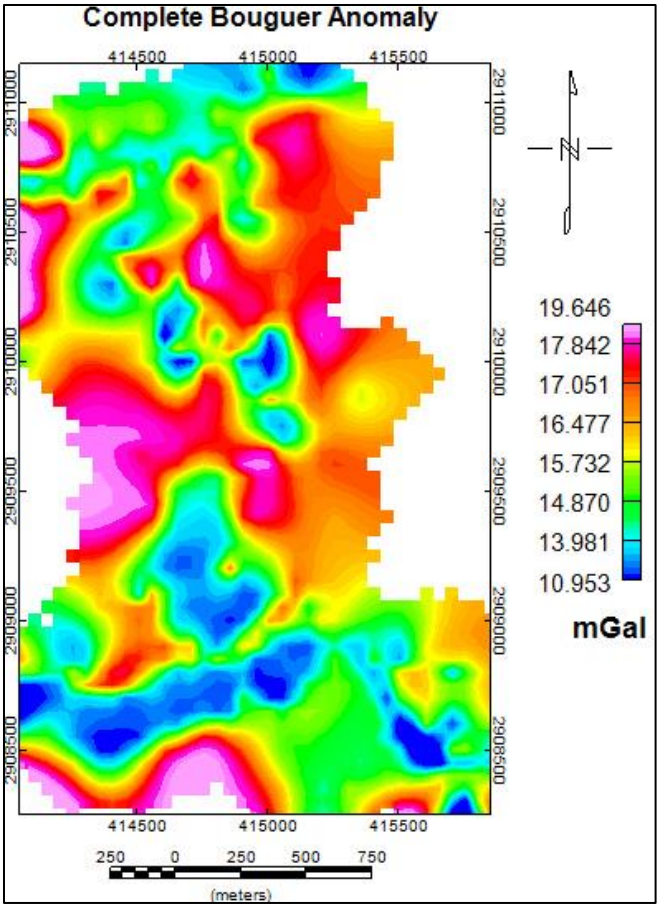

Figure 23 Complete Bouguer Anomaly map, which is the Bouguer anomaly corrected for the terrain effects (units in mGal)

5.3 Regional-Residual Separation

5.3.1 Two Dimensional FFT Filter Descriptions

The spatial frequencies of the filters used in separating the field are specified in terms of wavelengths (distance in meters). Cut-off rates determine the sharpness of the filter and the tapering of the energy spectrum. A high value of the cut-off has the effect of removing high frequencies but causes ringing on the edges of large amplitude changes.

The two-dimensional Fourier transform is equally useful for transforming and filtering map data, for example the gravity field as a function of distance east and north. The 2D forward Fourier transform is:

$$F(k_x, k_y) = \int_{-\sim}^{\sim} \int_{-\sim}^{\sim} f(x, y)\, e^{-i2\pi(k_x x + k_y y)} dx dy \qquad (23)$$

For extracting the regional anomaly, we filter as $R(k_x, k_y) = F(k_x, k_y)\, D(k_x, k_y)$, where *D* is the wavenumber low pass filter and subsequently return it to the spatial domain using the two-dimensional inverse Fourier transform:

$$r(x, y) = \left(\frac{1}{2\pi}\right)^2 \int_{-\sim}^{\sim} \int_{-\sim}^{\sim} R(k_x, k_y)\, e^{-i2\pi(k_x x + k_y y)} dk_x dk_y \qquad (24)$$

After getting $r(x, y), the$ regional anomaly in the spatial domain, we can derive the residual anomaly $t(x, y)$ by subtracting the regional from the total gravity anomaly as:

$$t(x, y) = f(x, y) - r(x, y) \qquad (25)$$

5.3.2 Data Preparation

To do this analysis, I used Oasis Montaj Geosoft® software. The pre-processing steps involve the preparation of the original spatial domain grid for filtering before the filters are applied. And then, the post-processing is aimed to return the filtered data to the same size and shape as the original grid and replacement of a regional trend.

Firstly, the nth-order trend or mean is removed from the gridded data to take our data and make the boundaries continuous for when we expand periodically (an implicit assumption of the discrete Fourier transform). And then the grid (which has now had the

trend removed from it) is expanded to prepare for the Fourier transform. The Fast Fourier Transform (FFT) in this study used the Cooley-Tukey algorithm.

The Cooley-Tukey algorithm requires grids to be of dimension 2 raised to an integer power n (i.e. 2, 4, 8, 16, 32, ...). So, if we have a grid which is 29 x 15 it would be expanded to 32 x 16 in order to meet the requirements of the FFT. Normally one has to pad with zeros out to higher n values to avoid wraparound effects with the FFT

Alternatively, the grid is then filled with dummies values using maximum entropy to fill the new expanded dimensions such that the grid becomes smoothly periodic. Since the grid is a single square/rectangular tile and copies of the tiles are laid out edge to edge, the grid pattern should smoothly match from tile to tile. The processing parameter shown on Table 5.

Table 5 Data preparation parameter for regional residual separation

Parameter	Value
Type of trend surface to remove	2^{nd} order
Trend based on	Edge points
% Expansion	10
Grid fill method	Maximum Entropy

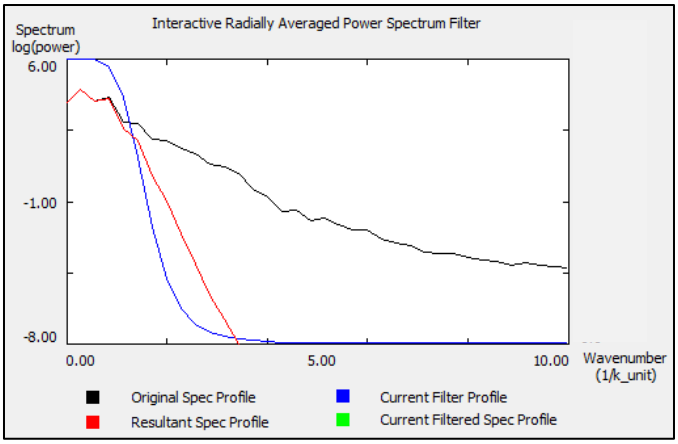

Figure 24 Radially averaged power spectrum. Butterworth filter is applied for regional anomaly

On Figure 24, the wavenumber unit is cycles per 1000 m while the filter axis on the right-hand side showing the fraction of spectrum value that is filtered from the whole spectrum. The blue line indicates its filter profile and its intersection with the whole spectrum (black line) obtained the resultant of spectrum profile for the regional anomaly (red line). The filter uses Butterworth filter to easily control the degree of filter roll off while leaving the central wavenumber fixed.

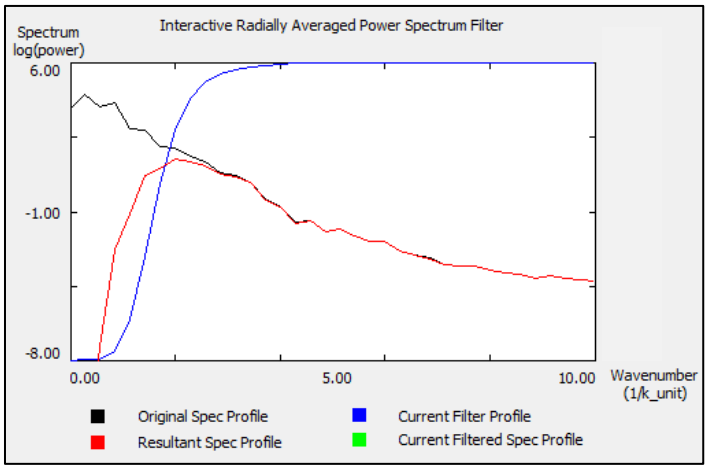

Figure 25 Radially averaged power spectrum. Butterworth filter is applied for residual anomaly

On Figure 25, the wavenumber unit is cycles per 1000 m while the filter axis on the right-hand side showing the fraction of spectrum value that is filtered from the whole spectrum. The blue line indicates its filter profile and its multiplication with the whole spectrum (black line) yields the resultant spectrum for the residual anomaly (red line). The filter used is a Butterworth filter to easily control the degree of filter roll off while leaving the central wavenumber flat.

5.3.3 Separation Result

Figure 26 indicates the regional anomaly on the study area. The anomaly value represents the deeper source density. While the residual anomaly on the Figure 27 represents the shallower anomaly. This residual anomaly will be used on the next analysis.

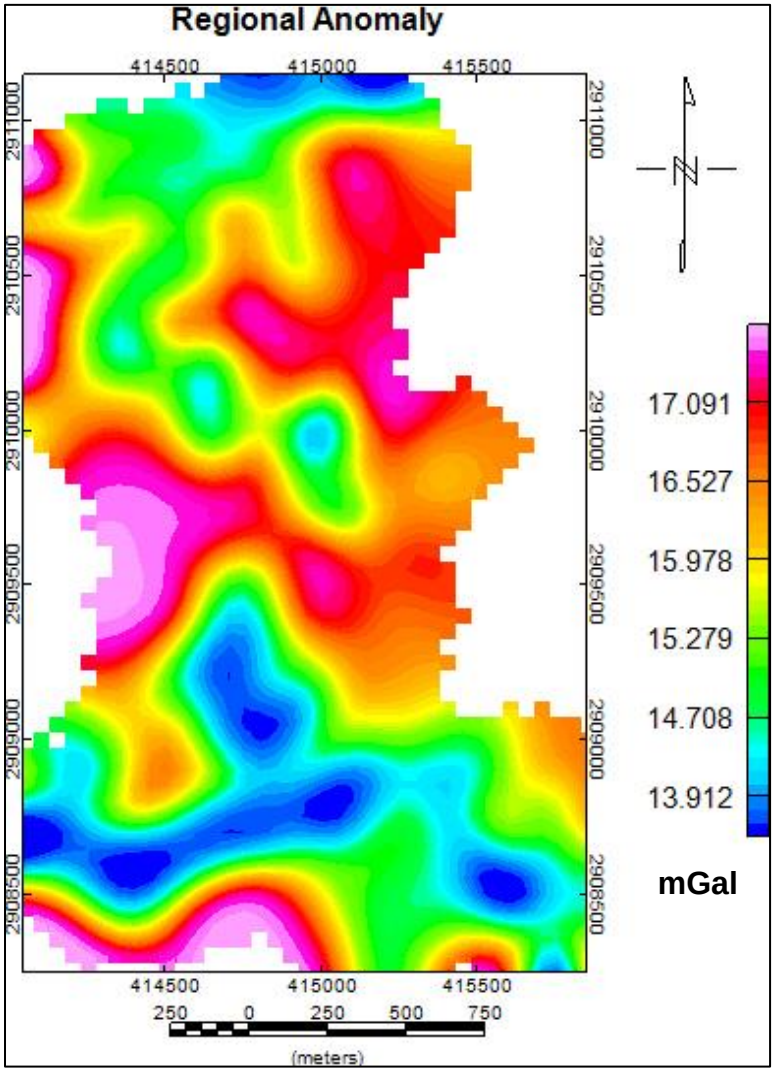

Figure 26 Regional anomaly

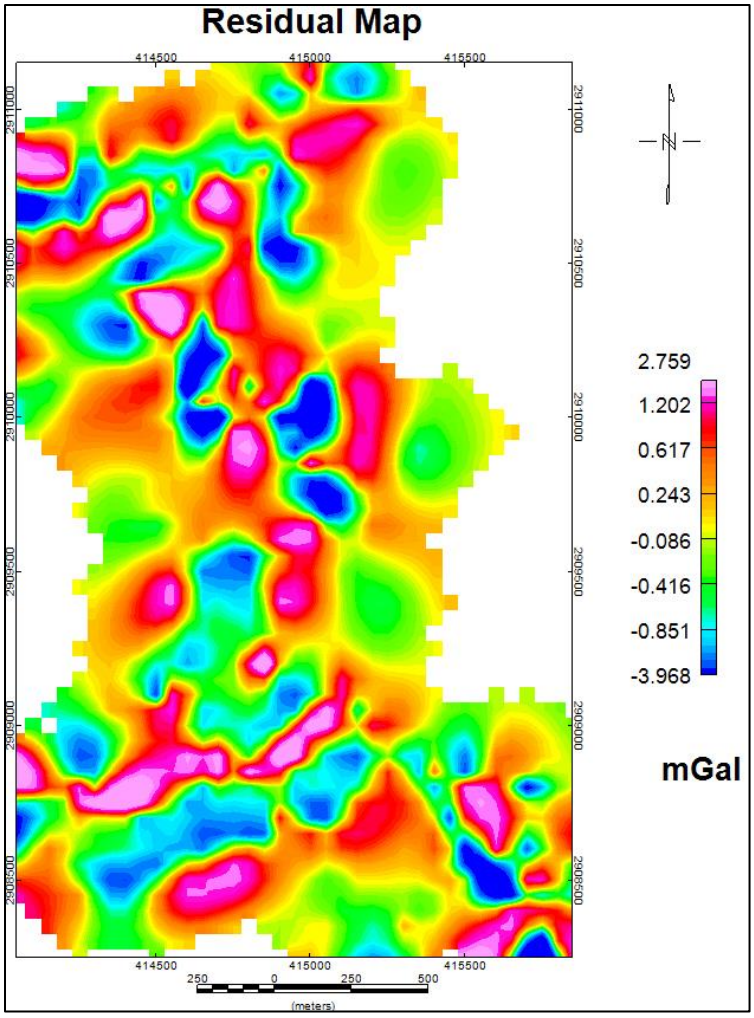

Figure 27 Residual anomaly from Butterworth filter

5.4 Second Vertical Derivatives

The second vertical derivative method of analytical regional – residual separation was applied to the available reduced data of the study area to calculate the second vertical derivative using Fast Fourier Transform (FFT). The complete Bouguer anomaly map was transformed the 2D spectral domain (Figure 28) and then filtered with second vertical derivates. Finally, it was back transformed into the spatial domain (Figure 29).

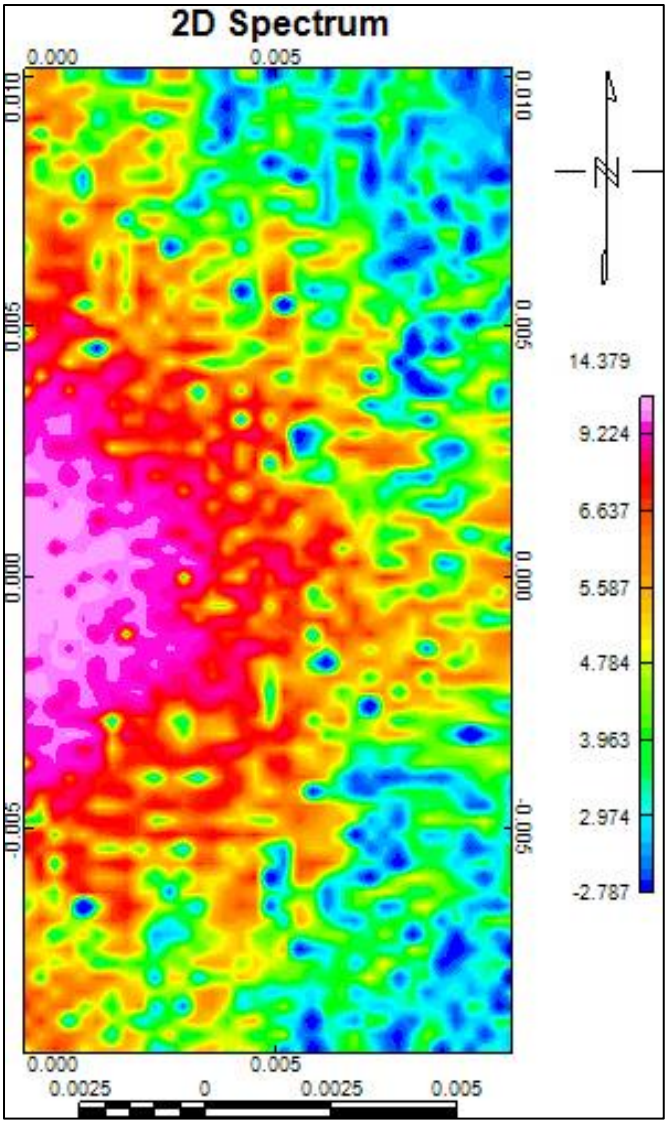

Figure 28 Two-dimension power spectrum

This filter will enhance the structure on the study area especially for near-surface fracture. As the fault or fractures can be defined by the rapid change of second vertical derivatives curve, the line shown on Figure 25 was delineated to get the idea of fault types on each structure.

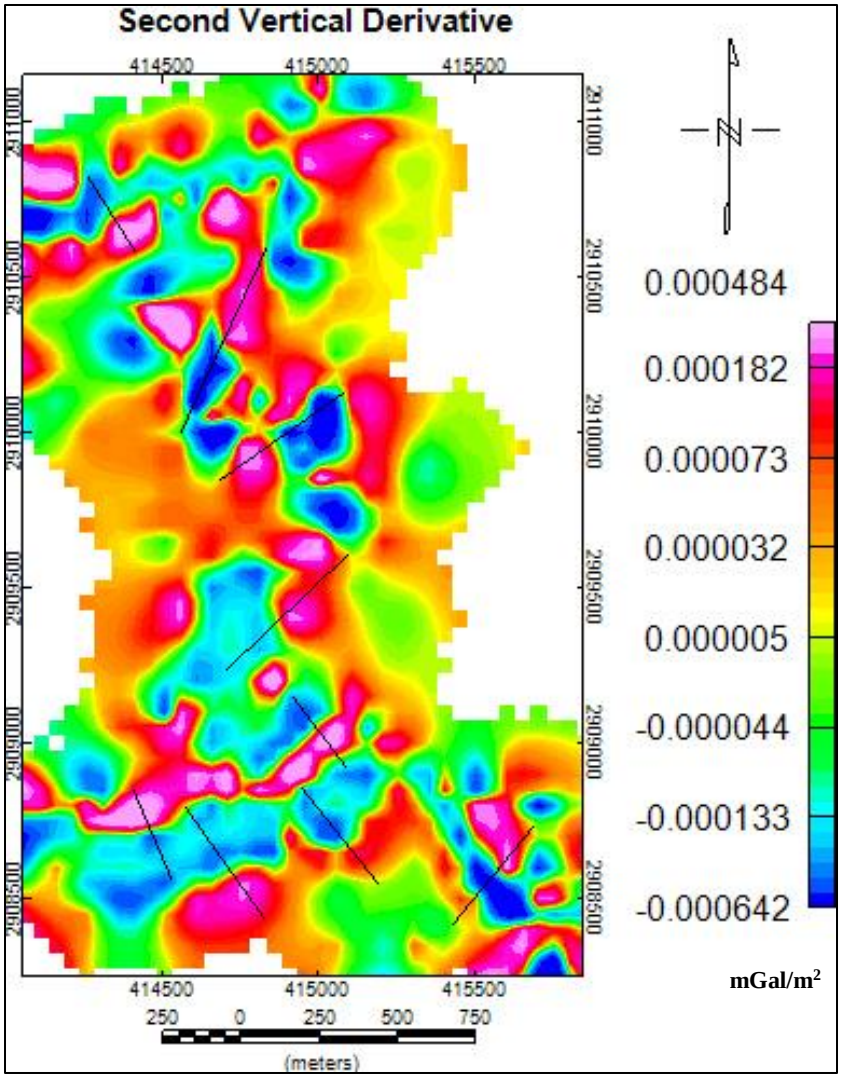

Figure 29 Second vertical derivative maps with the interpreted fault lines

5.5 Fault Type Determination

The analysis of second vertical derivative (SVD) is needed to confirm the vicinity of near-surface structure especially for fault structure. Using SVD, the structure is identified by its rapid change/contrast in the value. There is reduced probability of fault structures in the slight change values of the SVD.

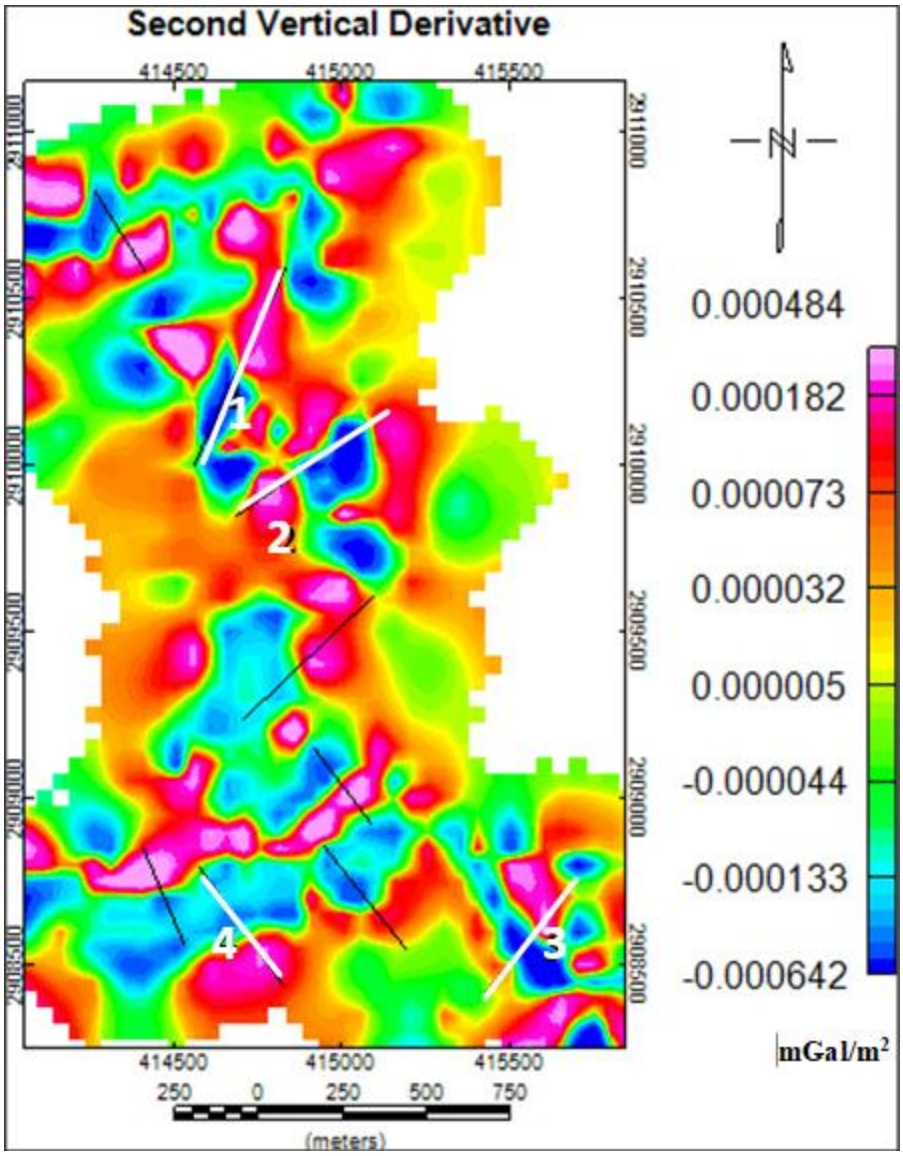

Figure 30 The interpreted fault lines crossing perpendicularly with the fault structure illuminated by SVD

Figure 30 shows the SVD analysis on the study area. The interpreted fault lies perpendicular with the black lines. The structure of Dammam Dome is affected by compressional regime of Hormuz Salt. The growth on this salt diapirism has begun in Jurassic and Cretaceous time in response to tectonic extension that took place within Arabian plate (Al-Fahmi et al., 2014). The compressional regime from the Hormuz Salt

caused the radial or concentric structure on the above formation and can be indicated by NW & NE structure orientation (Hariri, 2013).

Based on SVD calculation, the value of absolute maxima curve is greater than its minimum absolute curve on the normal fault structure.

$$\left|\frac{d^2g}{dz^2}_{max}\right| > \left|\frac{d^2g}{dz^2}_{min}\right|$$

Vice versa, the fault structure is a reverse/thrusting fault structure in a greater value of minimum absolute.

$$\left|\frac{d^2g}{dz^2}_{max}\right| < \left|\frac{d^2g}{dz^2}_{min}\right|$$

Figure 28 explains the indicated second vertical derivative absolute maximum value |SVD max| and minimum |SVD min| on the Line-1

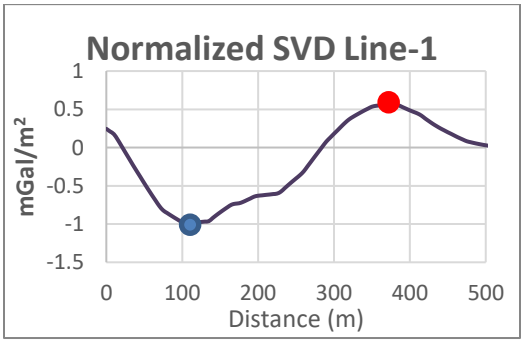

Figure 31 |SVD max| value indicated with red dot and |SVD min| value with the blue dot

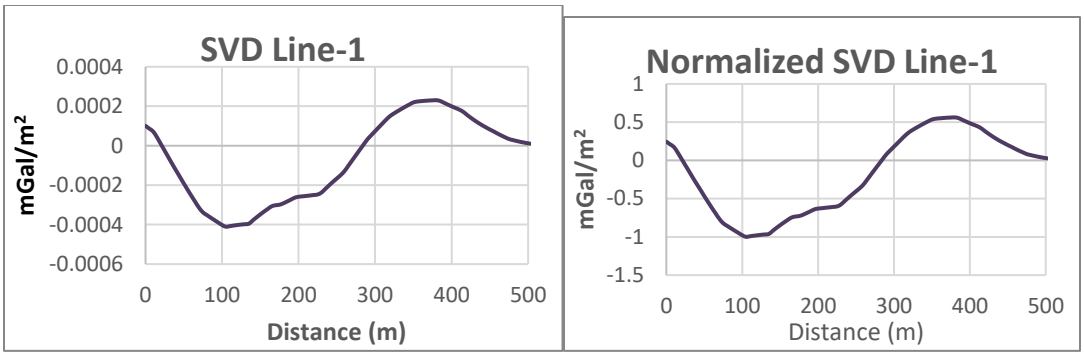

Figure 32 to Figure 35 on the next pages show the profile of residual anomaly, second vertical derivative (SVD), and the normalized SVD for 4 lines.

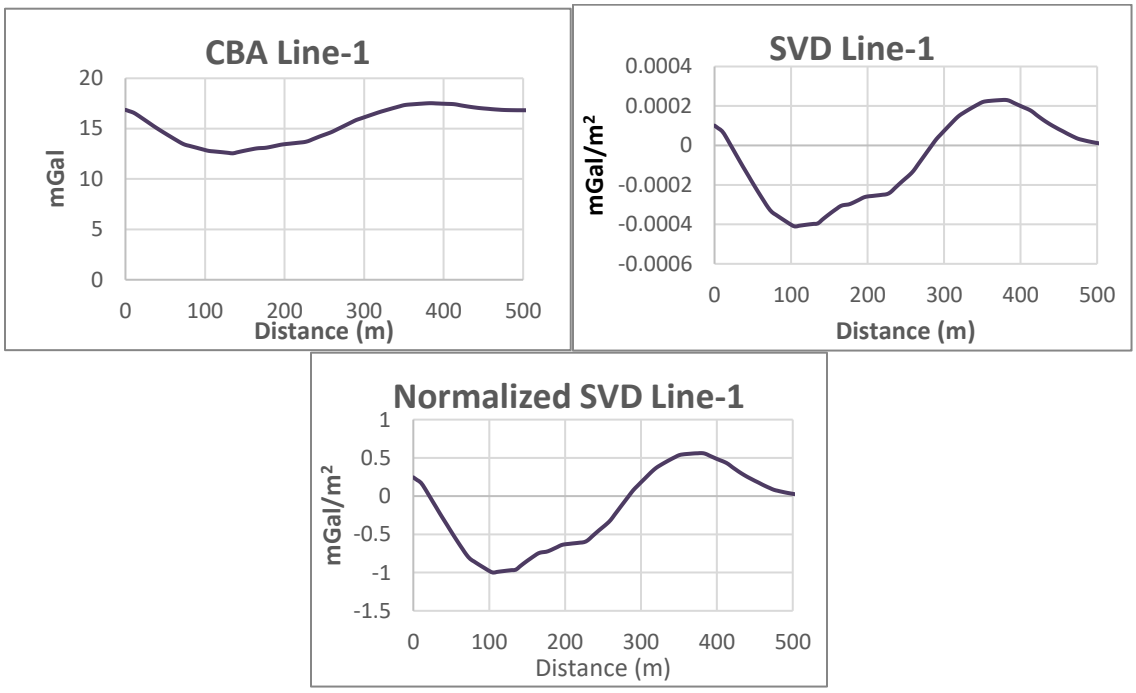

Figure 32 Attributes of residual and SVD on the Line-1

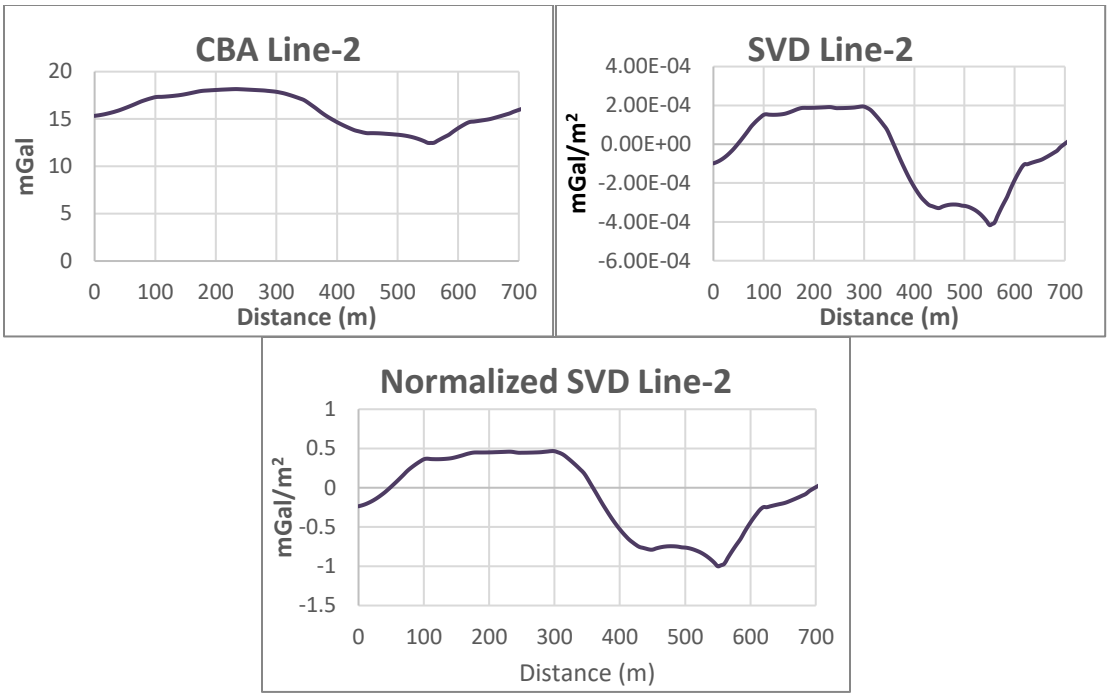

Figure 33 Attributes of residual and SVD on the Line-2

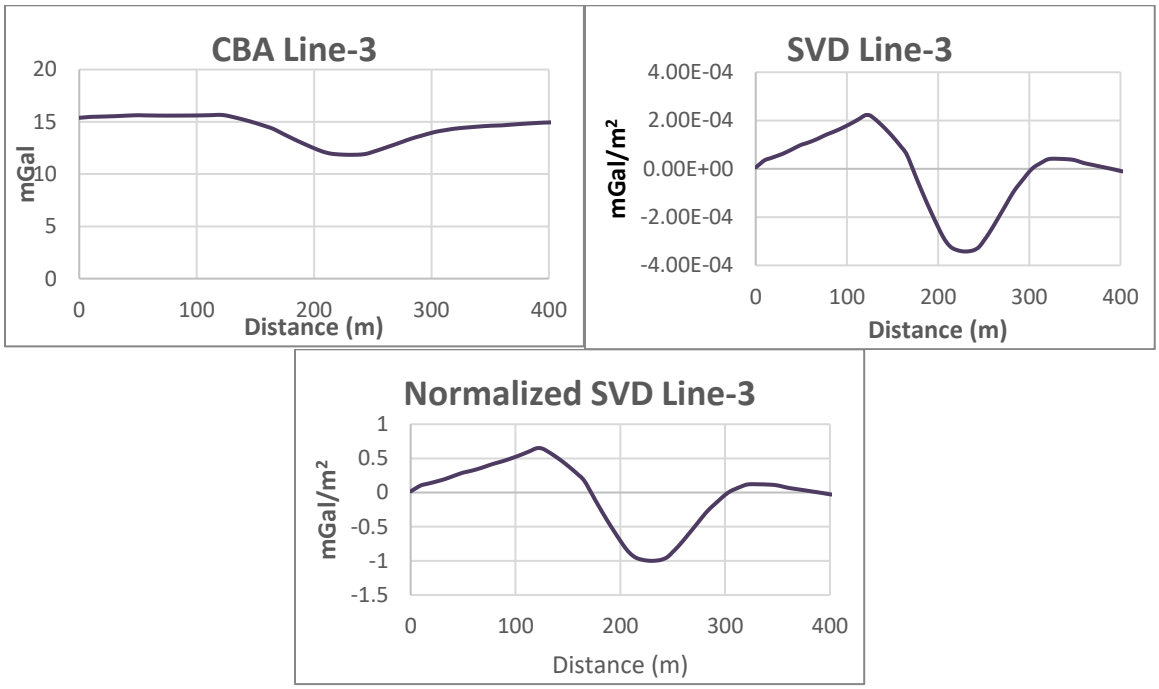

Figure 34 Attributes of residual and SVD on the Line-3

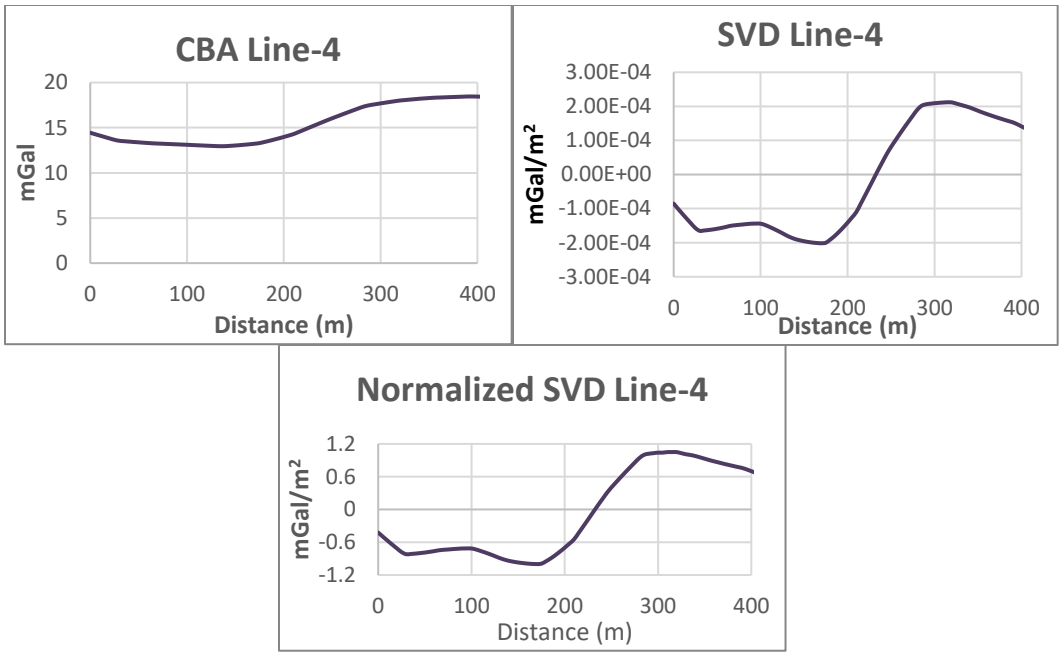

Figure 35 Attributes of residual and SVD on the Line-4

Figure 32 to Figure 35, the profile line 1, 2, 3 are showing the thrusting or reverse fault structure but Line-4 showing the normal fault structure. These findings supports the geological research on the Dammam Dome that conclude reverse faults dominated the structure on the area (Hariri, 2013).

5.6 Fault Lineament Orientation

The fault lineament delineations on the second vertical derivative map are shown in Figure 26. The lineaments have been mapped to get an idea of the dominant geological stress pattern of the study area.

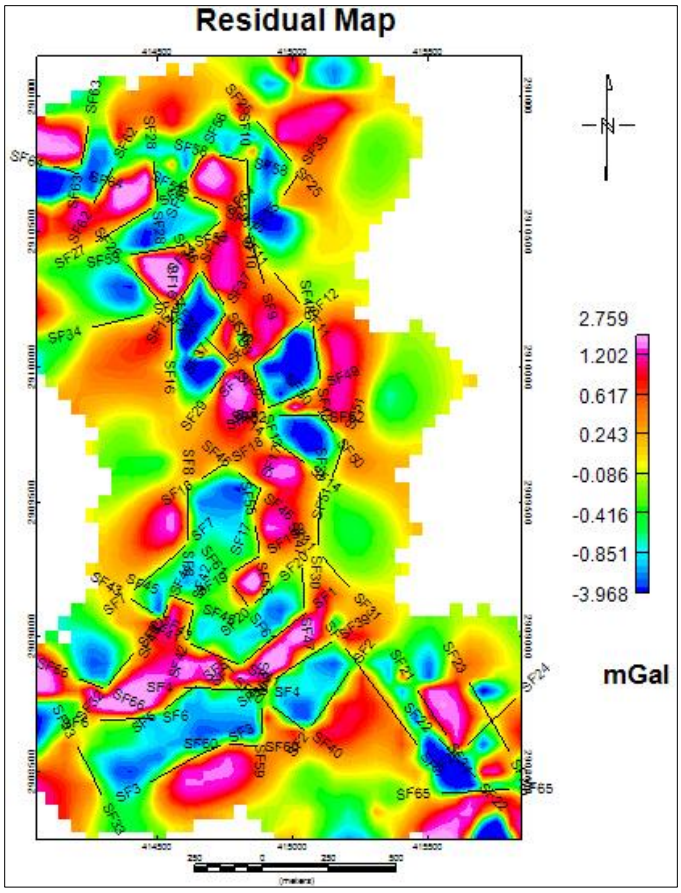

Figure 36 Interpreted fault structure on the residual map

On the Figure 36, there are 67 faults delineated in the zero value of second vertical derivative map. The interpreted direction of zero SVD value which separate the positive and negative anomaly is interpreted as the most probable fault structure. Those delineated fault structures then mapped to the rose diagram to get the dominant direction of tensional axis for the stress regime in the study area.

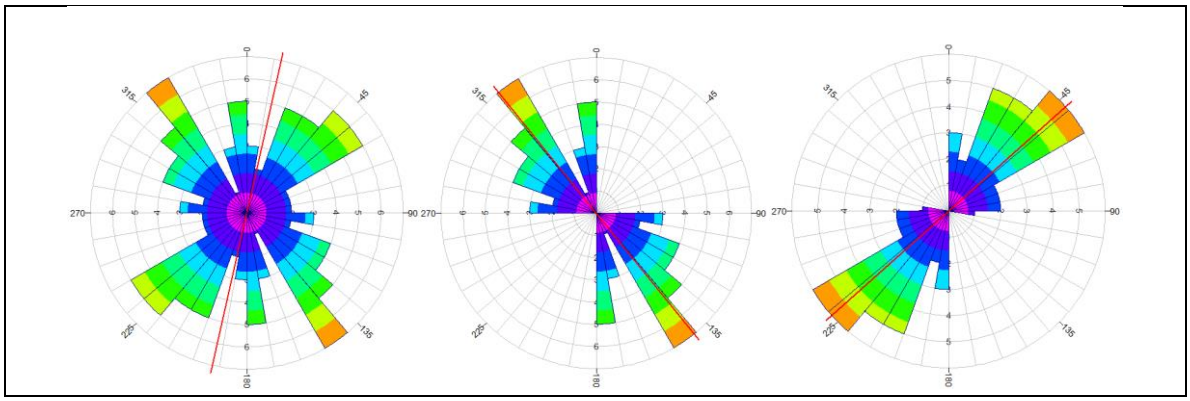

Figure 37 The sixty-seven faults orientation are delineated on the residual map. Left: The mean direction of total faults orientation is N 13^{o} E, and the filtered two major directions N 39^{o} W and N 48^{o} E are shown by the red line

As shown on Figure 37, the delineation of 67 faults orientation resulting N 39^{o} W in the NW fault direction and N 48^{o} E in the NE fault direction. See Appendix C for the statistical detail of each orientation delineation.

The dominant direction of fault strike in the study are NW and NE. The results are matched with the study on the Dammam Dome using GIS analysis (Hariri, 2013), outcrop and geo-mechanical study (Abdullatif, 2010), and borehole logs (Al-Fahmi et al., 2014) as shown on Figure 38.

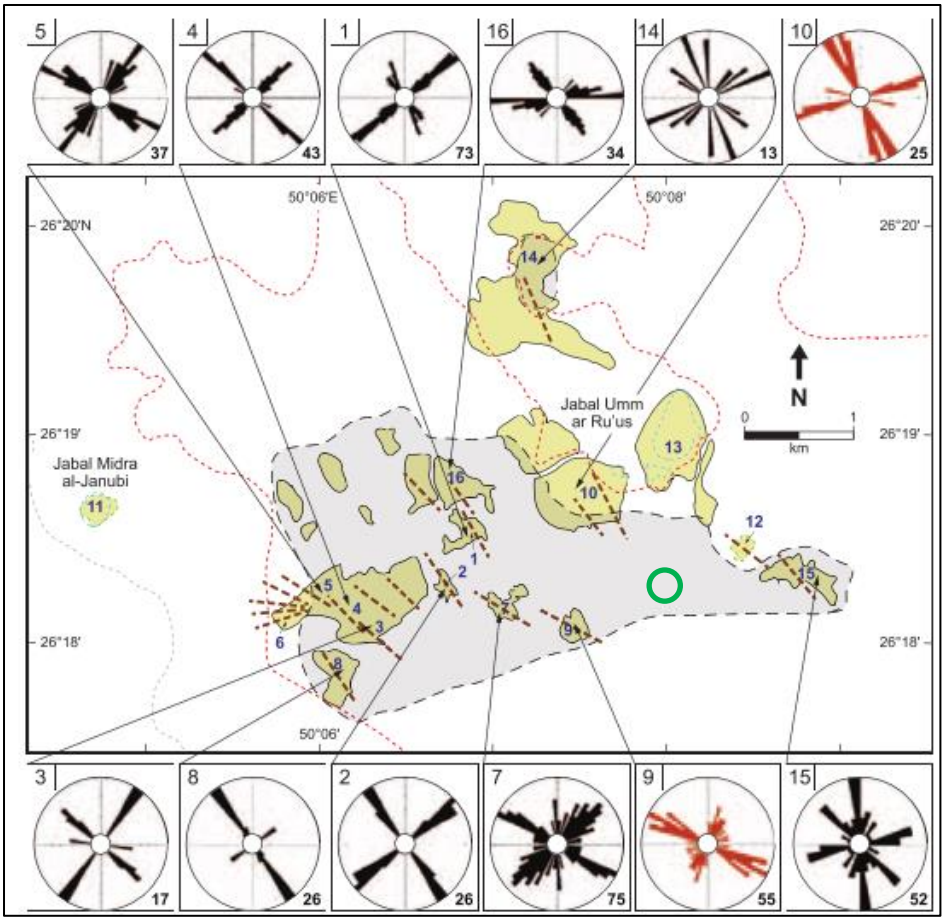

Figure 38 Various study on the dominant structures orientation on the Dammam Dome (Al-Fahmi et al., 2014). The red rose diagram was from satellite image study and the other from direct field studies. The study area is located on the green circle.

5.7 Fault Dip Estimation

Based on the empirical generalization formula for the synthetic model in Chapter 4, we can conclude the fault dip angle for those four interpreted faults.

Table 6 Estimated fault dip and fault type of 4 interpreted faults

Fault Line	Delta Normalized SVD (mGal/m^2)	Estimated Fault Dip (^{o})	Fault Type
Line-1	1.56	21	Thrust Fault
Line-2	1.47	15	Thrust Fault
Line-3	1.65	28	Thrust Fault
Line-4	2.05	67	Normal Fault

On the Table 4, it can be concluded that the dominant structures on the study area are thrust fault. However, the normal fault found in the study area are a local effect of geological force in the dome structure.

The result of fault dip estimation from the synthetic model analysis is limited by several factors. As explained previously, the dip is obtained from an empirical based formula which assumes that the only unknown is dip, the other parameters (formation thickness, density, and depth) remaining fixed and known. In this case, deviation of 6% from the generated model will produce slight errors on the dip estimation. In the actual field situation, the parameters may vary due to local geology changes in the study area. For the purpose of simply assessing the geological fault trend of the study, such deviations are acceptable. However, for more advanced use, such as volumetric estimation or detailed modeling, a more refined approach is needed such as gravity inversion and or joint inversion with another geophysical technique.

5.8 Forward Modeling

As explained on the Chapter 3, the methodology for generating the forward model is Talwani algorithm (Talwani & Ewing, 1960). The forward modeling is built on the line where the potential cavities situated. On Figure 39 the delineated line was chosen due to the strong negative and positive anomaly on the residual map. This feature indicated the karst potential on the area.

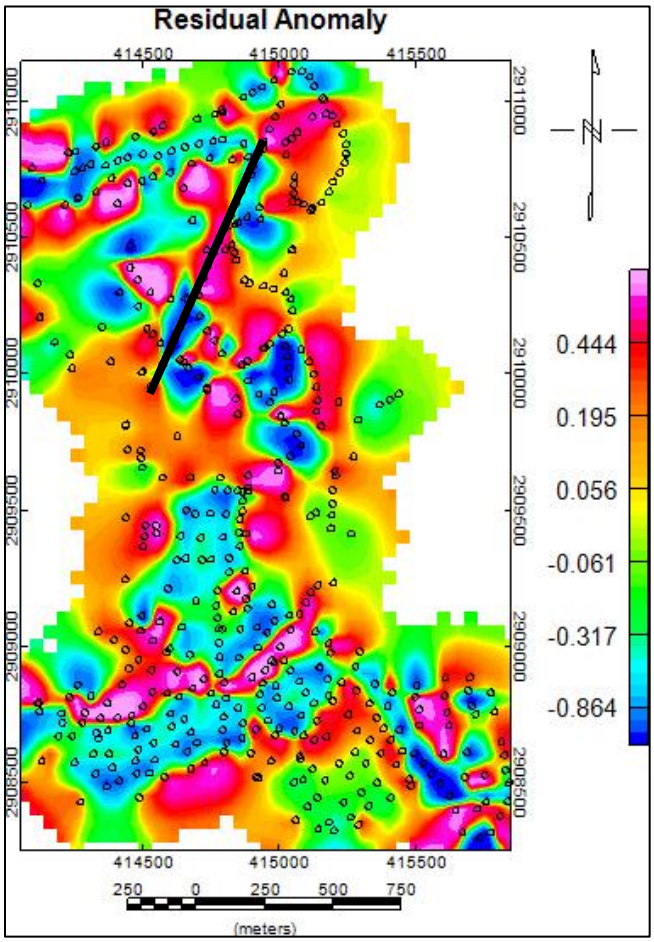

Figure 39 Delineated line for forward modeling

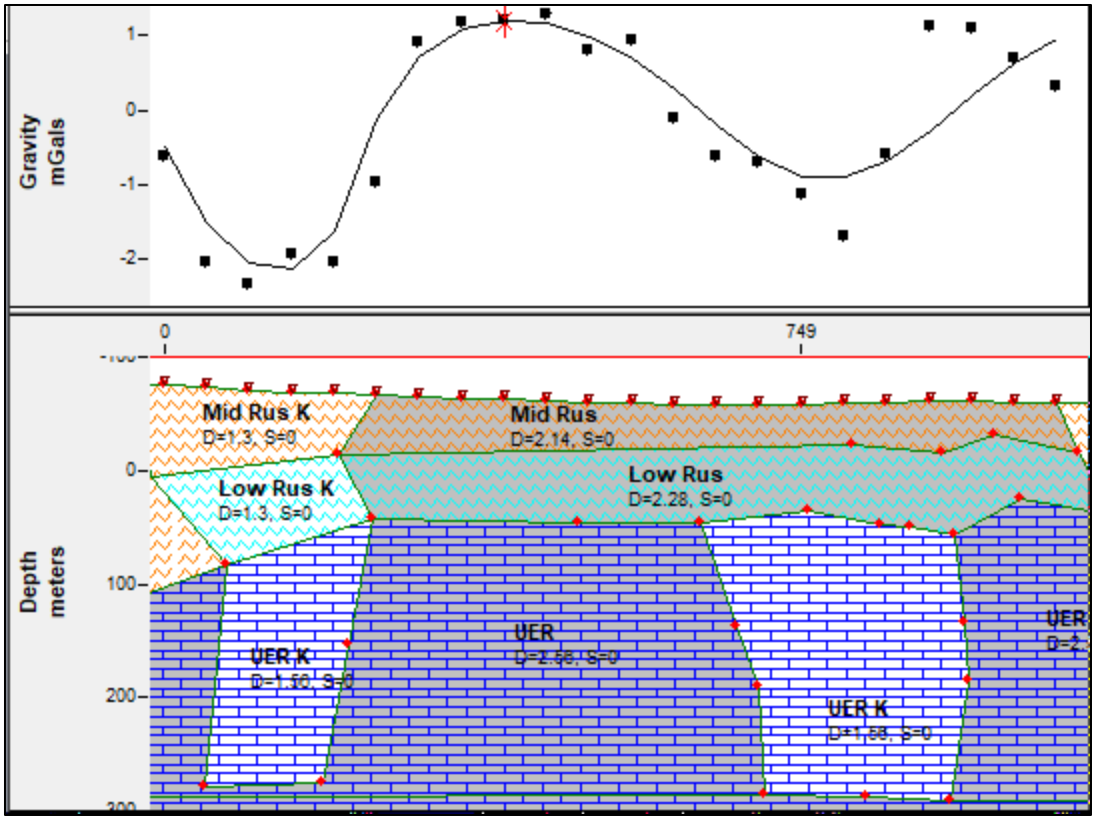

Figure 40 The calculated residual gravity profile and its forward modeling result showing the formation density distribution

On the Figure 40, the profile of residual anomaly in the delineated black line is used to do a forward modeling. The density variation and lateral variation is interactively modified to get the best fit between the residual anomaly on the station (black dots) and the calculated profile (black line). The total misfit from the modeling is 0.5 mGal.

The lighter color of the formation on Figure 40 is indicated by 'K' letter to assign the karstified formation. The formation has 1 g/cm^3 lower density than the surrounding layer. It is interpreted as probable karstified region. The most probable feature for that karstified region is cavity filled with partially saturated sand (Al-Shuhail et al., 2004a).

Table 7 The formation density and interpreted karstified formation density

Formation	Density (g/cm^3)
Middle Rus	2.14
Lower Rus	2.28
Umm Er Radhuma	2.56
Middle Rus Karstified	1.14
Lower Rus Karstified	1.30
Umm Er Radhuma Karstified	1.56

The lower density on the karstified formation in the study area are interpreted as cavity filled with partially saturated sand. The karstified formation has lower density than the surrounding formation due to the less dense material filled on the cavity. The interpreted density of karstified formation shown on Table 7.

This feature is probably affected by the high concentration of fault structure on the profile. As the UER formation is a ground water reservoir in the Eastern Province area, most probably the fault on the study area is a good conduit for water that make the dolomite limestone on the formation dissolved (Al-Fahmi et al., 2014).

CHAPTER 6

CONCLUSIONS AND RECOMMENDATIONS

6.1 Conclusions

Some analysis and result has been interpreted in the previous chapters. Those conclude some important points of the research in the study area:

1. The second vertical derivative method indicates the near-surface structures in the study area are dominated by high concentration of fault structure.
2. Thrust fault is dominant in the near-surface as the second vertical derivative high value is greater than the lower value. This indicates the main force in the study area is due to the dome structure which resulting thrust fault. The presence of normal fault is a local structure affected by the main tensional stress.
3. The structure orientation delineated in the second vertical derivative map resulting the dominant NW and NE fault orientation in the study area. The average directions are N 48^o E and N 39^o W.
4. The empirical formula generation for fault synthetic model concluded the dominant structures are thrusting fault. In 4 interpreted fault lines the fault dip are consecutively: 21^o, 15^o, 28^o, and 67^o.
5. The karstified formation on the study area are interpreted as a model having a cavity filled with partially saturated sand

6.2 Recommendations

To get the better result in studying the near-surface structure on this study area, there are some recommendations:

1. To get better results of forward modeling, the interface of the near-surface layer can be obtained by doing seismic refraction, resistivity, or TDEM surveying.
2. Use the inversion method to validate and enhance the forward model.
3. Do a joint interpretation using wider data range like seismic data, satellite or airborne gravity, which can be combined with the magnetic method.
4. Undertake drilling to tie the analysis to the geology and validate the model.

APPENDIX

A. GRAVITY MEASUREMENT DATASHEET

Table 8 Gravity measurements data sheet

Stn #	Latittude (degree)	Longitude (degree)	Elevation h (m)	Time	g tide corrected (mGal)	drift correction (mGal)	g drift corrected (mGal)	Δg	Latitude Correction	Free Air Correction	Bouguer Correction	Bouguer Anomaly
9009	26.3061237	50.1465645	70.001	10:25:10	2617.856	0.000	2617.856	0.000	0.000	21.595	-4.989	16.607
1	26.304937	50.142496	80.062	10:45:37	2616.946	0.005	2616.941	-0.915	-0.085	24.699	-5.706	18.164
2	26.302675	50.14245	75.371	10:49:32	2617.936	0.006	2617.930	0.074	-0.247	23.252	-5.371	18.202
3	26.30062	50.142439	67.863	10:54:10	2617.989	0.007	2617.982	0.126	-0.394	20.936	-4.836	16.620
4	26.298879	50.141458	65.024	10:57:48	2618.055	0.008	2618.047	0.191	-0.519	20.060	-4.634	16.136
5	26.296517	50.139243	61.019	11:01:44	2617.936	0.009	2617.927	0.071	-0.688	18.824	-4.348	15.235
6	26.2965	50.13928	62.497	11:03:02	2617.664	0.009	2617.655	-0.201	-0.689	19.280	-4.454	15.315
7	26.29322	50.140849	67.467	11:09:28	2617.329	0.010	2617.319	-0.537	-0.924	20.813	-4.808	16.392
8	26.293391	50.143006	62.411	11:12:52	2617.740	0.011	2617.729	-0.127	-0.912	19.254	-4.448	15.591
9	26.294338	50.144919	61.180	11:16:25	2618.940	0.012	2618.928	1.072	-0.844	18.874	-4.360	16.430
10	26.294082	50.147302	59.151	11:18:26	2619.538	0.012	2619.526	1.670	-0.862	18.248	-4.215	16.564
11	26.294064	50.147405	59.015	11:20:14	2619.538	0.013	2619.525	1.669	-0.864	18.206	-4.206	16.533
12	26.292666	50.148782	54.017	11:22:16	2620.235	0.013	2620.222	2.366	-0.964	16.664	-3.849	16.144
13	26.292533	50.151095	49.121	11:25:52	2620.768	0.014	2620.754	2.898	-0.973	15.154	-3.501	15.524
14	26.293839	50.153033	46.954	11:29:37	2621.356	0.015	2621.341	3.485	-0.880	14.485	-3.346	15.504
15	26.294373	50.156503	33.015	11:34:15	2623.148	0.016	2623.132	5.276	-0.841	10.185	-2.353	13.950
16	26.296305	50.156086	42.161	11:38:32	2623.143	0.017	2623.126	5.270	-0.703	13.007	-3.005	15.975
17	26.29743	50.154281	46.664	11:42:20	2622.464	0.018	2622.446	4.590	-0.623	14.396	-3.325	16.283
18	26.29854	50.149956	60.204	11:49:00	2621.656	0.019	2621.637	3.781	-0.543	18.573	-4.290	18.606
9009	26.3061237	50.1465645	70.001	11:59:47	2617.878	0.022	2617.856	0.000	0.000	21.595	-4.989	16.607
9009	26.3061237	50.1465645	70.001	15:37:36	2618.245	0.000	2618.245	0.000	0.000	21.595	-4.989	16.607
19	26.304264	50.150159	64.898	15:53:26	2619.813	0.003	2619.810	1.565	-0.133	20.021	-4.625	17.094
20	26.302868	50.149462	65.461	15:58:10	2619.254	0.004	2619.250	1.005	-0.233	20.195	-4.665	16.767
21	26.302186	50.150759	60.975	16:02:36	2620.016	0.005	2620.011	1.766	-0.282	18.811	-4.345	16.513
22	26.300557	50.150116	59.372	16:08:33	2620.208	0.007	2620.201	1.956	-0.399	18.316	-4.231	16.440
23	26.298285	50.151097	56.105	16:12:34	2619.810	0.008	2619.802	1.557	-0.561	17.308	-3.998	15.429
9009	26.3061237	50.1465645	70.001	16:37:21	2618.258	0.000	2618.258	0.000	0.000	21.595	-4.989	16.607
24	26.3034	50.148308	70.184	16:52:17	2618.829	-0.007	2618.836	0.578	-0.195	21.652	-5.002	17.423
25	26.303369	50.148339	70.021	16:54:20	2619.202	-0.008	2619.210	0.952	-0.197	21.601	-4.990	17.761

26	26.302163	50.146886	69.120	17:01:36	2619.020	-0.011	2619.031	0.773	-0.284	21.323	-4.926	17.455
27	26.30275	50.149255	65.925	17:09:48	2619.206	-0.015	2619.221	0.963	-0.242	20.338	-4.698	16.845
28	26.299231	50.143723	68.453	17:18:54	2619.051	-0.019	2619.070	0.812	-0.494	21.118	-4.878	17.545
29	26.29922	50.143718	68.473	17:19:48	2618.602	-0.020	2618.622	0.364	-0.494	21.124	-4.880	17.102
30	26.300251	50.146557	65.478	17:25:37	2619.408	-0.022	2619.430	1.172	-0.421	20.200	-4.666	17.127
31	26.297965	50.147845	64.544	17:41:57	2618.826	-0.030	2618.856	0.598	-0.584	19.912	-4.600	16.494
32	26.297338	50.145359	65.995	17:49:08	2618.627	-0.033	2618.660	0.402	-0.629	20.360	-4.703	16.688
33	26.29689	50.143465	66.660	17:54:00	2618.429	-0.036	2618.465	0.207	-0.661	20.565	-4.750	16.682
34	26.296187	50.140986	68.261	17:59:15	2618.262	-0.038	2618.300	0.042	-0.712	21.059	-4.865	16.948
9009	26.3061237	50.1465645	70.001	18:07:34	2618.216	-0.042	2618.258	0.000	0.000	21.595	-4.989	16.607
9009	26.3061237	50.1465645	70.001	18:13:21	2617.907	0.000	2617.907	0.000	0.000	21.595	-4.989	16.607
35	26.306064	50.148128	66.084	18:23:28	2619.254	0.006	2619.248	1.341	-0.004	20.387	-4.709	17.023
36	26.306081	50.148139	66.060	18:27:44	2619.254	0.008	2619.246	1.339	-0.003	20.379	-4.708	17.013
37	26.306788	50.147329	63.138	18:31:38	2619.536	0.011	2619.525	1.618	0.048	19.478	-4.499	16.549
38	26.307758	50.146686	62.470	18:42:16	2620.235	0.017	2620.218	2.311	0.117	19.272	-4.452	17.014
39	26.308877	50.14542	62.943	18:46:50	2620.083	0.020	2620.063	2.156	0.197	19.418	-4.486	16.891
40	26.310079	50.145082	64.671	18:50:20	2620.713	0.022	2620.691	2.784	0.283	19.951	-4.609	17.843
41	26.312548	50.144848	59.256	18:55:52	2621.581	0.025	2621.556	3.649	0.460	18.280	-4.223	17.246
42	26.312567	50.144817	59.219	18:57:16	2616.136	0.026	2616.110	-1.797	0.462	18.269	-4.220	11.790
43	26.308065	50.140354	76.567	19:24:05	2616.137	0.042	2616.095	-1.812	0.139	23.621	-5.456	16.214
44	26.308998	50.141518	74.962	19:30:47	2615.422	0.046	2615.376	-2.531	0.206	23.126	-5.342	15.047
45	26.307853	50.141856	80.672	19:34:14	2615.479	0.048	2615.431	-2.476	0.124	24.887	-5.749	16.539
46	26.307503	50.143	78.894	19:42:38	2615.479	0.053	2615.426	-2.481	0.099	24.339	-5.622	16.137
47	26.307512	50.143024	78.785	19:43:23	2615.222	0.053	2615.169	-2.738	0.099	24.305	-5.615	15.853
48	26.307044	50.143348	79.056	19:45:13	2616.120	0.054	2616.066	-1.841	0.066	24.389	-5.634	16.848
49	26.305382	50.144336	78.907	19:54:53	2616.602	0.060	2616.542	-1.365	-0.053	24.343	-5.623	17.408
50	26.303572	50.146946	73.336	19:57:42	2616.595	0.062	2616.533	-1.374	-0.183	22.624	-5.226	16.207
51	26.303684	50.146949	73.385	19:57:35	2618.641	0.062	2618.579	0.672	-0.175	22.639	-5.230	18.257
9009	26.3061237	50.1465645	70.001	20:17:00	2617.980	0.073	2617.907	0.000	0.000	21.595	-4.989	16.607
9009	26.3061237	50.1465645	70.001	9:03:21	2617.907	0.000	2617.907	0.000	0.000	21.595	-4.989	16.607
52	26.305733	50.142418	83.177	9:23:51	2615.994	0.019	2615.975	-1.932	-0.028	25.660	-5.928	17.829
53	26.305755	50.142436	83.207	9:32:21	2615.726	0.026	2615.700	-2.207	-0.026	25.669	-5.930	17.559
54	26.307614	50.140433	80.853	9:32:46	2615.740	0.027	2615.713	-2.194	0.107	24.943	-5.762	16.881
55	26.307614	50.140433	80.853	9:42:32	2615.460	0.036	2615.424	-2.483	0.107	24.943	-5.762	16.592
56	26.308485	50.139781	72.260	9:49:54	2616.625	0.042	2616.583	-1.324	0.169	22.292	-5.150	15.649
57	26.309312	50.139237	76.416	9:56:31	2617.985	0.048	2617.937	0.030	0.228	23.574	-5.446	17.930
58	26.309292	50.139231	76.468	9:57:21	2617.989	0.049	2617.940	0.033	0.227	23.590	-5.449	17.947
59	26.310432	50.139138	71.517	10:02:54	2619.057	0.054	2619.003	1.096	0.309	22.063	-5.097	17.754
59	26.31303056	50.13874722	69.234	10:10:00	2619.753	0.060	2619.693	1.786	0.495	21.359	-4.934	17.716

60	26.314244	50.138908	64.719	10:20:24	2620.640	0.070	2620.570	2.663	0.582	19.966	-4.612	17.435
61	26.314767	50.140247	63.861	10:29:06	2621.053	0.078	2620.975	3.068	0.619	19.701	-4.551	17.599
62	26.314761	50.140233	63.870	10:37:55	2621.638	0.086	2621.552	3.645	0.619	19.704	-4.552	18.179
63	26.315123	50.141636	62.807	10:43:37	2621.942	0.091	2621.851	3.944	0.645	19.376	-4.476	18.200
64	26.315687	50.143715	62.222	10:48:30	2621.949	0.095	2621.854	3.947	0.685	19.196	-4.434	18.023
65	26.316229	50.145891	63.297	10:54:27	2621.414	0.101	2621.313	3.406	0.724	19.527	-4.511	17.699
66	26.317226	50.147813	56.694	10:59:02	2621.862	0.105	2621.757	3.850	0.795	17.490	-4.040	16.505
67	26.316578	50.149649	59.542	11:04:44	2622.240	0.110	2622.130	4.223	0.749	18.369	-4.243	17.600
68	26.314799	50.150477	56.162	11:08:41	2622.184	0.114	2622.070	4.163	0.622	17.326	-4.002	16.865
69	26.313172	50.149587	56.476	11:14:12	2622.210	0.119	2622.091	4.184	0.505	17.423	-4.025	17.078
70	26.311593	50.148497	56.527	11:19:22	2622.059	0.123	2621.936	4.029	0.392	17.439	-4.028	17.047
71	26.311603	50.148519	56.505	11:23:40	2621.468	0.127	2621.341	3.434	0.393	17.432	-4.027	16.446
72	26.304518	50.148048	70.191	13:34:34	2619.813	0.246	2619.567	1.660	-0.115	21.654	-5.002	18.427
73	26.30575	50.149623	62.860	13:35:24	2619.797	0.247	2619.550	1.643	-0.027	19.392	-4.480	16.583
74	26.306548	50.150271	58.781	13:42:58	2621.257	0.253	2621.004	3.097	0.030	18.134	-4.189	17.011
75	26.308318	50.147514	59.302	13:50:40	2620.523	0.260	2620.263	2.356	0.157	18.295	-4.226	16.267
76	26.30832	50.147486	59.338	13:55:22	2619.726	0.265	2619.461	1.554	0.157	18.306	-4.229	15.474
77	26.306933	50.145419	71.099	14:01:54	2618.267	0.271	2617.996	0.089	0.058	21.934	-5.067	16.899
78	26.307839	50.144541	71.191	14:08:30	2616.887	0.277	2616.610	-1.297	0.123	21.962	-5.073	15.470
79	26.308471	50.143692	73.337	14:15:24	2616.142	0.283	2615.859	-2.048	0.168	22.624	-5.226	15.182
80	26.30895	50.143187	74.039	14:25:40	2616.057	0.292	2615.765	-2.142	0.202	22.841	-5.276	15.220
81	26.309686	50.142852	72.745	14:42:37	2615.366	0.307	2615.059	-2.848	0.255	22.442	-5.184	14.154
82	26.310145	50.142168	70.322	14:47:18	2614.788	0.312	2614.476	-3.431	0.288	21.694	-5.011	12.964
83	26.307921	50.144412	71.534	14:54:01	2618.332	0.318	2618.014	0.107	0.129	22.068	-5.098	16.949
84	26.306985	50.145412	70.897	15:01:51	2618.810	0.325	2618.485	0.578	0.062	21.872	-5.052	17.336
85	26.306638	50.146478	68.479	15:02:16	2618.807	0.325	2618.482	0.575	0.037	21.126	-4.880	16.784
86	26.307898	50.146904	61.386	15:09:25	2620.119	0.332	2619.787	1.880	0.127	18.938	-4.375	16.316
87	26.308579	50.145673	62.163	15:19:16	2620.898	0.341	2620.557	2.650	0.176	19.177	-4.430	17.222
88	26.310165	50.143302	73.356	15:23:55	2619.447	0.345	2619.102	1.195	0.289	22.630	-5.228	18.308
89	26.310962	50.14255	67.141	15:29:47	2619.907	0.350	2619.557	1.650	0.347	20.713	-4.785	17.231
90	26.313084	50.142072	60.639	15:35:37	2621.466	0.355	2621.111	3.204	0.499	18.707	-4.321	17.091
9009	26.3061237	50.1465645	70.001	15:47:15	2618.273	0.366	2617.907	0.000	0.000	21.595	-4.989	16.607
9009	26.3061237	50.1465645	70.001	20:03:56	2618.013	0.000	2618.013	0.000	0.000	21.595	-4.989	16.607
91	26.312899	50.149195	56.499	20:14:50	2622.384	-0.014	2622.398	4.385	0.485	17.430	-4.026	17.304
92	26.312996	50.147292	57.643	20:20:05	2622.085	-0.021	2622.106	4.093	0.492	17.783	-4.108	17.276
93	26.312435	50.146412	58.207	20:24:16	2621.654	-0.027	2621.681	3.668	0.452	17.957	-4.148	17.024
94	26.311587	50.146051	59.857	20:29:35	2621.602	-0.034	2621.636	3.623	0.391	18.466	-4.266	17.432
95	26.315491	50.148674	59.953	20:34:51	2622.121	-0.041	2622.162	4.149	0.671	18.495	-4.272	17.701
96	26.314953	50.147442	60.276	20:39:07	2621.954	-0.046	2622.000	3.987	0.633	18.595	-4.295	17.654

97	26.314573	50.146285	59.325	20:43:23	2622.241	-0.052	2622.293	4.280	0.605	18.302	-4.228	17.749
98	26.31444	50.14479	58.479	20:48:21	2622.111	-0.058	2622.169	4.156	0.596	18.041	-4.167	17.434
99	26.31399	50.143373	58.731	20:51:46	2621.754	-0.063	2621.817	3.804	0.564	18.119	-4.185	17.174
100	26.313766	50.142433	60.156	20:56:52	2621.503	-0.070	2621.573	3.560	0.547	18.558	-4.287	17.283
101	26.313477	50.141275	62.533	21:01:20	2621.257	-0.076	2621.333	3.320	0.527	19.292	-4.456	17.628
102	26.313034	50.14013	64.268	21:07:31	2620.785	-0.084	2620.869	2.856	0.495	19.827	-4.580	17.607
9009	26.3061237	50.1465645	70.001	21:17:36	2617.916	-0.097	2618.013	0.000	0.000	21.595	-4.989	16.607
9009	26.3061237	50.1465645	70.001	15:42:11	2622.466	0.000	2622.466	0.000	0.000	21.595	-4.989	16.607
103	26.293498	50.154466	43.096	15:47:31	2621.953	-0.252	2622.205	-0.261	-0.904	13.295	-3.071	10.867
104	26.293902	50.154112	42.661	15:50:44	2621.747	-0.404	2622.151	-0.315	-0.875	13.161	-3.040	10.681
105	26.294239	50.153785	43.663	15:53:02	2621.561	-0.513	2622.074	-0.392	-0.851	13.470	-3.112	10.817
106	26.2945805	50.1534843	44.998	16:01:15	2621.565	-0.901	2622.466	0.000	-0.827	13.882	-3.207	11.502
107	26.2948933	50.153141	46.336	16:04:12	2621.336	-1.040	2622.376	-0.090	-0.804	14.295	-3.302	11.707
108	26.2956829	50.1525879	48.578	16:07:13	2621.116	-1.183	2622.299	-0.167	-0.748	14.986	-3.462	12.105
109	26.2964687	50.1521568	50.447	16:10:11	2621.131	-1.323	2622.454	-0.012	-0.691	15.563	-3.595	12.647
110	26.2972088	50.1516685	52.745	16:12:37	2620.965	-1.438	2622.403	-0.063	-0.638	16.272	-3.759	13.088
111	26.2977791	50.150959	55.822	16:15:15	2620.422	-1.562	2621.984	-0.482	-0.598	17.221	-3.978	13.359
112	26.2982292	50.150032	59.697	16:18:42	2619.963	-1.725	2621.688	-0.778	-0.565	18.417	-4.254	13.950
113	26.2989292	50.149456	61.859	16:21:33	2619.745	-1.860	2621.605	-0.861	-0.515	19.084	-4.408	14.330
114	26.2994633	50.1485023	63.506	16:24:31	2619.323	-2.000	2621.323	-1.143	-0.477	19.592	-4.526	14.400
115	26.2998161	50.1478615	64.085	16:27:37	2619.029	-2.147	2621.176	-1.290	-0.452	19.770	-4.567	14.365
116	26.3004112	50.1471291	64.662	16:30:20	2618.732	-2.275	2621.007	-1.459	-0.409	19.948	-4.608	14.290
117	26.3009243	50.1468582	65.356	16:33:07	2618.566	-2.407	2620.973	-1.493	-0.372	20.162	-4.658	14.384
118	26.3017616	50.146656	68.218	16:35:45	2618.381	-2.531	2620.912	-1.554	-0.312	21.045	-4.861	14.942
119	26.3021965	50.1466217	69.705	16:39:00	2618.282	-2.685	2620.967	-1.499	-0.281	21.504	-4.967	15.318
120	26.3026447	50.1466637	71.203	16:50:49	2618.174	-3.243	2621.417	-1.049	-0.249	21.966	-5.074	16.092
121	26.3029137	50.1467438	72.048	16:54:49	2618.192	-3.432	2621.624	-0.842	-0.230	22.227	-5.134	16.480
122	26.3032551	50.1467438	73.029	16:57:30	2618.108	-3.559	2621.667	-0.799	-0.205	22.529	-5.204	16.731
123	26.3035526	50.1467628	73.473	17:01:16	2618.136	-3.737	2621.873	-0.593	-0.184	22.666	-5.236	17.021
9009	26.3061237	50.1465645	70.001	17:25:25	2617.588	-4.878	2622.466	0.000	0.000	21.595	-4.989	16.607
9009	26.3061237	50.1465645	70.001	14:37:59	2617.285	0.000	2617.285	0.000	0.000	21.595	-4.989	16.607
124	26.2995071	50.1488838	63.016	15:09:55	2619.149	0.024	2619.125	1.840	-0.474	19.441	-4.491	17.264
125	26.2998905	50.1491203	62.619	15:13:14	2619.100	0.026	2619.074	1.789	-0.446	19.318	-4.463	17.091
126	26.3002281	50.1493073	62.060	15:15:35	2619.017	0.028	2618.989	1.704	-0.422	19.145	-4.423	16.849
127	26.3004723	50.1495438	61.230	15:18:19	2618.894	0.030	2618.864	1.579	-0.405	18.889	-4.363	16.510
128	26.2989902	50.1485367	63.570	15:24:09	2618.787	0.034	2618.753	1.468	-0.511	19.611	-4.530	17.060
129	26.2984219	50.1481705	64.192	15:26:47	2618.240	0.036	2618.204	0.919	-0.552	19.803	-4.575	16.699
130	26.2978878	50.1479492	64.482	15:29:11	2617.829	0.038	2617.791	0.506	-0.590	19.893	-4.595	16.394
131	26.2976437	50.147625	64.603	15:31:39	2617.701	0.040	2617.661	0.376	-0.607	19.930	-4.604	16.310

132	26.2974072	50.1471367	64.762	15:34:41	2617.641	0.042	2617.599	0.314	-0.624	19.979	-4.615	16.302
133	26.2972164	50.1461105	65.310	15:38:12	2617.664	0.044	2617.620	0.335	-0.638	20.148	-4.654	16.466
134	26.2970181	50.1449547	66.015	15:41:14	2617.540	0.047	2617.493	0.208	-0.652	20.366	-4.705	16.522
135	26.296854	50.1440086	66.427	15:44:18	2617.526	0.049	2617.477	0.192	-0.664	20.493	-4.734	16.615
136	26.2964153	50.143116	66.671	15:46:49	2617.384	0.051	2617.333	0.048	-0.695	20.568	-4.751	16.560
137	26.2960987	50.1427155	66.950	15:49:33	2617.394	0.053	2617.341	0.056	-0.718	20.654	-4.771	16.657
9009	26.3061237	50.1465645	70.001	16:00:49	2617.346	0.061	2617.285	0.000	0.000	21.595	-4.989	16.607
9009	26.3061237	50.1465645	70.001	6:36:57	2617.253	0.000	2617.253	0.000	0.000	21.595	-4.989	16.607
138	26.306839	50.152475	52.449	6:44:47	2621.136	0.002	2621.134	3.881	0.051	16.180	-3.738	16.273
139	26.30664	50.152154	52.848	6:49:21	2620.788	0.003	2620.785	3.532	0.037	16.304	-3.766	16.033
140	26.306478	50.151779	53.539	6:53:29	2620.231	0.004	2620.227	2.974	0.025	16.517	-3.815	15.650
141	26.305964	50.15099	56.933	6:56:09	2619.698	0.004	2619.694	2.441	-0.011	17.564	-4.057	15.959
142	26.304743	50.150837	60.554	6:58:45	2619.407	0.005	2619.402	2.149	-0.099	18.681	-4.315	16.614
143	26.30412	50.150175	63.754	7:03:27	2619.260	0.006	2619.254	2.001	-0.144	19.668	-4.543	17.269
144	26.303629	50.150053	63.375	7:06:16	2618.897	0.007	2618.890	1.637	-0.179	19.551	-4.516	16.851
145	26.303181	50.15006	63.943	7:08:53	2618.727	0.007	2618.720	1.467	-0.211	19.726	-4.557	16.847
146	26.302802	50.150039	63.922	7:09:53	2618.606	0.007	2618.599	1.346	-0.238	19.720	-4.555	16.748
147	26.302351	50.150028	63.107	7:13:22	2618.622	0.008	2618.614	1.361	-0.270	19.469	-4.497	16.602
148	26.302358	50.150003	63.202	7:15:41	2618.745	0.009	2618.736	1.483	-0.270	19.498	-4.504	16.747
149	26.310291	50.147838	57.513	7:18:59	2621.076	0.010	2621.066	3.813	0.299	17.743	-4.099	17.159
150	26.310291	50.147838	57.513	7:31:59	2621.104	0.012	2621.092	3.839	0.299	17.743	-4.099	17.184
9009	26.3061237	50.1465645	70.001	7:34:28	2617.266	0.013	2617.253	0.000	0.000	21.595	-4.989	16.607
9009	26.3061237	50.1465645	70.001	14:06:33	2618.243	0.000	2618.243	0.000	0.000	21.595	-4.989	16.607
151	26.304256	50.148057	70.752	14:19:22	2618.521	-0.006	2618.527	0.284	-0.134	21.827	-5.042	17.203
152	26.304108	50.146933	73.254	14:35:02	2618.083	-0.013	2618.096	-0.147	-0.144	22.599	-5.220	17.376
153	26.30401944	50.14591667	74.989	14:50:52	2617.249	-0.020	2617.269	-0.974	-0.151	23.134	-5.344	16.967
154	26.30401944	50.14480833	77.328	14:55:21	2617.445	-0.022	2617.467	-0.776	-0.151	23.856	-5.511	17.720
155	26.30400278	50.14379444	79.647	15:04:24	2616.78	-0.027	2616.807	-1.436	-0.152	24.571	-5.676	17.611
156	26.30434444	50.14304167	80.534	15:14:22	2616.462	-0.031	2616.493	-1.750	-0.127	24.845	-5.739	17.483
157	26.30465556	50.14298889	80.250	15:27:01	2618.26	-0.037	2618.297	0.054	-0.105	24.757	-5.719	19.197
9009	26.3061237	50.1465645	70.001	18:29:14	2618.122	0.000	2618.122	0.000	0.000	21.595	-4.989	16.607
158	26.304899	50.142974	79.879	19:00:47	2616.21	-0.048	2616.258	-1.864	-0.088	24.643	-5.693	17.174
9009	26.3061237	50.1465645	70.001	19:30:29	2618.028	-0.094	2618.122	0.000	0.000	21.595	-4.989	16.607
9009	26.3061237	50.1465645	70.001	15:26:44	2617.089	0.000	2617.089	0.000	0.000	21.595	-4.989	16.607
159	26.31039444	50.14746667	57.989	15:33:50	2620.771	-0.005	2620.776	3.687	0.306	17.890	-4.133	17.138
160	26.310474	50.146939	58.839	15:36:24	2620.669	-0.006	2620.675	3.586	0.312	18.152	-4.193	17.233
161	26.310581	50.146782	59.113	15:39:19	2620.616	-0.008	2620.624	3.535	0.319	18.236	-4.213	17.240
162	26.310585	50.146755	59.164	15:41:35	2620.492	-0.010	2620.502	3.413	0.320	18.252	-4.216	17.129
163	26.311239	50.14645	59.439	15:44:01	2620.618	-0.011	2620.629	3.540	0.366	18.337	-4.236	17.275

164	26.311501	50.146381	59.326	15:46:01	2620.745	-0.013	2620.758	3.669	0.385	18.302	-4.228	17.357
165	26.311747	50.146294	59.188	15:47:50	2620.808	-0.014	2620.822	3.733	0.403	18.259	-4.218	17.371
166	26.312403	50.1462	58.403	15:50:13	2621.087	-0.015	2621.102	4.013	0.450	18.017	-4.162	17.419
167	26.312984	50.149246	56.538	15:54:01	2621.302	-0.018	2621.320	4.231	0.491	17.442	-4.029	17.152
168	26.313113	50.148931	56.875	15:56:07	2621.32	-0.019	2621.339	4.250	0.501	17.546	-4.053	17.242
169	26.313174	50.148726	57.068	15:58:08	2621.347	-0.020	2621.367	4.278	0.505	17.605	-4.067	17.312
170	26.313209	50.148517	57.233	15:59:57	2621.369	-0.022	2621.391	4.302	0.508	17.656	-4.079	17.372
171	26.313485	50.148561	57.471	16:03:22	2621.144	-0.024	2621.168	4.079	0.527	17.730	-4.096	17.186
172	26.313772	50.148563	57.784	16:05:49	2621.125	-0.025	2621.150	4.061	0.548	17.826	-4.118	17.222
173	26.31403	50.148592	58.078	16:07:39	2621.188	-0.027	2621.215	4.126	0.566	17.917	-4.139	17.337
174	26.314759	50.148274	59.404	16:10:44	2621.077	-0.029	2621.106	4.017	0.619	18.326	-4.233	17.491
175	26.315165	50.148236	60.088	16:12:29	2621.081	-0.030	2621.111	4.022	0.648	18.537	-4.282	17.629
176	26.315294	50.148475	60.016	16:14:30	2621.132	-0.031	2621.163	4.074	0.657	18.515	-4.277	17.655
177	26.316012	50.149224	59.014	16:16:22	2621.184	-0.032	2621.216	4.127	0.708	18.206	-4.206	17.419
178	26.31612	50.149723	57.523	16:18:32	2621.383	-0.034	2621.417	4.328	0.716	17.746	-4.099	17.258
179	26.316061	50.149965	56.417	16:20:00	2621.383	-0.035	2621.418	4.329	0.712	17.405	-4.021	17.001
180	26.316054	50.14997	56.369	16:21:49	2621.36	-0.036	2621.396	4.307	0.711	17.390	-4.017	16.968
181	26.315767	50.150142	54.600	16:24:21	2621.333	-0.037	2621.370	4.281	0.691	16.844	-3.891	16.544
182	26.315472	50.150379	54.942	16:26:15	2621.315	-0.039	2621.354	4.265	0.670	16.950	-3.915	16.629
183	26.315104	50.150478	55.621	16:28:00	2621.281	-0.040	2621.321	4.232	0.643	17.159	-3.964	16.784
184	26.314815	50.150471	56.137	16:30:26	2621.269	-0.041	2621.310	4.221	0.623	17.318	-4.001	16.917
185	26.314514	50.150427	56.579	16:32:58	2621.283	-0.043	2621.326	4.237	0.601	17.455	-4.032	17.059
186	26.314171	50.150255	56.823	16:34:49	2621.317	-0.044	2621.361	4.272	0.577	17.530	-4.049	17.176
187	26.313859	50.150005	56.808	16:36:19	2621.297	-0.045	2621.342	4.253	0.554	17.525	-4.048	17.176
188	26.313528	50.149856	56.633	16:38:22	2621.276	-0.047	2621.323	4.234	0.530	17.471	-4.036	17.138
189	26.310818	50.148229	56.908	16:43:57	2620.956	-0.050	2621.006	3.917	0.336	17.556	-4.056	17.082
190	26.310191	50.148297	57.011	16:47:14	2620.798	-0.052	2620.850	3.761	0.291	17.588	-4.063	16.995
191	26.309956	50.148488	56.908	16:49:15	2620.687	-0.054	2620.741	3.652	0.275	17.556	-4.055	16.878
192	26.309587	50.148551	57.052	16:51:39	2620.518	-0.055	2620.573	3.484	0.248	17.601	-4.066	16.771
193	26.308984	50.148406	57.701	16:54:28	2620.156	-0.057	2620.213	3.124	0.205	17.801	-4.112	16.608
194	26.308806	50.148161	58.082	16:56:31	2619.801	-0.058	2619.859	2.770	0.192	17.918	-4.139	16.357
195	26.308478	50.147718	58.849	16:58:12	2619.468	-0.059	2619.527	2.438	0.169	18.155	-4.194	16.231
196	26.308292	50.14888	58.388	17:02:30	2619.947	-0.062	2620.009	2.920	0.155	18.013	-4.161	16.617
197	26.307882	50.149172	58.956	17:04:16	2619.783	-0.063	2619.846	2.757	0.126	18.188	-4.201	16.618
198	26.30747	50.149343	59.562	17:05:42	2619.634	-0.064	2619.698	2.609	0.096	18.375	-4.245	16.643
199	26.307047	50.149442	60.340	17:07:26	2619.467	-0.066	2619.533	2.444	0.066	18.615	-4.300	16.692
200	26.306609	50.149482	61.500	17:09:34	2619.205	-0.067	2619.272	2.183	0.035	18.973	-4.383	16.738
201	26.306242	50.149439	62.559	17:11:30	2618.965	-0.068	2619.033	1.944	0.008	19.299	-4.458	16.777
9009	26.3061237	50.1465645	70.001	17:22:02	2617.014	-0.075	2617.089	0.000	0.000	21.595	-4.989	16.607

9001	26.312494	50.146536	58.069	9:44:58	2621.132	0.000	2621.132	0.000	0.000	17.914	-4.138	13.776
202	26.306884	50.147891	62.615	9:50:22	2618.107	0.001	2618.106	-3.026	-0.402	19.317	-4.462	12.231
203	26.306533	50.147724	64.218	9:53:05	2617.966	0.001	2617.965	-3.167	-0.427	19.811	-4.576	12.495
204	26.30584	50.148283	66.037	9:55:45	2618.112	0.002	2618.110	-3.022	-0.477	20.372	-4.706	13.121
205	26.305489	50.14873	65.698	9:58:53	2618.588	0.002	2618.586	-2.546	-0.502	20.268	-4.682	13.541
206	26.307238	50.146927	63.537	10:02:01	2616.96	0.004	2616.956	-4.176	-0.376	19.601	-4.528	11.274
207	26.307341	50.1451	70.606	10:04:56	2616.251	0.004	2616.247	-4.885	-0.369	21.782	-5.032	12.234
208	26.307642	50.14473	71.034	10:07:31	2615.166	0.006	2615.160	-5.972	-0.348	21.914	-5.062	11.228
209	26.30823	50.144046	72.341	10:10:25	2614.864	0.007	2614.857	-6.275	-0.305	22.317	-5.155	11.192
210	26.30875	50.143392	73.872	10:19:15	2619.038	0.008	2619.030	-2.102	-0.268	22.789	-5.264	15.691
211	26.307298	50.148438	61.189	10:22:32	2619.213	0.009	2619.204	-1.928	-0.372	18.877	-4.361	12.960
212	26.307686	50.148415	59.789	10:25:19	2619.34	0.010	2619.330	-1.802	-0.344	18.445	-4.261	12.727
213	26.308057	50.14837	59.019	10:28:00	2619.561	0.010	2619.551	-1.581	-0.318	18.207	-4.206	12.738
214	26.308398	50.148299	58.508	10:31:56	2618.846	0.011	2618.835	-2.297	-0.293	18.050	-4.169	11.877
215	26.308147	50.14595	63.111	10:35:05	2619.181	0.011	2619.170	-1.962	-0.311	19.470	-4.498	13.321
216	26.309385	50.145128	64.277	10:38:37	2619.358	0.012	2619.346	-1.786	-0.223	19.830	-4.581	13.686
217	26.309975	50.14459444	67.156	10:41:30	2618.135	0.012	2618.123	-3.009	-0.180	20.718	-4.786	13.103
218	26.309935	50.14405	70.519	10:44:52	2619.96	0.013	2619.947	-1.185	-0.183	21.755	-5.025	15.728
219	26.310568	50.14284	70.989	10:50:18	2621.156	0.014	2621.142	0.010	-0.138	21.900	-5.059	16.989
220	26.311694	50.142531	60.776	14:24:48	2618.667	0.014	2618.653	-2.479	-0.057	18.749	-4.331	11.996
221	26.30511	50.148886	66.396	14:27:02	2618.325	0.015	2618.310	-2.822	-0.529	20.483	-4.732	13.459
222	26.304754	50.148492	68.419	14:29:31	2617.981	0.015	2617.966	-3.166	-0.554	21.107	-4.876	13.619
223	26.294966	50.155072	42.273	14:38:52	2622.142	0.016	2622.126	0.994	-1.255	13.041	-3.013	12.278
224	26.293322	50.1558	40.691	14:43:01	2622.429	0.016	2622.413	1.281	-1.373	12.553	-2.900	12.307
225	26.292128	50.155554	40.087	14:45:49	2622.284	0.017	2622.267	1.135	-1.458	12.367	-2.857	12.104
226	26.2965	50.155242	43.614	14:53:33	2622.039	0.017	2622.022	0.890	-1.145	13.455	-3.108	12.382
227	26.297166	50.153216	48.609	14:56:23	2621.308	0.018	2621.290	0.158	-1.098	14.996	-3.464	12.787
9001	26.312494	50.146536	58.069	15:09:51	2621.206	0.019	2621.187	0.055	0.000	17.914	-4.138	13.831
9002	26.312671	50.146851	57.793	7:45:07	2621.143	0.000	2621.143	0.000	0.000	17.829	-4.119	13.711
228	26.302816	50.146141	72.482	7:51:06	2617.465	0.001	2617.464	-3.679	-0.706	22.361	-5.165	14.223
229	26.302828	50.145569	73.320	7:52:50	2617.404	0.001	2617.403	-3.740	-0.705	22.619	-5.225	14.359
230	26.302816	50.145006	74.099	7:55:11	2617.143	0.001	2617.142	-4.001	-0.706	22.859	-5.281	14.284
231	26.302928	50.144677	74.903	7:57:05	2617.083	0.001	2617.082	-4.061	-0.698	23.107	-5.338	14.406
232	26.303598	50.146556	73.713	7:59:57	2617.566	0.001	2617.565	-3.578	-0.650	22.740	-5.253	14.559
233	26.303609	50.146197	74.159	8:01:42	2617.531	0.002	2617.529	-3.614	-0.649	22.878	-5.285	14.629
234	26.30361	50.145722	74.867	8:03:11	2617.454	0.002	2617.452	-3.691	-0.649	23.097	-5.335	14.719
235	26.302042	50.146034	70.218	8:06:19	2617.566	0.002	2617.564	-3.579	-0.761	21.662	-5.004	13.840
236	26.302025	50.14521	71.417	8:08:29	2617.363	0.002	2617.361	-3.782	-0.762	22.032	-5.089	13.923
237	26.302081	50.144464	72.436	8:10:27	2617.382	0.002	2617.380	-3.763	-0.758	22.346	-5.162	14.179

238	26.301354	50.146257	67.769	8:13:22	2617.728	0.003	2617.725	-3.418	-0.810	20.907	-4.829	13.470
239	26.301306	50.145596	68.852	8:15:12	2617.526	0.003	2617.523	-3.620	-0.814	21.241	-4.907	13.528
240	26.301292	50.145259	69.311	8:17:05	2617.416	0.003	2617.413	-3.730	-0.815	21.382	-4.939	13.528
241	26.301336	50.14467	70.052	8:18:56	2617.364	0.003	2617.361	-3.782	-0.812	21.611	-4.992	13.648
242	26.301279	50.144326	70.130	8:20:20	2617.335	0.003	2617.332	-3.811	-0.816	21.635	-4.998	13.642
243	26.300881	50.146276	66.654	8:22:55	2617.915	0.004	2617.911	-3.232	-0.844	20.563	-4.750	13.425
244	26.300272	50.145844	66.691	8:27:00	2617.954	0.004	2617.950	-3.193	-0.888	20.574	-4.753	13.516
245	26.29977	50.145805	66.433	8:29:08	2617.951	0.004	2617.947	-3.196	-0.924	20.495	-4.734	13.488
246	26.299374	50.145848	66.282	8:30:52	2617.868	0.004	2617.864	-3.279	-0.952	20.448	-4.723	13.397
247	26.299016	50.145889	66.193	8:32:28	2617.821	0.005	2617.816	-3.327	-0.978	20.421	-4.717	13.355
248	26.298541	50.145916	66.078	8:34:31	2617.649	0.005	2617.644	-3.499	-1.012	20.385	-4.709	13.189
249	26.298062	50.145945	65.946	8:36:16	2617.554	0.005	2617.549	-3.594	-1.046	20.344	-4.700	13.097
250	26.297514	50.145945	65.668	8:38:09	2617.435	0.005	2617.430	-3.713	-1.085	20.259	-4.680	12.951
251	26.299277	50.147954	64.135	8:41:06	2618.428	0.005	2618.423	-2.720	-0.959	19.786	-4.571	13.454
252	26.298893	50.147693	64.489	8:43:10	2618.011	0.006	2618.005	-3.138	-0.987	19.895	-4.596	13.148
253	26.298386	50.147356	64.869	8:45:06	2617.759	0.006	2617.753	-3.390	-1.023	20.012	-4.623	13.022
254	26.298044	50.14665	65.416	8:47:22	2617.59	0.006	2617.584	-3.559	-1.047	20.181	-4.662	13.007
255	26.298326	50.144093	67.805	8:50:15	2617.443	0.006	2617.437	-3.706	-1.027	20.918	-4.832	13.407
256	26.298143	50.144849	67.016	8:52:14	2617.523	0.006	2617.517	-3.626	-1.040	20.675	-4.776	13.313
257	26.299065	50.147304	64.788	8:55:18	2617.921	0.007	2617.914	-3.229	-0.974	19.987	-4.617	13.116
258	26.298992	50.146698	65.362	8:57:19	2617.838	0.007	2617.831	-3.312	-0.980	20.164	-4.658	13.174
259	26.298995	50.146034	66.030	8:59:16	2617.803	0.007	2617.796	-3.347	-0.979	20.370	-4.706	13.297
260	26.299047	50.144544	67.826	9:01:30	2617.555	0.007	2617.548	-3.595	-0.976	20.924	-4.834	13.471
261	26.299426	50.143063	66.248	9:04:06	2617.158	0.008	2617.150	-3.993	-0.949	20.437	-4.721	12.672
262	26.299678	50.146954	64.962	9:06:49	2618.308	0.008	2618.300	-2.843	-0.930	20.041	-4.629	13.499
263	26.299575	50.146436	65.539	9:08:50	2618.126	0.008	2618.118	-3.025	-0.938	20.219	-4.671	13.461
264	26.30032	50.144019	68.147	9:14:52	2617.215	0.009	2617.206	-3.937	-0.885	21.023	-4.856	13.115
265	26.299923	50.14506	67.470	9:18:16	2617.614	0.009	2617.605	-3.538	-0.913	20.814	-4.808	13.381
266	26.299996	50.14689	64.986	9:23:32	2618.276	0.010	2618.266	-2.877	-0.908	20.048	-4.631	13.448
267	26.297101	50.140715	67.350	9:30:37	2617.109	0.010	2617.099	-4.044	-1.115	20.777	-4.800	13.049
268	26.29675	50.141208	67.549	9:33:36	2617.16	0.010	2617.150	-3.993	-1.140	20.839	-4.814	13.172
269	26.294536	50.14061	67.983	9:38:11	2616.856	0.011	2616.845	-4.298	-1.299	20.973	-4.845	13.129
270	26.295408	50.140529	68.384	9:41:15	2617.222	0.011	2617.211	-3.932	-1.236	21.096	-4.873	13.527
271	26.295513	50.141418	68.229	9:44:49	2616.944	0.012	2616.932	-4.211	-1.229	21.049	-4.862	13.204
272	26.295862	50.140901	68.459	9:46:42	2617.02	0.012	2617.008	-4.135	-1.204	21.120	-4.879	13.310
273	26.295844	50.14016	68.385	9:49:05	2617.11	0.012	2617.098	-4.045	-1.205	21.097	-4.873	13.383
274	26.295399	50.140023	68.361	9:50:58	2617.022	0.012	2617.010	-4.133	-1.237	21.089	-4.872	13.321
275	26.296217	50.139313	65.931	9:53:28	2616.939	0.012	2616.927	-4.216	-1.178	20.340	-4.698	12.603
276	26.296152	50.140124	68.296	9:56:30	2617.071	0.013	2617.058	-4.085	-1.183	21.069	-4.867	13.300

277	26.295601	50.141843	67.818	9:59:07	2617.099	0.013	2617.086	-4.057	-1.222	20.922	-4.833	13.254
278	26.295338	50.141481	68.025	10:01:13	2617.143	0.013	2617.130	-4.013	-1.241	20.986	-4.848	13.366
279	26.294824	50.141297	67.690	10:03:16	2616.939	0.013	2616.926	-4.217	-1.278	20.882	-4.824	13.119
280	26.294172	50.141388	66.944	10:06:31	2616.631	0.014	2616.617	-4.526	-1.325	20.652	-4.771	12.680
281	26.293743	50.14181	65.466	10:08:44	2616.781	0.014	2616.767	-4.376	-1.355	20.196	-4.665	12.510
282	26.293925	50.142263	64.877	10:10:11	2616.855	0.014	2616.841	-4.302	-1.342	20.015	-4.623	12.431
283	26.294365	50.142017	66.133	10:13:11	2616.903	0.014	2616.889	-4.254	-1.311	20.402	-4.713	12.746
284	26.29483	50.141895	66.983	10:15:23	2617.021	0.015	2617.006	-4.137	-1.277	20.664	-4.774	13.032
285	26.295852	50.142708	66.896	10:18:47	2617.175	0.015	2617.160	-3.983	-1.204	20.637	-4.767	13.092
286	26.295438	50.142841	66.470	10:21:32	2617.408	0.015	2617.393	-3.750	-1.234	20.506	-4.737	13.253
287	26.294971	50.142966	65.598	10:24:19	2617.553	0.015	2617.538	-3.605	-1.267	20.237	-4.675	13.224
288	26.2946	50.142862	65.095	10:30:14	2617.417	0.016	2617.401	-3.742	-1.294	20.082	-4.639	12.995
289	26.294178	50.142907	64.207	10:32:41	2617.298	0.016	2617.282	-3.861	-1.324	19.808	-4.576	12.695
290	26.294192	50.14339	63.376	10:34:48	2617.671	0.016	2617.655	-3.488	-1.323	19.551	-4.516	12.870
291	26.294642	50.143572	63.860	10:36:46	2617.762	0.017	2617.745	-3.398	-1.291	19.701	-4.551	13.043
292	26.295199	50.143529	64.989	10:38:53	2617.687	0.017	2617.670	-3.473	-1.251	20.049	-4.631	13.196
293	26.295662	50.143269	66.090	10:40:57	2617.433	0.017	2617.416	-3.727	-1.218	20.389	-4.710	13.170
294	26.29674	50.14445	66.076	10:43:39	2617.463	0.017	2617.446	-3.697	-1.141	20.384	-4.709	13.119
295	26.296171	50.144141	65.634	10:45:26	2617.762	0.017	2617.745	-3.398	-1.182	20.248	-4.677	13.354
296	26.295744	50.144182	64.939	10:47:13	2617.87	0.018	2617.852	-3.291	-1.212	20.034	-4.628	13.327
297	26.295161	50.144333	63.571	10:49:21	2617.937	0.018	2617.919	-3.224	-1.254	19.612	-4.530	13.111
298	26.29492	50.144774	62.486	10:51:08	2618.005	0.018	2617.987	-3.156	-1.271	19.277	-4.453	12.939
299	26.295211	50.145129	62.732	10:53:24	2618.028	0.018	2618.010	-3.133	-1.250	19.353	-4.471	12.999
300	26.295561	50.144906	63.784	10:55:19	2617.956	0.018	2617.938	-3.205	-1.225	19.677	-4.545	13.152
301	26.295994	50.144651	64.923	10:57:09	2617.807	0.019	2617.788	-3.355	-1.194	20.029	-4.627	13.242
302	26.296858	50.145638	65.317	10:59:44	2617.617	0.019	2617.598	-3.545	-1.132	20.150	-4.655	13.083
303	26.296483	50.145831	64.678	11:01:29	2617.817	0.019	2617.798	-3.345	-1.159	19.953	-4.609	13.158
304	26.296074	50.1461	63.821	11:03:41	2617.956	0.019	2617.937	-3.206	-1.188	19.689	-4.548	13.123
305	26.295642	50.146064	63.018	11:06:12	2618.105	0.019	2618.086	-3.057	-1.219	19.441	-4.491	13.112
306	26.29522	50.146229	62.058	11:07:57	2618.113	0.020	2618.093	-3.050	-1.250	19.145	-4.423	12.922
307	26.295381	50.14679	62.133	11:09:40	2618.024	0.020	2618.004	-3.139	-1.238	19.168	-4.428	12.839
308	26.295876	50.146824	63.004	11:11:14	2617.905	0.020	2617.885	-3.258	-1.203	19.437	-4.490	12.892
309	26.296376	50.146639	63.931	11:13:24	2617.679	0.020	2617.659	-3.484	-1.167	19.723	-4.556	12.849
310	26.296692	50.146191	64.684	11:15:22	2617.621	0.020	2617.601	-3.542	-1.144	19.955	-4.610	12.947
311	26.297215	50.147534	64.337	11:17:49	2617.713	0.021	2617.692	-3.451	-1.107	19.848	-4.585	12.919
312	26.296834	50.147434	63.989	11:19:37	2617.68	0.021	2617.659	-3.484	-1.134	19.741	-4.560	12.831
313	26.296403	50.1475	63.344	11:22:02	2617.807	0.021	2617.786	-3.357	-1.165	19.542	-4.514	12.835
314	26.295966	50.147739	62.468	11:23:47	2617.849	0.021	2617.828	-3.315	-1.196	19.271	-4.452	12.701
315	26.295714	50.148157	61.651	11:25:44	2618.039	0.021	2618.018	-3.125	-1.214	19.019	-4.393	12.715

316	26.29563	50.148728	60.819	11:27:25	2618.223	0.021	2618.202	-2.941	-1.220	18.763	-4.334	12.707
317	26.296142	50.148961	60.957	11:30:45	2618.359	0.022	2618.337	-2.806	-1.184	18.805	-4.344	12.839
318	26.296435	50.148501	62.209	11:32:28	2618.335	0.022	2618.313	-2.830	-1.163	19.191	-4.433	13.091
319	26.296725	50.14807	63.254	11:34:31	2618.123	0.022	2618.101	-3.042	-1.142	19.514	-4.508	13.106
320	26.297124	50.148023	63.872	11:36:40	2617.954	0.022	2617.932	-3.211	-1.113	19.705	-4.552	13.055
321	26.297965	50.148317	64.206	11:38:44	2617.85	0.023	2617.827	-3.316	-1.053	19.807	-4.576	12.969
322	26.297625	50.148555	63.948	11:40:30	2618.07	0.023	2618.047	-3.096	-1.077	19.728	-4.557	13.152
323	26.297268	50.148881	62.776	11:42:41	2618.383	0.023	2618.360	-2.783	-1.103	19.367	-4.474	13.213
324	26.296905	50.149109	61.480	11:44:30	2618.615	0.023	2618.592	-2.551	-1.129	18.966	-4.381	13.163
325	26.29655	50.149426	60.174	11:46:58	2618.723	0.023	2618.700	-2.443	-1.154	18.564	-4.288	12.986
326	26.296807	50.149967	58.703	11:49:07	2618.991	0.024	2618.967	-2.176	-1.136	18.110	-4.183	12.887
327	26.297359	50.149914	59.319	11:51:01	2619.029	0.024	2619.005	-2.138	-1.096	18.300	-4.227	13.031
328	26.297728	50.149634	60.706	11:53:01	2618.761	0.024	2618.737	-2.406	-1.070	18.728	-4.326	13.066
329	26.297753	50.149636	60.719	11:55:26	2618.529	0.024	2618.505	-2.638	-1.068	18.732	-4.327	12.835
9002	26.312671	50.146851	57.793	12:03:56	2621.168	0.025	2621.143	0.000	0.000	17.829	-4.119	13.711
9003	26.312606	50.147333	57.571	13:50:53	2618.64	0.000	2618.640	0.000	0.000	17.761	-4.103	13.658
330	26.294932	50.146119	61.470	14:06:04	2618.022	0.000	2618.022	-0.618	-1.266	18.963	-4.381	15.231
331	26.294872	50.147112	60.997	14:08:20	2618.302	0.000	2618.302	-0.338	-1.270	18.818	-4.347	15.403
332	26.294621	50.147865	59.827	14:10:52	2618.461	0.000	2618.461	-0.179	-1.288	18.457	-4.264	15.302
333	26.294628	50.147861	59.847	14:13:07	2618.696	0.000	2618.696	0.056	-1.287	18.463	-4.265	15.542
334	26.29393	50.148711	57.043	14:15:00	2618.865	0.000	2618.865	0.225	-1.337	17.598	-4.065	15.095
335	26.294358	50.149392	57.012	14:18:26	2618.724	0.000	2618.724	0.084	-1.307	17.588	-4.063	14.916
336	26.294711	50.14896	58.861	14:20:24	2618.668	-0.001	2618.669	0.029	-1.281	18.159	-4.195	15.274
337	26.294803	50.148912	59.187	14:22:49	2618.403	-0.001	2618.404	-0.236	-1.275	18.259	-4.218	15.080
338	26.295495	50.148007	61.450	14:24:46	2618.277	-0.001	2618.278	-0.362	-1.225	18.957	-4.379	15.441
339	26.295674	50.147298	62.340	14:26:49	2618.18	-0.001	2618.181	-0.459	-1.212	19.232	-4.443	15.542
340	26.295486	50.149044	60.160	14:29:26	2618.329	-0.001	2618.330	-0.310	-1.226	18.559	-4.287	15.188
341	26.295968	50.149541	59.413	14:31:46	2618.659	-0.001	2618.660	0.020	-1.191	18.329	-4.234	15.306
342	26.29565	50.15102	54.099	14:34:41	2619.601	-0.001	2619.602	0.962	-1.214	16.689	-3.855	15.010
343	26.296187	50.150708	55.822	14:37:02	2619.362	-0.001	2619.363	0.723	-1.176	17.221	-3.978	15.142
344	26.296642	50.150106	58.149	14:40:24	2619.022	-0.001	2619.023	0.383	-1.143	17.939	-4.144	15.321
345	26.296091	50.15174	51.681	14:43:13	2620.007	-0.001	2620.008	1.368	-1.183	15.943	-3.683	14.811
346	26.296561	50.151482	52.870	14:46:11	2619.861	-0.001	2619.862	1.222	-1.149	16.310	-3.768	14.914
347	26.296979	50.150982	54.744	14:47:54	2619.661	-0.001	2619.662	1.022	-1.119	16.889	-3.901	15.128
348	26.295445	50.149901	57.854	15:13:02	2619.001	-0.001	2619.002	0.362	-1.229	17.848	-4.123	15.316
349	26.295339	50.14945	59.152	15:17:54	2618.597	-0.002	2618.599	-0.041	-1.236	18.248	-4.215	15.228
350	26.297242	50.150449	57.103	15:21:31	2619.369	-0.002	2619.371	0.731	-1.100	17.616	-4.069	15.378
351	26.294013	50.149049	56.703	15:26:57	2618.829	-0.002	2618.831	0.191	-1.331	17.493	-4.041	14.974
352	26.293425	50.149574	54.087	15:29:29	2619.322	-0.002	2619.324	0.684	-1.373	16.686	-3.854	14.888

353	26.293116	50.149218	54.109	15:31:51	2619.396	-0.002	2619.398	0.758	-1.395	16.693	-3.856	14.990
354	26.292332	50.150193	50.293	15:34:20	2619.747	-0.002	2619.749	1.109	-1.452	15.515	-3.584	14.492
355	26.292384	50.149626	51.792	15:36:32	2619.514	-0.002	2619.516	0.876	-1.794	15.978	-3.691	14.956
356	26.292601	50.150016	51.251	15:38:51	2619.507	-0.002	2619.509	0.869	-1.432	15.811	-3.652	14.460
357	26.29277	50.150824	49.867	15:41:11	2619.801	-0.002	2619.803	1.163	-1.420	15.384	-3.554	14.413
358	26.293265	50.150547	51.451	15:43:42	2619.619	-0.002	2619.621	0.981	-1.385	15.873	-3.667	14.572
359	26.293991	50.149864	54.844	15:46:06	2619.243	-0.002	2619.245	0.605	-1.333	16.919	-3.908	14.949
360	26.293153	50.151478	49.174	15:48:26	2619.962	-0.002	2619.964	1.324	-1.393	15.170	-3.504	14.383
361	26.293603	50.151198	50.598	15:50:19	2619.809	-0.002	2619.811	1.171	-1.361	15.609	-3.606	14.535
362	26.294554	50.150367	54.746	15:52:29	2619.238	-0.002	2619.240	0.600	-1.293	16.889	-3.901	14.880
363	26.29415	50.150775	52.708	15:54:16	2619.483	-0.002	2619.485	0.845	-1.321	16.261	-3.756	14.671
364	26.29344	50.15228	48.477	15:57:17	2620.285	-0.002	2620.287	1.647	-1.372	14.955	-3.455	14.520
365	26.293929	50.151785	49.739	15:59:09	2619.994	-0.002	2619.996	1.356	-1.337	15.344	-3.545	14.493
366	26.294942	50.150967	53.433	16:01:16	2619.439	-0.002	2619.441	0.801	-1.265	16.484	-3.808	14.742
367	26.294563	50.151358	51.647	16:03:04	2619.701	-0.002	2619.703	1.063	-1.292	15.933	-3.681	14.608
368	26.294044	50.152967	46.852	16:05:55	2620.588	-0.002	2620.590	1.950	-1.329	14.454	-3.339	14.394
369	26.294534	50.152467	48.297	16:08:13	2620.239	-0.002	2620.241	1.601	-1.294	14.900	-3.442	14.353
370	26.295337	50.151509	51.989	16:10:25	2619.807	-0.002	2619.809	1.169	-1.237	16.039	-3.705	14.740
371	26.294916	50.151908	50.265	16:12:58	2620.016	-0.002	2620.018	1.378	-1.267	15.507	-3.582	14.570
372	26.295727	50.152	50.529	16:16:14	2620.311	-0.003	2620.314	1.674	-1.209	15.588	-3.601	14.869
373	26.295363	50.152266	49.402	16:18:01	2620.416	-0.003	2620.419	1.779	-1.235	15.240	-3.521	14.733
374	26.294985	50.152695	47.795	16:19:56	2620.492	-0.003	2620.495	1.855	-1.262	14.745	-3.406	14.455
9003	26.312606	50.147333	57.571	16:42:31	2618.637	-0.003	2618.640	0.000	0.000	17.761	-4.103	13.658
9004	26.31248	50.146507	58.100	14:21:04	2621.201	0.000	2621.201	0.000	0.000	17.924	-4.140	13.783
375	26.313941	50.14184	61.606	14:26:39	2620.799	0.000	2620.799	-0.402	0.105	19.005	-4.390	14.109
376	26.314362	50.141614	62.426	14:29:13	2620.815	0.000	2620.815	-0.386	0.135	19.258	-4.449	14.289
377	26.314396	50.141066	63.174	14:31:25	2620.558	-0.001	2620.559	-0.642	0.137	19.489	-4.502	14.207
378	26.314266	50.140769	63.423	14:33:43	2620.399	-0.001	2620.400	-0.801	0.128	19.566	-4.520	14.117
379	26.316138	50.145941	63.223	14:41:36	2620.713	-0.001	2620.714	-0.487	0.262	19.504	-4.506	14.250
380	26.316079	50.145634	63.047	14:43:29	2620.782	-0.001	2620.783	-0.418	0.258	19.450	-4.493	14.281
381	26.315914	50.144983	62.680	14:47:12	2620.921	-0.001	2620.922	-0.279	0.246	19.337	-4.467	14.345
382	26.3155	50.14338	61.922	14:50:33	2621.15	-0.002	2621.152	-0.049	0.216	19.103	-4.413	14.424
383	26.31549	50.143385	61.905	14:53:38	2621.111	-0.002	2621.113	-0.088	0.216	19.098	-4.412	14.382
384	26.315325	50.142704	61.965	14:56:02	2620.961	-0.002	2620.963	-0.238	0.204	19.116	-4.416	14.258
385	26.316649	50.14668	63.427	15:01:29	2620.575	-0.002	2620.577	-0.624	0.299	19.567	-4.520	14.125
386	26.316812	50.14701	58.296	15:03:17	2620.745	-0.002	2620.747	-0.454	0.310	17.984	-4.154	13.066
387	26.316993	50.147368	57.763	15:05:10	2620.873	-0.002	2620.875	-0.326	0.323	17.820	-4.116	13.055
388	26.317512	50.148455	57.936	15:07:29	2621.124	-0.002	2621.126	-0.075	0.361	17.873	-4.129	13.310
389	26.317519	50.148832	56.891	15:09:42	2621.123	-0.003	2621.126	-0.075	0.361	17.551	-4.054	13.060

390	26.317344	50.149123	55.910	15:11:23	2621.136	-0.003	2621.139	-0.062	0.348	17.248	-3.984	12.853
391	26.317037	50.149293	54.329	15:13:50	2621.164	-0.003	2621.167	-0.034	0.326	16.760	-3.872	12.528
392	26.316641	50.149594	59.910	15:15:43	2621.318	-0.003	2621.321	0.120	0.298	18.482	-4.269	14.035
393	26.315112	50.146708	60.924	15:23:13	2621.097	-0.003	2621.100	-0.101	0.189	18.795	-4.342	14.164
394	26.315241	50.145916	61.265	15:25:40	2621.06	-0.003	2621.063	-0.138	0.198	18.900	-4.366	14.199
395	26.315185	50.145576	61.004	15:27:21	2621.023	-0.003	2621.026	-0.175	0.194	18.820	-4.347	14.104
396	26.315105	50.145056	60.781	15:30:11	2620.964	-0.004	2620.968	-0.233	0.188	18.751	-4.332	13.998
397	26.31499	50.144536	60.646	15:32:21	2621.04	-0.004	2621.044	-0.157	0.180	18.709	-4.322	14.050
398	26.314853	50.144032	60.331	15:34:39	2621.05	-0.004	2621.054	-0.147	0.170	18.612	-4.299	13.996
399	26.31468	50.143553	60.107	15:36:27	2620.995	-0.004	2620.999	-0.202	0.158	18.543	-4.283	13.900
400	26.314757	50.142987	60.776	15:38:34	2620.838	-0.004	2620.842	-0.359	0.163	18.749	-4.331	13.896
401	26.314624	50.142425	61.286	15:40:54	2620.801	-0.004	2620.805	-0.396	0.154	18.907	-4.368	13.990
402	26.314521	50.142073	61.734	15:42:49	2620.833	-0.004	2620.837	-0.364	0.146	19.045	-4.399	14.136
403	26.314986	50.141254	63.140	15:49:22	2620.62	-0.005	2620.625	-0.576	0.180	19.479	-4.500	14.223
404	26.314972	50.141269	63.122	15:51:16	2620.482	-0.005	2620.487	-0.714	0.179	19.473	-4.498	14.082
405	26.314811	50.140507	63.700	15:52:46	2620.255	-0.005	2620.260	-0.941	0.167	19.651	-4.539	14.004
406	26.314159	50.14047	63.678	16:18:53	2620.227	-0.006	2620.233	-0.968	0.120	19.645	-4.538	14.019
407	26.313842	50.139257	63.000	16:22:00	2619.964	-0.006	2619.970	-1.231	0.098	19.436	-4.490	13.618
408	26.313285	50.140594	63.754	16:25:52	2620.015	-0.007	2620.022	-1.179	0.058	19.668	-4.543	13.888
409	26.313252	50.140611	63.752	16:29:29	2620.503	-0.007	2620.510	-0.691	0.055	19.667	-4.543	14.378
410	26.313849	50.142964	59.136	16:32:20	2620.697	-0.007	2620.704	-0.497	0.098	18.244	-4.214	13.434
411	26.314143	50.143999	58.403	16:35:37	2620.958	-0.007	2620.965	-0.236	0.119	18.017	-4.162	13.500
412	26.314623	50.145453	59.013	16:39:58	2621.239	-0.007	2621.246	0.045	0.154	18.206	-4.206	13.892
413	26.314672	50.146867	59.763	16:44:14	2621.164	-0.008	2621.172	-0.029	0.157	18.437	-4.259	13.991
414	26.314074	50.146996	58.582	16:48:31	2621.184	-0.008	2621.192	-0.009	0.114	18.073	-4.175	13.774
9004	26.31248	50.146507	58.100	16:52:54	2621.193	-0.008	2621.201	0.000	0.000	17.924	-4.140	13.783
9009	26.3061237	50.1465645	70.001	14:02:17	2616.873	0.000	2616.873	0.000	0.000	21.595	-4.989	16.607
415	26.302416	50.143575	74.215	14:12:44	2617.132	0.000	2617.132	0.259	-0.266	22.895	-5.289	18.132
416	26.302167	50.143591	73.312	14:14:59	2617.108	0.000	2617.108	0.235	-0.283	22.617	-5.225	17.911
417	26.302411	50.14318	74.346	14:17:11	2617.097	-0.001	2617.098	0.225	-0.266	22.936	-5.298	18.128
418	26.302058	50.143138	73.062	14:19:01	2617.094	-0.001	2617.095	0.222	-0.291	22.540	-5.207	17.846
419	26.301716	50.143097	71.823	14:21:30	2617.104	-0.001	2617.105	0.232	-0.316	22.157	-5.118	17.586
420	26.298211	50.143982	67.713	14:25:13	2617.29	-0.001	2617.291	0.418	-0.567	20.889	-4.825	17.048
421	26.298595	50.143478	68.198	14:27:08	2617.229	-0.001	2617.230	0.357	-0.539	21.039	-4.860	17.075
422	26.298924	50.143026	67.177	14:28:34	2617.231	-0.001	2617.232	0.359	-0.516	20.724	-4.787	16.811
423	26.299167	50.142608	65.437	14:30:33	2617.181	-0.001	2617.182	0.309	-0.498	20.187	-4.663	16.331
424	26.29762	50.143433	66.997	14:33:59	2617.183	-0.001	2617.184	0.311	-0.609	20.669	-4.774	16.814
425	26.297952	50.142953	66.691	14:36:03	2617.135	-0.001	2617.136	0.263	-0.585	20.574	-4.753	16.670
426	26.29829	50.142465	65.669	14:37:46	2617.065	-0.001	2617.066	0.193	-0.561	20.259	-4.680	16.333

427	26.298613	50.142031	64.465	14:40:16	2617.093	-0.001	2617.094	0.221	-0.538	19.887	-4.594	16.053
428	26.297657	50.142592	66.364	14:43:48	2617.128	-0.002	2617.130	0.257	-0.606	20.473	-4.729	16.607
429	26.297128	50.142348	66.712	14:46:04	2617.148	-0.002	2617.150	0.277	-0.644	20.581	-4.754	16.747
430	26.29652	50.141817	67.506	14:48:08	2617.179	-0.002	2617.181	0.308	-0.688	20.826	-4.811	17.010
431	26.2967	50.140419	67.890	14:51:21	2616.79	-0.002	2616.792	-0.081	-0.675	20.944	-4.838	16.700
432	26.297574	50.144383	66.877	15:08:09	2617.255	-0.003	2617.258	0.385	-0.612	20.632	-4.766	16.863
433	26.296029	50.142188	67.478	15:11:12	2616.976	-0.003	2616.979	0.106	-0.723	20.817	-4.809	16.837
434	26.296002	50.141574	68.168	15:13:43	2616.879	-0.003	2616.882	0.009	-0.725	21.030	-4.858	16.906
435	26.296922	50.152306	50.514	15:19:39	2620.68	-0.003	2620.683	3.810	-0.659	15.583	-3.600	16.453
436	26.295835	50.153321	46.702	15:22:41	2621.129	-0.003	2621.132	4.259	-0.737	14.408	-3.328	16.075
437	26.296364	50.153296	47.353	15:24:05	2621.152	-0.003	2621.155	4.282	-0.699	14.608	-3.375	16.215
438	26.296777	50.153168	48.180	15:25:54	2621.137	-0.003	2621.140	4.267	-0.669	14.864	-3.434	16.367
439	26.295854	50.15441	44.346	15:28:36	2621.577	-0.003	2621.580	4.707	-0.735	13.681	-3.160	15.963
440	26.296268	50.154342	44.999	15:30:22	2621.514	-0.003	2621.517	4.644	-0.706	13.882	-3.207	16.026
441	26.296833	50.154246	45.932	15:32:41	2621.405	-0.004	2621.409	4.536	-0.665	14.170	-3.273	16.098
442	26.296218	50.155402	43.045	15:35:40	2621.897	-0.004	2621.901	5.028	-0.709	13.279	-3.068	15.949
443	26.297006	50.155113	44.444	15:37:53	2621.809	-0.004	2621.813	4.940	-0.653	13.711	-3.167	16.136
444	26.297435	50.155177	44.881	15:39:23	2621.847	-0.004	2621.851	4.978	-0.622	13.846	-3.198	16.247
445	26.296934	50.155956	42.892	15:42:08	2622.097	-0.004	2622.101	5.228	-0.658	13.232	-3.057	16.061
446	26.294891	50.154218	43.521	15:44:24	2621.464	-0.004	2621.468	4.595	-0.804	13.426	-3.101	15.724
447	26.295305	50.156355	41.015	15:47:02	2622.311	-0.004	2622.315	5.442	-0.775	12.653	-2.923	15.947
448	26.29488	50.156463	40.593	15:48:36	2622.353	-0.004	2622.357	5.484	-0.805	12.523	-2.893	15.919
449	26.294129	50.155004	41.884	15:50:46	2621.877	-0.004	2621.881	5.008	-0.859	12.921	-2.985	15.804
450	26.294195	50.155744	41.012	15:52:34	2622.277	-0.004	2622.281	5.408	-0.854	12.652	-2.923	15.992
451	26.293338	50.156596	31.059	15:55:14	2622.429	-0.004	2622.433	5.560	-0.915	9.582	-2.213	13.844
452	26.293941	50.156635	31.904	15:57:36	2622.406	-0.005	2622.411	5.538	-0.872	9.842	-2.274	13.979
453	26.293077	50.15547	41.270	16:00:14	2622.137	-0.005	2622.142	5.269	-0.934	12.732	-2.941	15.993
454	26.2923	50.155968	39.540	16:04:50	2622.164	-0.005	2622.169	5.296	-0.990	12.198	-2.818	15.666
455	26.292848	50.156317	39.537	16:06:36	2622.322	-0.005	2622.327	5.454	-0.951	12.197	-2.818	15.784
456	26.292303	50.154943	41.900	16:09:16	2621.998	-0.005	2622.003	5.130	-0.990	12.926	-2.986	16.060
457	26.293017	50.154686	43.292	16:11:13	2621.725	-0.005	2621.730	4.857	-0.938	13.355	-3.085	16.066
458	26.294562	50.145416	60.811	16:20:10	2618.272	-0.005	2618.277	1.404	-0.828	18.760	-4.334	16.659
459	26.294064	50.143935	62.224	16:22:27	2617.594	-0.006	2617.600	0.727	-0.864	19.196	-4.434	16.352
460	26.294574	50.139407	60.595	16:25:32	2616.707	-0.006	2616.713	-0.160	-0.827	18.693	-4.318	15.042
9009	26.3061237	50.1465645	70.001	16:34:54	2616.867	0.000	2616.867	0.000	0.000	21.595	-4.989	16.607
462	26.310633	50.145262	63.627	16:43:08	2619.584	-0.001	2619.585	2.718	-0.132	19.629	-4.534	17.945
463	26.311157	50.14542	62.247	16:45:06	2620.083	-0.001	2620.084	3.217	-0.095	19.203	-4.436	18.079
464	26.311576	50.145365	61.450	16:48:14	2620.424	-0.001	2620.425	3.558	-0.065	18.957	-4.379	18.201
465	26.313615	50.144482	57.293	16:50:41	2620.506	-0.002	2620.508	3.641	0.081	17.675	-4.083	17.151

9009	26.3061237	50.1465645	70.001	16:53:08	2616.865	-0.002	2616.867	0.000	-0.455	21.595	-4.989	17.062
9009	26.3061237	50.1465645	70.001	15:16:20	2616.7	0.000	2616.700	0.000	0.000	21.595	-4.989	16.607
466	26.302411	50.14318	64.588	15:02:12	2618.381	0.004	2618.377	1.677	-0.266	19.925	-4.603	17.266
467	26.302058	50.143138	65.373	15:08:37	2620.914	0.002	2620.912	4.212	-0.291	20.167	-4.659	20.012
468	26.301716	50.143097	65.026	15:11:11	2620.878	0.001	2620.877	4.177	-0.316	20.061	-4.634	19.919
469	26.298211	50.143982	61.222	15:19:22	2616.697	0.001	2616.696	-0.004	-0.567	18.887	-4.363	15.087
470	26.298595	50.143478	63.531	15:24:35	2616.751	0.002	2616.749	0.049	-0.539	19.599	-4.527	15.660
471	26.298924	50.143026	61.708	15:28:01	2616.785	0.003	2616.782	0.082	-0.516	19.037	-4.398	15.237
472	26.302413	50.142495	60.871	15:32:30	2616.773	0.004	2616.769	0.069	-0.266	18.779	-4.338	14.775
473	26.302992	50.142422	61.484	15:33:04	2616.784	0.005	2616.779	0.079	-0.224	18.968	-4.382	14.890
474	26.303244	50.142467	61.947	15:35:55	2616.675	0.005	2616.670	-0.030	-0.206	19.111	-4.415	14.872
475	26.303784	50.142454	62.699	15:37:32	2616.443	0.006	2616.437	-0.263	-0.168	19.343	-4.468	14.779
476	26.304342	50.14245	69.328	15:39:52	2615.045	0.006	2615.039	-1.661	-0.128	21.388	-4.941	14.913
477	26.305474	50.142448	60.348	15:43:31	2616.669	0.007	2616.662	-0.038	-0.047	18.617	-4.301	14.325
478	26.302051	50.142455	57.542	15:46:16	2616.991	0.008	2616.983	0.283	-0.292	17.752	-4.101	14.226
479	26.301722	50.143591	60.285	15:48:24	2616.666	0.009	2616.657	-0.043	-0.315	18.598	-4.296	14.574
480	26.301666	50.142452	60.480	15:52:51	2617.011	0.010	2617.001	0.301	-0.319	18.658	-4.310	14.968
481	26.301155	50.142449	55.966	15:54:30	2616.939	0.010	2616.929	0.229	-0.356	17.265	-3.988	13.861
482	26.299619	50.142174	57.546	15:57:16	2616.902	0.011	2616.891	0.191	-0.466	17.753	-4.101	14.309
483	26.299168	50.141761	56.470	15:58:33	2616.893	0.012	2616.881	0.181	-0.498	17.421	-4.024	14.076
484	26.298746	50.141373	58.503	16:01:08	2616.75	0.012	2616.738	0.038	-0.528	18.048	-4.169	14.445
485	26.298346	50.141024	56.777	16:02:40	2616.596	0.013	2616.583	-0.117	-0.557	17.516	-4.046	13.910
486	26.297917	50.140664	58.349	16:04:09	2616.533	0.013	2616.520	-0.180	-0.588	18.001	-4.158	14.250
487	26.297482	50.140302	56.786	16:05:33	2616.603	0.013	2616.590	-0.110	-0.619	17.518	-4.047	13.980
488	26.297104	50.139938	72.803	16:10:26	2614.763	0.015	2614.748	-1.952	-0.646	22.460	-5.188	15.966
489	26.305827	50.142634	72.393	16:13:34	2614.685	0.016	2614.669	-2.031	-0.021	22.333	-5.159	15.165
490	26.306258	50.142114	74.729	16:15:42	2614.487	0.016	2614.471	-2.229	0.010	23.054	-5.325	15.490
491	26.306566	50.141658	75.415	16:17:29	2614.276	0.017	2614.259	-2.441	0.032	23.265	-5.374	15.419
492	26.306859	50.141284	75.466	16:21:20	2614.688	0.018	2614.670	-2.030	0.053	23.281	-5.378	15.821
493	26.308058	50.139994	68.504	16:24:02	2616.785	0.018	2616.767	0.067	0.139	21.133	-4.882	16.179
494	26.309258	50.139235	64.363	16:25:56	2617.565	0.019	2617.546	0.846	0.225	19.856	-4.587	15.891
495	26.309986	50.139172	62.047	16:29:05	2618.188	0.020	2618.168	1.468	0.277	19.142	-4.422	15.911
496	26.310856	50.139264	60.660	16:30:31	2618.316	0.020	2618.296	1.596	0.339	18.714	-4.323	15.648
497	26.311306	50.139366	59.793	16:32:39	2618.308	0.021	2618.287	1.587	0.371	18.446	-4.261	15.401
498	26.311744	50.139375	59.300	16:35:01	2618.757	0.021	2618.736	2.036	0.403	18.294	-4.226	15.701
499	26.3061237	50.1465645	49.375	16:48:49	2618.384	0.021	2618.363	1.663	0.053	23.281	-5.378	15.821
9009	26.312555	50.146917	70.001	16:40:37	2616.723	0.023	2616.700	0.000	0.461	21.595	-4.989	16.146

B. DIFFERENTIAL GPS DATASHEET

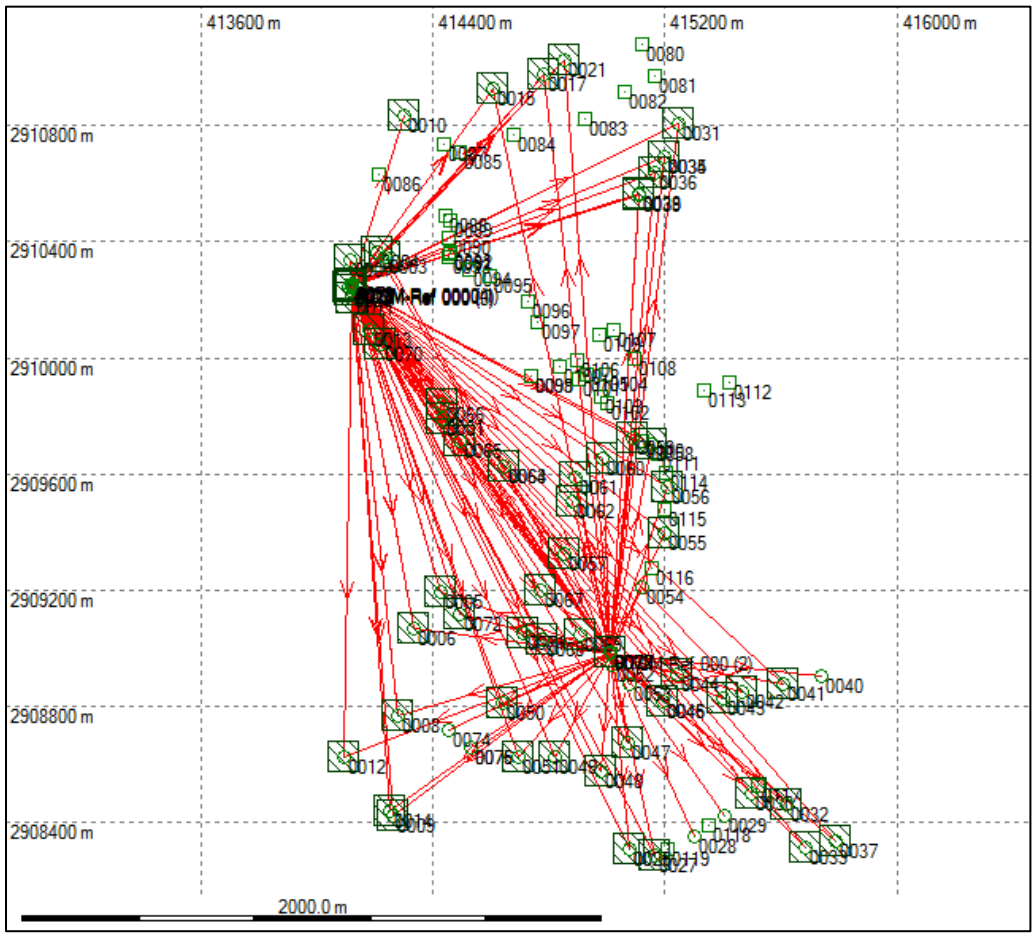

Figure 41 Base and rover station coordinate from differential GPS data processing in Leica Geo Office (R).

Point Id	Latitude	Longitude	Ortho. Hgt.	Sd. Latitude	Sd. Longitude	Sd. Height	Hgt. Qlty
0001	26° 18' 18.21480" N	50° 08' 34.08860" E	79.0443	0.0024	0.0023	0.0066	0.0066
0002	26° 17' 52.17692" N	50° 08' 55.31982" E	63.8531	0.0047	0.0047	0.0158	0.0158
0003	26° 18' 36.25923" N	50° 08' 26.98156" E	67.1093	0.0000	0.0000	0.0000	0.0000
0004	26° 18' 36.69742" N	50° 08' 25.85554" E	64.7400	0.0052	0.0051	0.0137	0.0137
0005	26° 17' 58.83588" N	50° 08' 34.05647" E	64.4385	0.0055	0.0050	0.0172	0.0172
0006	26° 17' 54.65867" N	50° 08' 30.84256" E	64.1681	0.0047	0.0046	0.0134	0.0134
0007	26° 18' 35.79542" N	50° 08' 22.57267" E	65.1095	0.0080	0.0071	0.0257	0.0257
0008	26° 17' 45.01797" N	50° 08' 28.83248" E	68.5866	0.0045	0.0046	0.0159	0.0159
0009	26° 17' 33.79016" N	50° 08' 28.44743" E	62.0010	0.0051	0.0051	0.0173	0.0173
0010	26° 18' 52.02472" N	50° 08' 29.14630" E	62.8436	0.0101	0.0096	0.0229	0.0229
0011	26° 18' 31.54900" N	50° 08' 22.88738" E	70.3253	0.0113	0.0088	0.0303	0.0303
0012	26° 17' 40.21066" N	50° 08' 22.24871" E	67.9499	0.0067	0.0068	0.0244	0.0244
0013	26° 18' 28.10185" N	50° 08' 25.05580" E	77.1169	0.0074	0.0076	0.0189	0.0189
0014	26° 17' 34.22441" N	50° 08' 27.90908" E	67.3889	0.0056	0.0056	0.0196	0.0196
0015	26° 18' 55.07511" N	50° 08' 40.18872" E	61.8101	0.0092	0.0088	0.0206	0.0206
0016	26° 18' 32.82185" N	50° 08' 22.78617" E	73.2848	0.0035	0.0036	0.0112	0.0112
0017	26° 18' 56.74789" N	50° 08' 46.43059" E	62.9524	0.0064	0.0061	0.0148	0.0148
0018	26° 18' 33.02071" N	50° 08' 22.78073" E	69.4860	0.0053	0.0082	0.0174	0.0174
0019	26° 18' 32.91192" N	50° 08' 22.48223" E	71.4926	0.0054	0.0067	0.0176	0.0176
0020	26° 18' 32.45528" N	50° 08' 22.54152" E	72.0173	0.0043	0.0054	0.0141	0.0141
0021	26° 18' 58.44876" N	50° 08' 49.03367" E	63.1762	0.0077	0.0073	0.0167	0.0167
0022	26° 18' 32.81260" N	50° 08' 22.77317" E	73.2575	0.0057	0.0069	0.0181	0.0181
0023	26° 18' 32.82175" N	50° 08' 22.78604" E	73.2846	0.0032	0.0037	0.0094	0.0094
0024	26° 18' 32.82178" N	50° 08' 22.78618" E	73.2852	0.0052	0.0056	0.0143	0.0143
0025	26° 17' 30.21142" N	50° 08' 57.77628" E	51.3851	0.0077	0.0073	0.0275	0.0275
0026	26° 17' 30.21168" N	50° 08' 57.77631" E	51.3829	0.0044	0.0041	0.0155	0.0155
0027	26° 17' 29.47850" N	50° 09' 00.90589" E	50.8245	0.0054	0.0051	0.0191	0.0191
0028	26° 17' 31.63630" N	50° 09' 05.87122" E	49.7687	0.0059	0.0055	0.0204	0.0204
0029	26° 17' 33.92025" N	50° 09' 09.65029" E	48.5751	0.0084	0.0077	0.0288	0.0288
0030	26° 17' 36.48454" N	50° 09' 12.93484" E	47.4202	0.0094	0.0087	0.0322	0.0322
0031	26° 18' 51.33872" N	50° 09' 03.18634" E	56.8734	0.0056	0.0050	0.0113	0.0113
0032	26° 17' 35.21601" N	50° 09' 17.32670" E	43.0809	0.0081	0.0073	0.0271	0.0271
0033	26° 17' 30.50350" N	50° 09' 19.57511" E	39.8285	0.0092	0.0091	0.0324	0.0324
0034	26° 18' 47.71311" N	50° 09' 01.60336" E	56.0203	0.0072	0.0063	0.0144	0.0144

Figure 42 Data processing table of differential GPS on Leica Geo Office (R). All coordinates are in Appendix A.

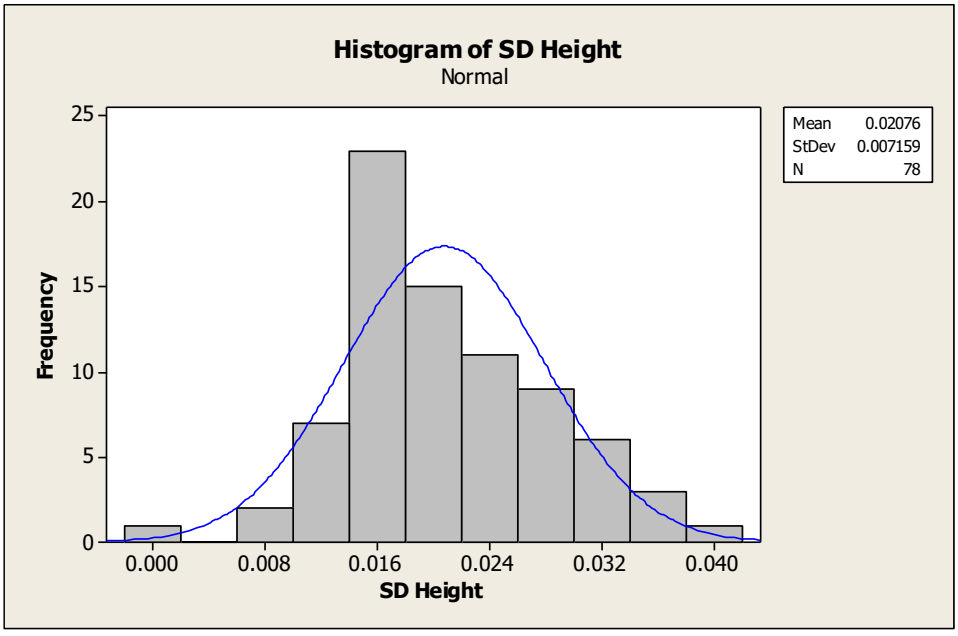

Figure 43 Histogram of height deviation (in meter) from differential GPS measurement

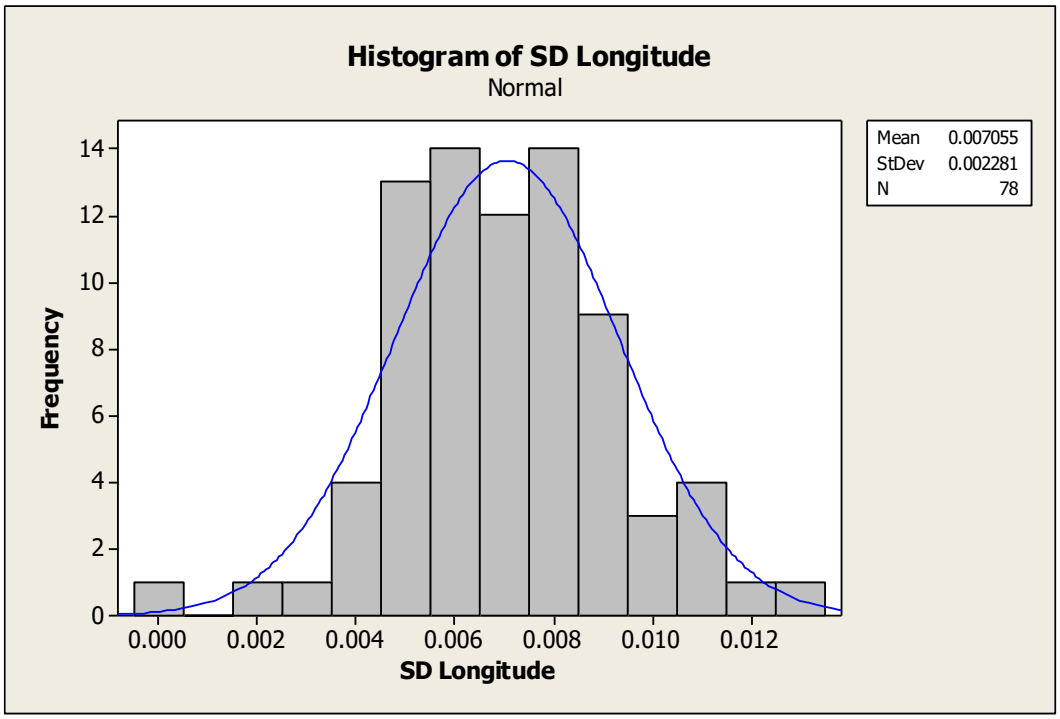

Figure 44 Histogram of longitude standard deviation (in meter) from differential GPS measurement

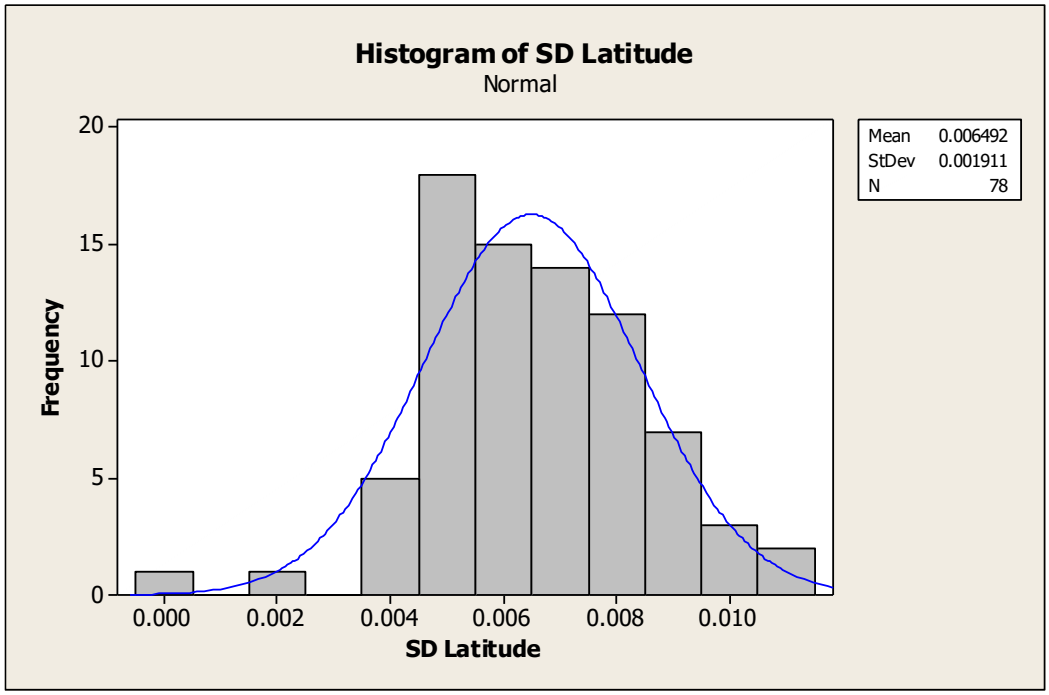

Figure 45 Histogram of latitude standard deviation (in meter) from differential GPS measurement

C. STRUCTURAL LINEAMENT DELINEATION

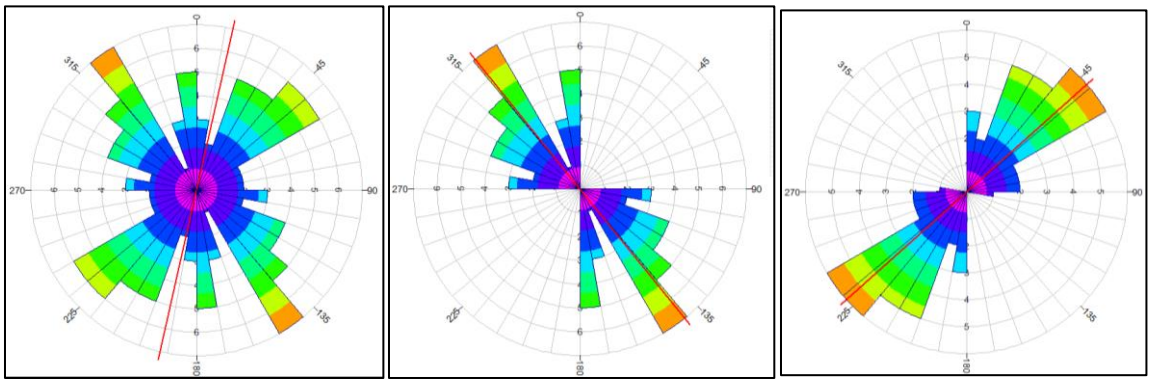

Figure 46 The structure trend orientation on the SVD map is shown by the red line. Left: the mean orientation of total faults is N 12.7º E. Center: The mean NW orientation is N 39º W. Right: The mean NE orientation is N 48º W.

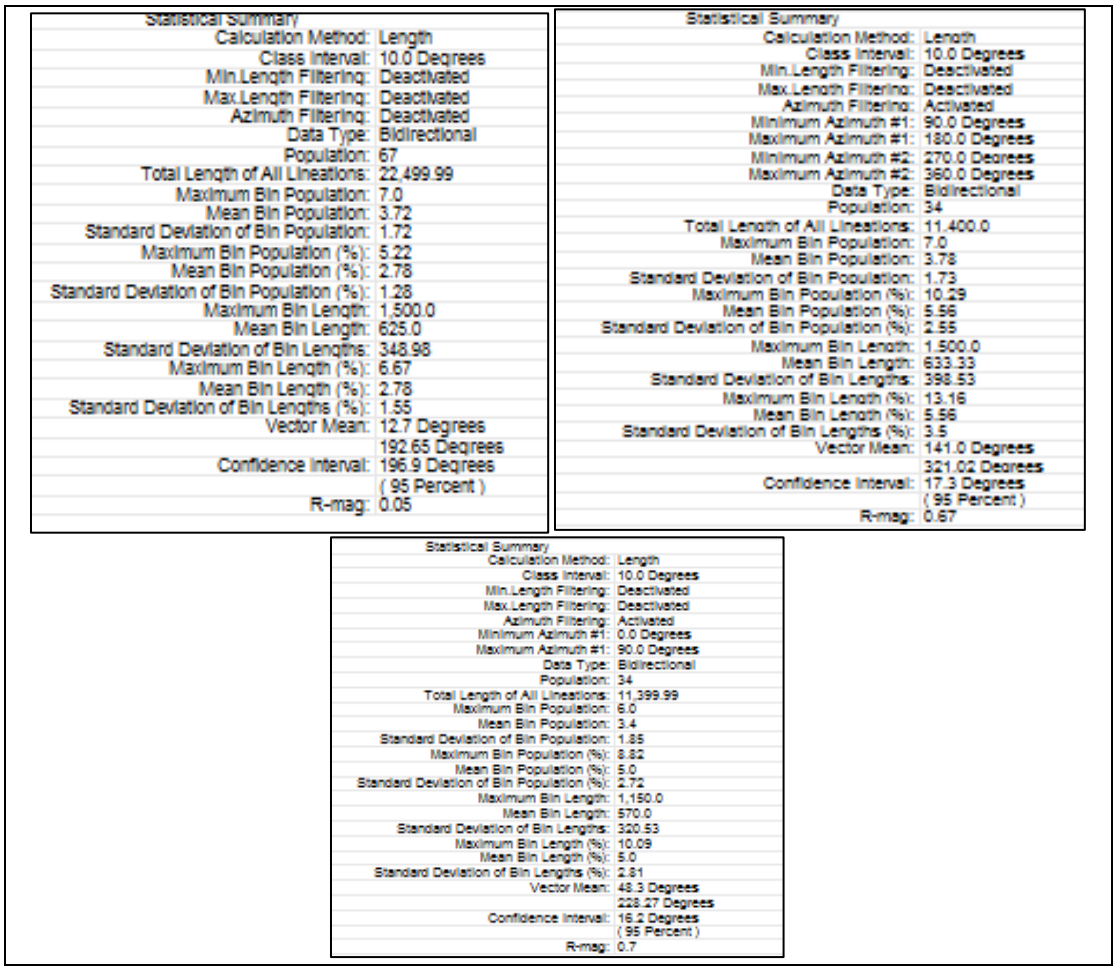

Statistical Summary	
Calculation Method:	Length
Class Interval:	10.0 Degrees
Min.Length Filtering:	Deactivated
Max.Length Filtering:	Deactivated
Azimuth Filtering:	Deactivated
Data Type:	Bidirectional
Population:	67
Total Length of All Lineations:	22,499.99
Maximum Bin Population:	7.0
Mean Bin Population:	3.72
Standard Deviation of Bin Population:	1.72
Maximum Bin Population (%):	5.22
Mean Bin Population (%):	2.78
Standard Deviation of Bin Population (%):	1.28
Maximum Bin Length:	1,500.0
Mean Bin Length:	625.0
Standard Deviation of Bin Lengths:	348.98
Maximum Bin Length (%):	6.67
Mean Bin Length (%):	2.78
Standard Deviation of Bin Lengths (%):	1.55
Vector Mean:	12.7 Degrees
	192.65 Degrees
Confidence Interval:	196.9 Degrees
	(95 Percent)
R-mag:	0.05

Statistical Summary	
Calculation Method:	Length
Class Interval:	10.0 Degrees
Min.Length Filtering:	Deactivated
Max.Length Filtering:	Deactivated
Azimuth Filtering:	Activated
Minimum Azimuth #1:	90.0 Degrees
Maximum Azimuth #1:	180.0 Degrees
Minimum Azimuth #2:	270.0 Degrees
Maximum Azimuth #2:	360.0 Degrees
Data Type:	Bidirectional
Population:	34
Total Length of All Lineations:	11,400.0
Maximum Bin Population:	7.0
Mean Bin Population:	3.78
Standard Deviation of Bin Population:	1.73
Maximum Bin Population (%):	10.29
Mean Bin Population (%):	5.56
Standard Deviation of Bin Population (%):	2.55
Maximum Bin Length:	1,500.0
Mean Bin Length:	633.33
Standard Deviation of Bin Lengths:	398.53
Maximum Bin Length (%):	13.16
Mean Bin Length (%):	5.96
Standard Deviation of Bin Lengths (%):	3.5
Vector Mean:	141.0 Degrees
	321.02 Degrees
Confidence Interval:	17.3 Degrees
	(95 Percent)
R-mag:	0.67

Statistical Summary	
Calculation Method:	Length
Class Interval:	10.0 Degrees
Min.Length Filtering:	Deactivated
Max.Length Filtering:	Deactivated
Azimuth Filtering:	Activated
Minimum Azimuth #1:	0.0 Degrees
Maximum Azimuth #1:	90.0 Degrees
Data Type:	Bidirectional
Population:	34
Total Length of All Lineations:	11,399.99
Maximum Bin Population:	6.0
Mean Bin Population:	3.4
Standard Deviation of Bin Population:	1.85
Maximum Bin Population (%):	8.82
Mean Bin Population (%):	5.0
Standard Deviation of Bin Population (%):	2.72
Maximum Bin Length:	1,150.0
Mean Bin Length:	570.0
Standard Deviation of Bin Lengths:	320.53
Maximum Bin Length (%):	10.09
Mean Bin Length (%):	5.0
Standard Deviation of Bin Lengths (%):	2.81
Vector Mean:	48.3 Degrees
	228.27 Degrees
Confidence Interval:	16.2 Degrees
	(95 Percent)
R-mag:	0.7

Figure 47 Statistical summary of fault delineation on whole map (left), NW trending (right), NE trending (bottom)

References

Abdullatif, O. (2010). Geomechanical properties and rock mass quality of the carbonate rus formation, dammam dome, saudi arabia. The Arabian Journal for Science and Engineering, 35(July 2010), 25.

Abu Taleb, M. G., & Egeli, I. (1981). Some geotechnical problems in the Eastern Province of Saudi Arabia. In Proceedings of the Symposium on Geotechnical Problems in Saudi Arabia (pp. 813–819). Riyadh: King Saud University.

Al-Fahmi, M., Cooke, M. L., & Cole, J. C. (2014). Modeling of the Dammam outcrop fractures : Case study for fracture development in salt- cored structures development in salt-cored structures. GeoArabia, 19(July), 49–80.

Al-Saad, H., & Ibrahim, M. I. (2002). Stratigraphy, micropaleontology, and paleoecology of the Miocene Dam Formation, Qatar. GeoArabia, 7(1), 9–28.

Al-Shuhail, A. A., Hariri, M. M., & Makkawi, M. H. (2004a). Using ground-penetrating radar to delineate fractures in the Rus Formation, Dammam Dome, Eastern Saudi Arabia. International Geology Review, 46(1), 91–96. https://doi.org/10.2747/0020-6814.46.1.91

Al-Shuhail, A. A., Hariri, M. M., & Makkawi, M. H. (2004b). Using Ground-Penetrating Radar to Delineate Fractures in the Rus Formation, Dammam Dome, Eastern Saudi Arabia. International Geology Review, 46(1), 91–96. https://doi.org/10.2747/0020-6814.46.1.91

Alsharhan, A. S., Rizk, Z. A., Nairn, A. E. M., Bakhit, D. W., & Alhajari, S. A. (2001). Hydrogeology of an Arid Region: The Arabian Gulf and Adjoining Areas. Elsevier. https://doi.org/10.1016/B978-0-444-50225-4.X5000-3

Bishop, I., Styles, P., Emsley, S. J., & Ferguson, N. S. (1997). The detection of cavities using the microgravity technique: case histories from mining and karstic environments. Engineering Geology, 12(1), 153–166. https://doi.org/10.1144/GSL.ENG.1997.012.01.13

Butler, D. K. (1984). Microgravimetric and gravity gradient techniques for detection of subsurface cavities. Geophysics, 49(7), 1084–1096. https://doi.org/10.1190/1.1441723

Buttkus, B. (2000). Spectral Analysis and Filter Theory in Applied Geophysics. Spectral Analysis and Filter Theory in Applied Geophysics. Berlin, Heidelberg: Springer Berlin Heidelberg. https://doi.org/10.1007/978-3-642-57016-2

Chamberlain, A. T., Sellers, W., Proctor, C., & Coard, R. (2000). Cave detection in limestone using ground penetrating radar. Journal of Archaeological Science,

27(10), 957–964. https://doi.org/10.1006/jasc.1999.0525

Colley, G. C. (1963). The detection of caves by gravity measurements. Geophysical Prospecting, 11(1), 1–9. https://doi.org/10.1111/j.1365-2478.1963.tb02019.x

Crosch, J., Touma, F., & Richards, D. (1985). Solution cavities in the limestone of eastern Saudi Arabia. In Second Saudi Engineering Conference (pp. 2879–2907).

Davies, J. A., & Lord, J. A. (1980). The effects of cavities in limestone on the construction of a high rise building in Al Khobar, Saudi Arabia. Proceedings of the Symposium on Geotechnical Problems in Saudi Arabia, 123–131.

Elkhrachy, I. (2016). Vertical accuracy assessment for SRTM and ASTER Digital Elevation Models: A case study of Najran city, Saudi Arabia. Ain Shams Engineering Journal, 2, 1–11. https://doi.org/10.1016/j.asej.2017.01.007

Elkins, T. A. (1951). The second derivative method of gravity interpretation. Geophysics, 16(1), 29–50. https://doi.org/10.1190/1.1437648

Fiore, V. di, Angelino, A., Passaro, S., & Bonanno, A. (2013). High resolution seismic reflection methods to detect near surface tuff-cavities: A case study in the Neapolitan area, Italy. Journal of Cave and Karst Studies, 75(1), 51–59. https://doi.org/10.4311/2011ES0248

Gambetta, M., Armadillo, E., Carmisciano, C., Stefanelli, P., Cocchi, L., & Tontini, F. C. (2011). Determining geophysical properties of a near-surface cave through integrated microgravity vertical gradient and electrical resistivity tomography measurements. Journal of Cave and Karst Studies, 73(1), 11–15. https://doi.org/10.4311/jcks2009ex0091

Greenhalgh, S., & Marescot, L. (2013). Gravity Surveying. ETH Zurich.

Guoqiang, X., Jianping, S., & Xian, Y. (2004). Detecting shallow caverns in China using TEM. The Leading Edge, 23(7), 694–695. Retrieved from http://dx.doi.org/10.1190/1.1776743

Hariri, M. M. (2013). Fractures system within Dammam Dome and its relationship to the doming process, Eastern Saudi Arabia. Arabian Journal of Geosciences, 7(11), 4943–4956. https://doi.org/10.1007/s12517-013-1125-9

Hinze, W. J., Frese, R. R. B. von, Frese, R. Von, & Saad, A. H. (2013). Gravity and Magnetic Exploration: Principles, Practices, and Applications. https://doi.org/10.1017/CBO9780511843129

Jado, A. R., & Johnson, D. H. (1983). Solution caverns in the Dammam Dome, Dhahran, Saudi Arabia. Arabian Journal of Science and Engineering, 8(1), 69–73.

Khaldaoui, F., Djediat, Y., Djeddi, M., & Ydri, A. (2015). Characterization by electrical resistivity imaging 3D and GPR of dissolutions in Quaternary carbonate sandstone

formations in Algiers-West. In International Conference on Engineering Geophysics, Al Ain, United Arab Emirates, 15-18 November 2015 (pp. 268–270). Society of Exploration Geophysicists. https://doi.org/10.1190/iceg2015-075

Longman, I. M. (1959). Formulas for computing the tidal accelerations due to the moon and the sun. Journal of Geophysical Research, 64(12), 2351–2355. https://doi.org/10.1029/JZ064i012p02351

Martín, A., Núñez, M. A., Gili, J. A., & Anquela, A. B. (2011). A comparison of robust polynomial fitting, global geopotential model and spectral analysis for regional-residual gravity field separation in the Doñana National Park (Spain). Journal of Applied Geophysics, 75(2), 327–337. https://doi.org/10.1016/j.jappgeo.2011.06.037

Metwaly, M., & Alfouzan, F. (2013). Application of 2-D geoelectrical resistivity tomography for subsurface cavity detection in the eastern part of Saudi Arabia. Geoscience Frontiers, 4(4), 469–476. https://doi.org/10.1016/j.gsf.2012.12.005

Milton, D. I. (1967). Geology of the Arabian Peninsula: Kuwait. Geological Survey Professional Paper 560-F.

Momayez, M., Hassani, F. P., Hara, A., & Sadri, A. (1996). Application of GPR in Canadian mines. CIM Bulletin, 89(1001), 107–110. Retrieved from http://www.scopus.com/inward/record.url?eid=2-s2.0-0030159363&partnerID=tZOtx3y1

Nettleton, L. L. (1971). Elementary gravity and magnetics for geologists and seismologists. Houston: Society of Exploration Geophysicists.

Pánisová, J., & PaŠteka, R. (2009). The use of microgravity technique in archaeology: A case study from the St. Nicolas church in pukanec, slovakia. Contributions to Geophysics and Geodesy, 39(3), 237–254. https://doi.org/10.2478/v10126-009-0009-1

Pernod, P., Piwakowski, B., Delannoy, B., & Tricot, J. . (1989). Detection of shallow underground cavities by seismic methods: physical modelling approach (Acoustical). Boston, MA: Springer. https://doi.org/https://doi.org/10.1007/978-1-4613-0791-4_74

Pumphrey, H. C. (2014). Gravity surveying : a brief introduction. Edinburgh.

Putiška, R., Dostál, I., & Kušnirák, D. (2012). Determination of dipping contacts using electrical resistivity tomography. Contributions to Geophysics and Geodesy, 42(2), 161–180. https://doi.org/10.2478/v10126-012-0007-6

Reynolds, J. M. (1997). An Introduction to Applied and Environmental Geophysics. Wiley-Blackwell (Vol. 1). Wiley-Blackwell.

Setiyono, K., Gallo, S., Boulange, C., Bruere, F., Moreau, F., Rondeleux, B., & Snow, J.

(2015). Near surface velocity model of Dukhan Field from multi-physics survey to enhance PSDM seismic imaging. International Petroleum Technology Conference, 1–19. https://doi.org/10.2523/IPTC-18293-MS

Styles, P., McGrath, R., Thomas, E., & Cassidy, N. J. (2005). The use of microgravity for cavity characterization in karstic terrains. Quarterly Journal of Engineering Geology and Hydrogeology, 38(2), 155–169. https://doi.org/10.1144/1470-9236/04-035

Talwani, M., & Ewing, M. (1960). Rapid computation of gravitational attractionn of three dimensional bodies of arbitrary shape. Geophysics, 25(1), 203–225. https://doi.org/10.1190/1.1438687

Telford, W. M., Geldart, L. P., & Sheriff, R. E. (1990). Applied Geophysics (2nd ed.). Cambridge: Cambridge University Press. https://doi.org/10.1017/CBO9781139167932

Tleel, J. W. (1974). Surface Geology of Dammam Dome, Eastern Province, Saudi Arabia. AAPG Bulletin (Vol. 57). American Association of Petroleum Geologists. Retrieved from http://archives.datapages.com/data/bulletns/1971-73/data/pg/0057/0003/0550/0558.htm

Weijermars, R. (1999). Surface geology, lithostratigraphy and Tertiary growth of the Dammam Dome, Saudi Arabia: A new field guide. GeoArabia, 4(2), 199–226.

Vitae

Name : Muhammad Hanif

Nationality : Indonesia

Date of Birth : November 10th, 1991

Email : hanifgeos@gmail.com

Address : Jalan Gegerkalong Girang Kiara 1 No. 29 Bandung

Postal Code: 40153, Indonesia

Academic Background:

B.Sc of Geophysics, Institute Technology of Bandung (ITB), 2013

M.Sc of Geophysics, King Fahd University of Petroleum & Minerals (KFUPM), 2018

Publication:

Hanif, M., Greenhalgh, S., Kaka, S.I. (2018). Gravity investigations of near-surface faulting and cavities of the Dammam Dome on the KFUPM campus, Saudi Arabia. Arabian Journal of Geosciences (submitted)